

JOHANNES GUTENBERG UNIVERSITY MAINZ

Isoprene Oxidation and its Impacts on the Atmospheric Composition

by

Domenico Taraborrelli

A thesis submitted in partial fulfillment for the
degree of Doctor of Philosophy

in the
Faculty of Chemistry, Pharmacy and Geosciences
Institute of Inorganic and Analytical Chemistry

November 2009

PhD defense 01/26/2010

“An error does not become truth by reason of multiplied propagation, nor becomes truth error because nobody sees it.”

Mahatma Gandhi

Abstract

by Domenico Taraborrelli

Terrestrial vegetation, especially tropical rain forest, releases vast quantities of volatile organic compounds (VOCs) to the atmosphere, which are removed by oxidation reactions and deposition of reaction products. The oxidation is mainly initiated by hydroxyl radicals (OH), primarily formed through the photodissociation of ozone. Previously it was thought that, in unpolluted air, biogenic VOCs deplete OH and reduce the atmospheric oxidation capacity. Conversely, in polluted air VOC oxidation leads to noxious oxidant build-up by the catalytic action of nitrogen oxides ($\text{NO}_x = \text{NO} + \text{NO}_2$). However, aircraft measurements of atmospheric trace gases performed over the pristine Amazon forest revealed unexpectedly high OH concentrations. Isoprene was the dominant VOC emitted in that region and its oxidation computed to be the largest OH sink. In this work the hypothesis that natural isoprene oxidation efficiently recycles OH in low- NO_x air has been investigated in great detail. A highly explicit oxidation mechanism for isoprene has been developed including recent experimental and theoretical advancements. Major OH-recycling routes have been implemented and shown to substantially enhance oxidation under low- NO_x conditions. Enhanced OH concentrations persisted under reduced light conditions typical of vegetation canopies. When compared to aircraft measurements the new oxidation mechanism shows to reproduce the OH concentrations within the uncertainty range. Furthermore, simulations showed substantial production of a dihydroxyepoxide from isoprene that may be a potentially important precursor of organic aerosols in the atmosphere. A new reduced oxidation mechanism based on traditional knowledge has been developed and tested for global atmospheric studies. The inclusion in this mechanism of the new oxidation routes will allow to study the impacts of enhanced VOC oxidation on atmospheric composition, surface-atmosphere exchanges, aerosols and climate.

Zusammenfassung

von Domenico Taraborrelli

Terrestrische Vegetation, vor allem tropischer Regenwald, emittiert grosse Mengen flüchtiger organischer Verbindungen (VOCs) in die Atmosphäre, die durch Oxidationsreaktionen und Deposition der Reaktionsprodukte wieder entfernt werden. Die Oxidation wird vor allem durch Hydroxyl-Radikale (OH) initiiert, die hauptsächlich durch Photodissoziation von Ozon gebildet werden. Zuvor ging man davon aus, dass biogene VOCs OH in unverschmutzter Luft abbauen und dadurch die atmosphärische Oxidationskapazität verringern. Umgekehrt, führt die Oxidation von VOCs in verschmutzter Luft durch die katalytische Wirkung von Stickstoffoxiden ($\text{NO}_x = \text{NO} + \text{NO}_2$) zu schädlicher Oxidationsmittelbildung. Flugzeugmessungen atmosphärischer Spurengase, die über dem unberührten Amazonas-Regenwald durchgeführt worden sind, haben jedoch unerwartet hohe OH-Konzentrationen aufgezeigt. Das VOC mit der höchsten Emission in dieser Region war Isopren, dessen Oxidation als stärkste OH-Senke berechnet wurde. In dieser Arbeit wurde die Hypothese genauestens untersucht, dass die natürliche Isopren-Oxidation in niedrig- NO_x Luft OH effizient erneuert. Es wurde ein sehr detaillierter Oxidationsmechanismus für Isopren entwickelt, in dem neueste experimentelle und theoretische Fortschritte umgesetzt worden sind. Die Haupt-OH-Rückgewinnungswege wurden angewendet wodurch gezeigt wurde, dass sie wesentlich zur Oxidation unter niedrig- NO_x Bedingungen beitragen. Verstärkte OH-Konzentrationen blieben unter verminderten Lichtverhältnissen, wie sie unter dichten Vegetationsdächern typisch sind, dauerhaft erhalten. Im Vergleich zu Flugzeugmessungen, der neue Oxidationsmechanismus reproduziert die OH-Konzentrationen innerhalb des Unsicherheitsbereiches. Darüber hinaus zeigten Simulationen eine erhebliche Produktion eines Isopren-Dihydroxyepoxids, das ein potenziell wichtiger Vorläufer organischer Aerosole in der Atmosphäre sein könnte. Es wurde einen neuen vereinfachten Oxidationsmechanismus auf Basis des traditionellen Wissenstands entwickelt und seine Anwendung für globale atmosphärische Studien getestet. Die Eingliederung der neuen Oxidationswege in diesen Mechanismus ermöglicht es folgende Auswirkungen der verstärkten VOC-Oxidation zu studieren die Zusammensetzung der Atmosphäre, den Austausch zwischen Erdoberfläche und Atmosphäre, Aerosole und Klima.

Contents

Abstract	iii
Zusammenfassung	iv
Acknowledgements	v
List of Figures	x
List of Tables	xiii
Abbreviations	xv
1 Introduction	1
1.1 Isoprene from vegetation	1
1.2 Role in the Earth system	1
1.3 Isoprene oxidation chemistry	3
1.3.1 Experimental work	3
1.3.2 Oxidation mechanisms	3
2 Mainz Isoprene Mechanism 2: Development	6
2.1 Background	6
2.2 Reduction principles	7
2.3 The whole mechanism	9
2.4 The OH-pathway	9
2.5 O ₃ -pathway	11
2.6 The NO ₃ -pathway	11
2.7 Unsaturated C ₅ –C ₄ -products	12
2.7.1 Aldehydes	12
2.7.2 Ketones	12
2.8 C ₃ –C ₂ -products	12
3 Mainz Isoprene Mechanism 2: Evaluation	13
3.1 Box model setup	13
3.2 Oxidation pathways of isoprene and RO ₂	15
3.3 Low-NO _x regimes	15

3.3.1	MCM behaviour	15
3.3.2	MIM2 and MIM behaviour and biases	16
3.4	Mid-NO _x regimes	20
3.4.1	MCM behaviour	20
3.4.2	MIM2 and MIM behaviour and biases	22
3.5	High-NO _x regimes	22
3.5.1	MCM behaviour	22
3.5.2	MIM2 and MIM behaviour and biases	22
3.6	Organic nitrogen and peroxides	25
3.6.1	Alkyl nitrates	25
3.6.2	Peroxy acyl nitrates	27
3.7	C ₂ –C ₅ peroxides	28
3.8	Impact on the global scale	29
3.9	Implementation in a global model	29
3.10	OH and isoprene	31
3.11	New species	33
3.11.1	Glyoxal	33
3.11.2	Propene	34
3.11.3	Acetaldehyde	34
3.12	Incorporation of new experimental results	34
4	Development of a new detailed isoprene oxidation mechanism	38
4.1	Motivation	38
4.2	Strategy	39
4.2.1	Starting point	39
4.2.2	Development directions	40
4.3	Reactions with OH	40
4.3.1	SAR formalism	40
4.3.2	OH-addition to double bonds	40
4.3.3	H-abstraction by OH	42
4.3.4	Reaction with OH: measurements vs. predictions	45
4.3.5	Alkyl radicals	46
4.3.6	Excited RO ₂ radicals	48
4.3.6.1	General atmospheric fate	48
4.3.6.2	CH ₃ CO ₃ [*] radical	48
4.3.6.3	HCOCH ₂ O ₂ [*] radical	49
4.3.6.4	HCOCO ₃ [*] radical	50
4.3.6.5	HOCH ₂ CO ₃ [*] radical	50
4.3.6.6	HOCH(O ₂)CHO [*] radical	50
4.3.6.7	Vinyl peroxy radical (CH ₂ =CHO ₂ [*])	51
4.3.6.8	CH ₃ COCH(O ₂)OH [*] and CH ₃ CO ₂ (OH)CHO [*] radicals	51
4.3.6.9	Methyl vinyl peroxy radical (CH ₃ C(O ₂)=CH ₂ [*])	52
4.3.7	Stabilised RO ₂	53
4.3.7.1	Reaction with HO ₂	53
4.3.7.2	Reaction with NO	54
4.3.7.3	Reaction with other RO ₂ and NO ₃	55
4.3.7.4	Peroxy ring-closure	55

4.3.8	Fate of alkoxy radicals RO \cdot	56
4.3.9	Reaction of OH with major compounds	58
4.3.9.1	Methacrolein	58
4.3.9.2	isoprene	59
4.4	Reactions of O $_3$ with unsaturated VOC	60
4.4.1	General mechanism	60
4.4.2	Fate of Criegee intermediates	61
4.4.2.1	General	61
4.4.2.2	$\cdot\text{CH}_2\text{OO}\cdot$	63
4.4.2.3	$\text{CH}_3\cdot\text{CHOO}\cdot$	64
4.4.2.4	$\text{HOCH}_2\cdot\text{CHOO}\cdot$	64
4.4.2.5	$\text{HCO}\cdot\text{CHOO}\cdot$	65
4.4.2.6	$\text{HOOCH}_2\cdot\text{CHOO}\cdot$	65
4.4.2.7	$\text{HOCH}_2\text{C}(\text{OO}\cdot)\text{CH}_3$	65
4.4.2.8	$\text{HOOCH}_2\text{C}(\text{OO}\cdot)\text{CH}_3$	66
4.4.2.9	$\text{HCO}\cdot\text{C}(\text{OO}\cdot)\text{CH}_3$	66
4.4.2.10	$\text{CH}_3\text{C}(\text{O})\cdot\text{CHOO}\cdot$	67
4.4.3	Fate of stabilised Criegee Intermediates	68
4.4.4	Branching ratios and rate constants	68
4.4.5	Unsaturated hydroperoxides	69
4.5	Photolysis reactions	71
4.5.1	PAN	71
4.5.2	Glycolaldehyde	71
4.5.3	Methyl vinyl ketone and methacrolein	71
4.6	MCM extended	73
4.6.1	Version 1	73
4.6.2	Version 2	74
5	Enhanced isoprene oxidation	76
5.1	Unconstrained simulations	76
5.1.1	Simulation parameters	76
5.1.2	Case 1: NO $_x$ -free boundary layer	76
5.1.3	Case 2: NO $_x$ -rich boundary layer	79
5.1.4	Case 3: within the canopy	82
5.2	Box model constrained with field measurements	82
5.2.1	Simulation setup	82
5.2.2	Case 1: isoprene-poor troposphere	83
5.2.3	Case 2: isoprene-rich boundary layer	85
6	Conclusions and outlook	88
6.1	Conclusions	88
6.1.1	A new oxidation mechanism for 3D models	88
6.1.2	A new master oxidation mechanism	89
6.2	Outlook	90
6.2.1	Budgeting of OH recycling routes	90
6.2.2	New chemistry and the global atmospheric composition	90
6.2.3	Further mechanism development	91

6.2.4 Investigation of new routes	91
6.3 Catalytic oxidation in the atmosphere	92
A MIM2 mechanism	94
Bibliography	109

List of Figures

2.1	The OH-addition pathway in MIM2. The three short-lived peroxy radicals from isoprene are delimited by dashed lines. The branching ratios of each reaction are indicated in light blue.	10
3.1	Low-NO _x scenario: comparison of MCM, MIM, MIMvK and MIM2. . . .	17
3.2	Low-NO _x scenario: relative biases, 100*(mechanism-MCM)/MCM, of MIM, MIMvK and MIM2.	18
3.3	Mid-NO _x scenario: comparison of MCM, MIM, MIMvK and MIM2. . . .	20
3.4	Mid-NO _x scenario: relative biases, 100*(mechanism-MCM)/MCM, of MIM, MIMvK and MIM2.	21
3.5	High-NO _x scenario: comparison of MCM, MIM, MIMvK and MIM2. . . .	23
3.6	High-NO _x scenario: relative biases, 100*(mechanism-MCM)/MCM, of MIM, MIMvK and MIM2.	24
3.7	Alkyl nitrates in MIM2 under different NO _x -regimes	25
3.8	Nitrogen reservoirs in low-NO _x scenario. In all the plots the actual mixing ratios of each species are presented with MIMvK (black line), original MIM (red line), MIM2 (blue line) and MCM (green line). The alkyl nitrates shown here are the sum of all alkyl nitrates except NOA (shown separately).	27
3.9	Nitrogen reservoirs in mid-NO _x scenario. In all the plots the actual mixing ratios of each species are presented with MIMvK (black line), original MIM (red line), MIM2 (blue line) and MCM (green line). The alkyl nitrates shown here are the sum of all alkyl nitrates except NOA (shown separately).	28
3.10	Nitrogen reservoirs in high-NO _x scenario. In all the plots the actual mixing ratios of each species are presented with MIMvK (black line), original MIM (red line), MIM2 (blue line) and MCM (green line). The alkyl nitrates shown here are the sum of all alkyl nitrates except NOA (shown separately).	29
3.11	Organic peroxides other than CH ₃ OOH for all four mechanisms in this study under low-NO _x conditions. In all the plots the actual mixing ratios of each species are presented with MIMvK (black line), original MIM (red line), MIM2 (blue line) and MCM (green line). C ₃ -peroxides are not shown because MIM and MIMvK do not have any.	30
3.12	Organic peroxides other than CH ₃ OOH for all four mechanisms in this study under mid-NO _x conditions. In all the plots the actual mixing ratios of each species are presented with MIMvK (black line), original MIM (red line), MIM2 (blue line) and MCM (green line). C ₃ -peroxides are not shown because MIM and MIMvK do not have any.	31

3.13	Organic peroxides other than CH ₃ OOH for all four mechanisms in this study under high-NO _x conditions. In all the plots the actual mixing ratios of each species are presented with MIMvK (black line), original MIM (red line), MIM2 (blue line) and MCM (green line). C ₃ -peroxides are not shown because MIM and MIMvK do not have any.	32
3.14	Seasonal relative change 100*(MIM2-MIMvK)/MIMvk for OH (left panel) and isoprene (right panel).	33
3.15	Relative differences of the modified MIM2 for some major species under the low-NO _x scenario.	36
4.1	Ratio of observed to modelled OH mixing ratio during the GABRIEL campaign as a function of isoprene mixing ratio (Kubistin et al. (2008)).	39
4.2	Site specific addition of OH to different double bonds. The reactions are ordered according to the increasing stability of the resulting organic radicals, from primary to tertiary (Peeters et al. (2007)).	41
4.3	Tautomeric equilibrium between the two forms for the radical from the reaction of OH with hydroxyacetone.	51
4.4	Example of homogeneous gas-phase production of tetrols in isoprene oxidation involving reactions between peroxy radicals.	55
4.5	Competition between peroxy ring-closure and reactions with other radicals for one isomer of the peroxy radicals from isoprene under very low-NO _x . Numbers close to arrows are the (pseudo-)unimolecular rate constants for the reactions indicated.	56
4.6	General fate of alkoxy radicals from VOC oxidation (Atkinson, 1997a). The reaction frequencies shown are for atmospheric conditions at 298 K and 1 bar.	57
4.7	OH addition to isoprene, subsequent O ₂ addition and RO ₂ with relative yields for each isomer taken from Paulot et al. (2009a). The two pairs of RO ₂ in the upper and lower part of the graph are geometric isomers and treated in the mechanism as single species.	60
4.8	General mechanism of ozonolysis. The diradical species are the Criegee intermediates. R _i (i = 1, 4) can be either an alkyl radical or a H atom.	61
4.9	Criegee intermediates. a) Resonance between the diradical and the zwitterionic form. b) The conformers <i>syn</i> and <i>anti</i>	62
4.10	Possible fates of Criegee intermediates that are <i>anti</i> monosubstituted conformers (a) and <i>syn</i> monosubstituted and disubstituted conformers (b).	62
4.11	Quantitative decomposition of a simple Criegee intermediate.	66
4.12	Decomposition of a Criegee intermediate from ozonolysis of an isoprene hydroperoxides. The <i>syn</i> and <i>anti</i> conformers have final OH yields of 2 and 1, respectively.	67
4.13	Branching ratios for ozonolysis of generic alkenes.	69
4.14	Ozonolysis of one internally double bonded hydroperoxide for which the total OH yield is estimated to be higher than one (see text).	70
4.15	A general representation of epoxide formation from β hydroperoxide alkyl radicals above a tropical pristine forest.	73
4.16	1,5- and 1,6-H-shifts for isoprene derived peroxy radicals as proposed by Peeters et al. (2009).	74

5.1	Comparison of MCME v1 and v2 with MCM for a NO _x -free boundary layer.	77
5.2	Comparison of MCME v1 and v2 with MCM for a NO _x -rich boundary layer.	80
5.3	Comparison of MCME v1 and v2 with MCM for a within-canopy scenario.	81
5.4	Results for simulations constrained with GABRIEL measurements in the free troposphere for which isoprene is below the detection limit and assumed to be not present.	84
5.5	Results for simulations constrained with GABRIEL measurements in the boundary layer for which isoprene is about 3 nmol/mol. MCMEv2seg includes a 50% reduction of $k_{OH+C_5H_8}$	86
6.1	Molecular decompositions that could be theoretically investigated for further mechanism development.	92
A.1	A selection of the most prominent among the news species present now in MIM2. A comparison between MIM2 and MCM in the low-NO _x scenario is shown.	95
A.2	A selection of the most prominent among the news species present now in MIM2. A comparison between MIM2 and MCM in the mid-NO _x scenario is shown.	96
A.3	A selection of the most prominent among the news species present now in MIM2. A comparison between MIM2 and MCM in the high-NO _x scenario is shown.	97

List of Tables

2.1	Number of reactions and species for each mechanism.	9
3.1	Initial mixing ratios of species under the three scenarios here presented. . .	14
3.2	Diurnal averages for the 5th day of simulation for the cumulative loss of isoprene and RO ₂ (CH ₃ O ₂ included) and the relative differences between MCM and MIM2 for selected species.	16
4.1	Site-specific rate constants and group substituent factors of the extended SAR for OH addition to double bonds and comparison with Kwok and Atkinson (1995) (KA95). k are for 298 K and 1 bar and expressed in cm ³ molec ⁻¹ s ⁻¹ and F_a is unitless.	43
4.2	Parameters of the new SAR for H abstraction by OH and comparison with the one by Kwok and Atkinson (1995) (KA95). k_p , k_s and k_t are the rate constants for the -CH ₃ , -CH ₂ - and >CH- groups. They are given for 298 K and 1 bar and expressed in cm ³ molec ⁻¹ s ⁻¹ and F is unitless.	44
4.3	Comparison of predicted (this study and Kwok and Atkinson (1995)) with experimental rate constants (k_{OH}) for selected organic compounds at 298 K and 1 bar. k_{OH} is expressed in cm ³ molecule ⁻¹ s ⁻¹	45
4.4	Number of reactions and species for the MCME mechanism and comparison to the other ones considered in this study.	72
5.1	Initial mixing ratios of species under the three scenarios here used.	78
5.2	Measured OH concentrations and modeled-to-measured ratios for the different mechanisms after 20 minutes simulations time. MCMEv2seg include a 50% reduction in the rate constant of isoprene + OH.	85
A.1	MIM2 species. For the lumped species based on isomers in MCM only the condensed formulae are shown. For lumped species representing non-isomeric species the condensed formulae are not shown.	98
A.1	MIM2 species (continued)	99
A.2	Composition of lumped species in MIM2 is given in terms of MCM species.	100
A.3	List of MIM2 reactions. The expressions for the simple MCM rate coefficients (KRO2NO, KRO2HO2, KAPHO2, KAPNO, KRO2NO3, KNO3AL) are shown in Tab. A.4. The expressions for the complex MCM rate coefficients (KFPAN, KBPAN and KMT16) are shown in Tab. A.5. M is the concentration of air in molec cm ⁻³ and T is the temperature in K.	101
A.3	MIM2 reactions (continued)	102
A.3	MIM2 reactions (continued)	103
A.3	MIM2 reactions (continued)	104
A.3	MIM2 reactions (continued)	105

A.3	MIM2 reactions (continued)	106
A.4	MCM simple rate constants. T is the temperature in K.	107
A.5	Parameters for the MCM complex rate constants used in MIM2. M is the concentration of air in molec cm ⁻³ and T is the temperature in K.	107
A.6	Photolysis Parameters (l, m and n) from MCM and used in the box model evaluation (Saunders et al., 2003). They J-values (in s ⁻¹) are computed with the expression $J = l \times (\cos(\theta))^m \times \exp(-n \sec(\theta))$, where θ is the solar zenith angle.	108

Abbreviations

BVOC	B iogenic V olatile O rganic C ompound
MIM	M ainz I soprene M echanism
MIMvK	M ainz I soprene M echanism von K uhlmann's version
MIM2	M ainz I soprene M echanism 2
MCM	M aster C hemical M echanism
MCMEv1	M aster C hemical M echanism E xtended version 1
MCMEv2	M aster C hemical M echanism E xtended version 2
SOA	S econdary O rganic A erosol

Chapter 1

Introduction

1.1 Isoprene from vegetation

The terrestrial vegetation acts as a source of biogenic volatile organic compounds (BVOCs), which are of widely recognized importance for atmospheric chemistry and climate. Isoprene (2-methyl-1,3-butadiene, C_5H_8) and monoterpenes (made up of two isoprene units) are among the most important BVOCs. Globally, isoprene dominates the emissions by far and strongly affects the composition of the troposphere. Its emissions depend strongly on temperature and light ([Fehsenfeld et al. \(1992\)](#)). Global emission estimates of isoprene are in the range 410–680 Tg/yr (362–601 Tg(C)/yr) ([Müller et al. \(2008\)](#) and [Arneth et al. \(2008, and references therein\)](#)). Given the magnitude of its emissions, isoprene is considered the dominant BVOC emitted into the atmosphere.

1.2 Role in the Earth system

BVOCs play numerous roles in the Earth system and provide interlinkages between its biological, chemical and physical components. Initially, the biological role of isoprene was not very well understood and thought to be basically conferring thermo-tolerance to plants by interacting with the membranes of the plant ([Sharkey and Singaas \(1995\)](#), [Sharkey et al. \(2001\)](#), [Singaas et al. \(1997\)](#)). Then its role in protecting plants from O_3 and H_2O_2 was discovered ([Loreto and Velikova \(2001\)](#), [Loreto et al. \(2001\)](#)). It was also reported that isoprene plays a role in the plant-insect interactions ([Laothawornkitkul et al. \(2008a,b\)](#), [Loivamäki et al. \(2008\)](#)). [Niinemets et al. \(2004\)](#) proposed that isoprene has a protective role, acting as a metabolic “safety valve”. This view is also supported by the emissions of a BVOC being largely controlled by its own physicochemical properties like solubility and volatility ([Penuelas and Llusà \(2004\)](#)).

Isoprene oxidation by OH can, in the presence of sufficient NO_x , lead to the formation of O_3 in the troposphere allowing the oxidation of NO to NO_2 without removal of an O_3 molecule (Atkinson and Arey (2003b)). Under low- NO_x conditions a net consumption of O_3 takes place. Nitrogen-containing products like nitrates are recognized as important in the long-range transport of NO_x in the atmosphere. Nitrates from isoprene oxidation represent a large fraction of the atmospheric organic N-reservoir. Recently, alkyl nitrates from isoprene have been shown to be taken up by foliage and incorporated into the leaf amino acids (Lockwood et al. (2008)). This may be the basis for a potentially significant role of isoprene, helping nitrogen-limited forests sequestering nitrogen from the atmosphere and provide a self-fertilizing mechanism.

Isoprene not only influences gas phase atmospheric chemistry, but can also lead to the formation of Secondary Organic Aerosols (SOAs). The mechanisms by which BVOC oxidation may lead to SOAs in clean air are still not fully understood (Kulmala (2003)), but it is clear that BVOC oxidation products generally have lower vapour pressures than the primary compounds, and so may more readily condense on pre-existing molecular clusters. Recent field and laboratory evidence indicates that the oxidation of isoprene forms SOA (Carlton et al. (2009, and references therein)). Global biogenic emissions of isoprene are sufficiently large that the formation of SOA in even small yields would result in substantial production of atmospheric particulate matter. Aerosols directly affect climate by scattering solar radiation. They also indirectly alter the Earth's radiative balance by acting as cloud condensation nuclei, changing cloud albedo and the degree of cloud cover, so potentially leading to net cooling of the Earth's surface during the day. Although it is known that a substantial fraction of the aerosol particles in remote regions is organic material, and that the oxidation of BVOCs may lead to the formation of SOAs, it is not yet clear how important SOA formation is in altering the climate system. There is the possibility that SOA formation from BVOC emissions cools the Earth and so moderates temperature dependent BVOC emission from plants. On the other hand, a recent study showed how new particle formation in forests is inhibited by isoprene emissions (Kiendler-Scharr et al. (2009)). Hence, there is the potential for feedbacks between BVOC emissions, SOA and climate. Therefore, a comprehensive knowledge of isoprene chemistry is essential to understand the role of isoprene in the Earth system, since atmospheric oxidation is the link between the biological and climatic roles of isoprene.

1.3 Isoprene oxidation chemistry

1.3.1 Experimental work

The main oxidation pathways of isoprene are reactions with OH, O₃ and NO₃, with the OH-pathway being by far the most important. This is due to the high reaction rate with OH and to the coincidence of the strong light- and temperature-dependent emissions (Fehsenfeld et al. (1992), Yokouchi (1994)) with the peak in OH concentrations during the day. Many experimental studies have been conducted so far, and product yields for many species, with and without NO_x, have been determined. For instance, the OH-pathway has been investigated extensively in a number of studies (Benkelberg et al. (2000), Kwok et al. (1995), Lee et al. (2005), Miyoshi et al. (1994), Paulot et al. (2009a,b), Paulson et al. (1992a), Ruppert and Becker (2000), Sprengnether et al. (2002), Tuazon and Atkinson (1990a)). Fewer studies on the stable products from the O₃-pathway have been performed (Aschmann and Atkinson (1994), Atkinson et al. (1994), Grosjean et al. (1993), Paulson et al. (1992b), Sauer et al. (1999)), while a number of studies focused specifically on the OH-yields (Atkinson et al. (1992), Gutbrod et al. (1997), Lewin et al. (2001), Neeb and Moortgat (1999), Paulson et al. (1998), Rickard et al. (1999)). Chemical properties have been determined for only a few oxidation products (Atkinson et al. (2006)). A substantial fraction of the global isoprene production occurs in regions of the Southern Hemisphere where NO mixing ratios are below 60 pmol/mol (Emmons et al. (1997), Müller et al. (2008), Torres and Buchan (1988)). Under these conditions, after HCHO, the organic hydroperoxides (ROOH) are the next most abundant products, with a maximum product yield ranging between 32 and 48% (Benkelberg et al. (2000), Jenkin et al. (1997)). Their chemical properties have not been measured yet, but they are predicted to be very reactive and critical to adequately represent the isoprene chemistry in low-NO_x conditions. Other important products under all NO_x-regimes are methy vinyl ketone (MVK), methacrolein (MACR), C₅-carbonyls, glycolaldehyde, glyoxal, hydroxyacetone and methylglyoxal.

1.3.2 Oxidation mechanisms

The knowledge of isoprene chemistry is still incomplete, many uncertainties remain, and only a few detailed isoprene mechanisms exist. Three of them are described in Fan and Zhang (2004), Madronich and Calvert (1989) and Carter and Atkinson (1996), with the last one being evaluated against a chamber study (Carter (2000)). Another detailed mechanism of isoprene oxidation is included in the Master Chemical Mechanism (MCM v3.1) (Jenkin et al. (1997), Saunders et al. (2003)). It can be freely accessed at the

website: <http://mcm.leeds.ac.uk/MCM>. This isoprene mechanism is highly explicit, providing a description of the complete degradation of isoprene and its degradation products, initiated (where appropriate) by reaction with OH, O₃, NO₃ and photolysis. However, it already contains some level of reduction compared with the related subset mechanisms of Jenkin and Hayman (1995) and Jenkin et al. (1998), which treat the OH-initiated degradation to first generation products in greater detail. The reduction in the MCM of the more detailed chemistry consisted of neglecting the formation of two minor hydroxy peroxy radicals from the OH-addition pathway, which together represent about 10% of the reaction products.

Recently, the MCM has been evaluated against NO_x-air chamber experiments (Pinho et al. (2005)). Moreover, it has been applied in many recent field studies (Biesenthal et al. (1998), Carslaw et al. (1999a, 2001), Warneke et al. (2001), Williams et al. (2001)). However, detailed mechanisms like the MCM are not suitable for global atmospheric chemistry simulations due to computational limitations, and a reduced mechanism must be employed, although this is known to lead to loss of accuracy and information (Carslaw et al. (1999b), Whitehouse et al. (2004a,b, and references therein)). Moreover, inaccuracies in the representation of important intermediate species adds further uncertainties to 3-D atmospheric models due to the interplay between chemistry, transport and deposition. Therefore, assessments of all these uncertainties in the models must be performed. In this work we re-evaluate the Mainz Isoprene Mechanism (MIM, Pöschl et al. (2000)), which is an earlier reduction of MCM. We present and evaluate a new reduced mechanism of intermediate size for isoprene, which we call MIM2. We show that, unlike MIM, MIM2 preserves the basic features of the corresponding detailed mechanism and shows similar nonlinear behaviour. A set of reduction principles that form the basis of its development is presented in Chapter 2. A box model evaluation of MIM2 and MIM against MCM for three NO_x scenarios is presented in Chapter 3. Despite their complexity, MIM2 as well as MCM have substantially underestimated the HO_x levels during a field campaign in a pristine environment with intense vegetation (Butler et al. (2008), Kubistin et al. (2008), Lelieveld et al. (2008), Martinez et al. (2008)). In the past such underestimation has been thought to be related to the presence of unknown very reactive BVOCs that would react with O₃ and produce OH (Tan et al. (2001)). Here another approach to resolve this model-observation discrepancy is taken. In such environments isoprene is the largest sink for OH in the boundary layer. Furthermore, the current detailed isoprene oxidation mechanisms represents a rather old and limited experimental knowledge. Therefore, an alternative hypothesis is advanced. The OH sink due to isoprene has been largely overestimated, that is OH might be recycled to a substantial extent during oxidation. To examine this, a very detailed oxidation mechanism has been developed and presented in Chapter 4. Finally in Chapter 5 the new mechanism is tested

in a box model in both the free mode and constrained to field measurements. In contrast to MCM, substantial improvements for HO_x and other intermediates are shown. Implications for the atmospheric composition and biosphere-atmosphere exchanges are also discussed. Finally, the results are summarized and an outlook for future research is presented in Chapter 6.

Chapter 2

Mainz Isoprene Mechanism 2: Development

2.1 Background

The chemistry of terpenes (e.g. isoprene and monoterpenes) has a large range of oxidation reaction pathways and products (Atkinson and Arey (2003a,b)). To our knowledge, all VOC oxidation mechanisms employed in global atmospheric chemistry models neglect most of the products and isomers arising from terpene oxidation (Brasseur et al. (1998), Folberth et al. (2006), Geiger et al. (2003), Horowitz et al. (2007), Houweling et al. (1998), von Kuhlmann et al. (2004), Wang and Shallcross (2000), Wang et al. (1998)). Furthermore, mechanisms like MIM often include lumped species which represent many compounds, sometimes with very different chemical structures and properties. Thus, they fail to reproduce the nonlinear behaviours of its tropospheric chemistry under different conditions, e.g., differences in product yields in the absence and presence of NO_x (Jenkin et al. (1998), Ruppert and Becker (2000)). For example, MIM considers only one product for each class of C_5 - and C_4 -compounds: one carbonyl species instead of four isomers, two alkyl nitrates instead of eight compounds and one hydroperoxide instead of four isomers. It can only poorly reproduce the experimental results or the diurnal cycle of the total nitrates (see Sect. 3.6.1). MIM, as well as many other condensed mechanisms, has to be taken as an entity without changing individual rate constants or reaction products. For instance, while the average MCM alkyl nitrate yield is 10%, in MIM a 4.4% yield based on an experimental study by Chen et al. (1998) was adopted and the results were tuned accordingly. Afterwards, von Kuhlmann et al. (2004) increased this yield in MIM to 12% following Sprengnether et al. (2002), which we have found leads to undesirable side effects on the results of the mechanism (see Sect. 3). Changing such

yields in MIM was accepted only because of the large experimental uncertainties in the literature, with estimates ranging between 4.4 and 15% (Chen et al. (1998), Giacomelli et al. (2005), Patchen et al. (2007), Sprengnether et al. (2002)). However, we note that modifications of a highly-tuned reduced mechanism like MIM, or usage of any subset of its reactions, can lead to serious misinterpretation of either field or experimental data. Nevertheless, to date there have been several applications of such modified version of MIM. There are two global atmospheric chemistry models, MATCH-MPIC (Lawrence et al. (2003), von Kuhlmann et al. (2003)) and ECHAM5/MESSy (Jöckel et al. (2006), Pozzer et al. (2007)) in which this modified MIM was included. Moreover, 19 out of the 44 reactions of MIM were used to update the isoprene mechanism of the well-established mechanism RACM (Stockwell et al. (1997)) and were tested against a chamber study (EUPHORE) (Geiger et al. (2003)). This mechanism was then used to analyse long-term measurements of atmospheric OH concentrations (Rohrer and Berresheim (2006)). After a slight modification, the mechanism was used to perform a product and a kinetic study of isoprene chemistry with the SAPHIRE chamber (Karl et al. (2006)).

2.2 Reduction principles

Keeping in mind the background described above, the following principles for mechanism reduction have been conceived and adopted for designing MIM2:

1. **Take the MCM for isoprene as the reference (Saunders et al. (2003, and references therein)), with any errors or omissions it may contain.**
2. **Consider only C₂–C₅-species to be isoprene-related and hence belonging to the reduced mechanism.**
3. **Make the mechanism detailed enough to accurately reproduce the diurnal cycle of important intermediate species like carbonyls, hydroperoxides and alkyl and peroxy acyl nitrates.** This is expected to be of relevance in order to properly simulate the atmospheric composition with 3-D models where transport and dry and wet deposition of species play a key role. MIM was intended to perform well in reproducing the concentrations of O₃, OH, NO_x, H₂O₂, CH₃OOH, CO and isoprene. While this generally works well, it will be shown in Sect. 3 that its biases with respect to MCM are sometimes significant even for these species.
4. **Include any isoprene oxidation products which can be measured using modern instrumentation, and any other species which represent significant minor pathways but were neglected in previous mechanisms.**

Such species are glyoxal, glycolaldehyde, propene, acetaldehyde, α -nitrooxy acetone, C₅-hydroperoxides, diols, and C₅-carbonyls. Recently, measurements of oxygenated organics during field campaigns and in laboratory experiments have become widespread (Sinreich et al. (2007), Volkamer et al. (2005), Williams et al. (2001); de Gouw and Warneke (2007, and references therein)). For glyoxal, a species absent in MIM, satellite retrievals have recently become possible and are becoming more reliable (Myriokefalitakis et al. (2008), Wittrock et al. (2006)).

5. **Neglect long-lived species only if they are formed in very small amounts (<30 pmol/mol under all NO_x regimes studied).** This principle ensures that their elimination from the mechanism does not significantly affect species like O₃ and OH. For instance this was the case for some peroxy acyl nitrates like the MCM species GLYPAN and C4PAN6.
6. **Substitute all the species which react quickly at frequencies greater than 1 s⁻¹ with the respective products of the major loss pathway.** The species satisfying such principle are the Criegee biradicals (see Sect. 2.5) and alkoxy radicals with typical lifetimes being less than 1 s. Whitehouse et al. (2004a) successfully applied a similar principle for all species that are set to decompose at a rate of 10⁶ s⁻¹ in MCM. This was based on the idea that the long term behaviour of a chemical mechanism can be accurately represented by assuming that the faster time-scales equilibrate with respect to the slower ones.
7. **Lump species that are always in a nearly constant ratio and have very similar reactivities.** Species that react through the same paths, in reactions with same rate coefficients, can be lumped together without any loss of accuracy to the mechanism (Whitehouse et al. (2004b)). Moreover, the loss of accuracy is small when species with very similar reactivities are lumped together. Hence, in this study, every lumped species is assumed to have reactivities and products equal to the corresponding weighted averages of the respective components. For an example see Sect. 2.4.
8. **Adopt the MCM nomenclature and give lumped species a name starting with L and being as similar as possible to the MCM names of the species it represents.**

Designing MIM2 with such principles in mind has led to a mechanism that allows further mechanism development building directly on MIM2, which is not possible with MIM or most other contemporary reduced mechanisms. It is thus straightforward to test the effects of any new laboratory kinetic developments in atmospheric chemistry models using MIM2. Moreover, the fairly large number of C₂–C₅-species included in MIM2 allows

TABLE 2.1: Number of reactions and species for each mechanism.

Mechanism	Stable species ^a	Species ^a	Reactions ^b
MCM	150	180	583(+12)
MIM	12	15	42(+2)
MIM2	53	68	195(+4)

^a Note that only C₂–C₅ species have been taken into account.

^b Inside the parentheses are the number of photolysis reactions of PAN-like compounds that must be included when modeling the upper troposphere.

global models like ECHAM5/MESSy (Jöckel et al. (2006)) to include rather detailed organic aqueous-phase chemistry, which appears to be potentially important by often acting as a strong sink for trace gases like glyoxal (Carlton et al. (2007), Hastings et al. (2005), Loeffler et al. (2006), Volkamer et al. (2007)) and MVK and MACR (Chen et al. (2007)), and which may also have implications for cloud microphysics (Nenes et al. (2002)).

2.3 The whole mechanism

The size of MIM2 with respect to MCM and MIM is presented in Table 2.1.

MIM2 consists of 69 species, of which 53 are long-lived and hence need to be transported in atmospheric chemistry models (see Table A.1). These species are involved in 178 reactions (see Table A.3). When implemented in 3-D atmospheric chemistry models, photolysis reactions of the 4 peroxy acyl nitrates must be added. These photolysis reactions are not considered in MCM because it was designed to simulate the lower troposphere. However, the photolysis of peroxy acyl nitrates can become the dominant sink in the upper troposphere (Nizkorodov et al. (2005), Talukdar et al. (1995)).

2.4 The OH-pathway

Under atmospheric conditions the OH-addition pathway for isoprene oxidation is by far the most important. The MCM considers the production of only four isomers of peroxy radicals, RO₂, which is a reduction of an even more detailed mechanism (Jenkin and Hayman (1995), Jenkin et al. (1998)) that takes into account six possible isomers. In Fig. 2.1 a flow diagram illustrating the OH-pathway is shown.

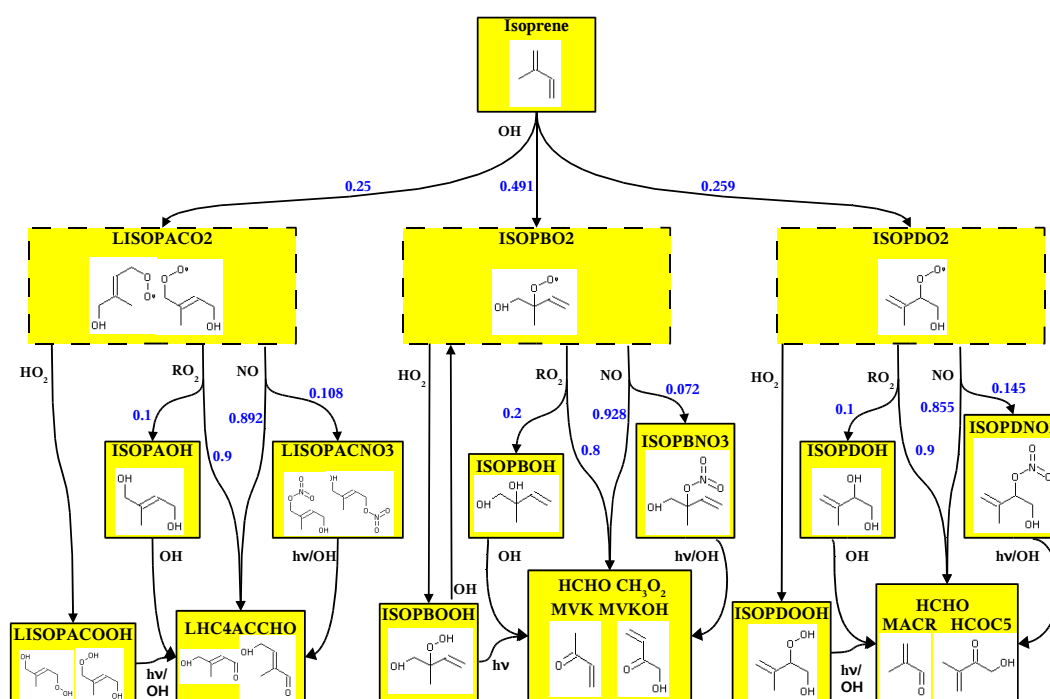


FIGURE 2.1: The OH-addition pathway in MIM2. The three short-lived peroxy radicals from isoprene are delimited by dashed lines. The branching ratios of each reaction are indicated in light blue.

MIM2, as well as MCM, implicitly assumes the OH-addition to occur only at position 1 and 4 with branching ratios being 0.655 and 0.345, respectively. The O_2 -addition to the resulting alkyl radicals is assumed to be instantaneous. MIM2 considers the production of three different kinds of peroxy radicals (RO_2), namely LISOPACO2, ISOPBO2 and ISOPDO2. They react with NO, NO_3 , HO_2 and RO_2 according to the MCM protocol (Jenkin et al. (1997), Saunders et al. (2003)). Unlike MIM, MIM2 retains the permutation reaction formalism adopted in MCM and the production of diols from such reactions. It is a simplified parameterization in which each RO_2 reacts with a pool of $R'O_2$ at a pseudo-first-order rate (Madronich and Calvert (1990)). The average alkyl nitrate yield from $RO_2 + NO$ reactions in MIM2 is 10%, as in the MCM. The yields of single isomers depend on the structure and are quite uncertain, and MIM2 enables sensitivity studies changing such yields. The species represented by LISOPACO2, namely ISOPAO2 and ISOPCO2, are not produced in equal amounts in MCM v3.1, but simulation tests showed that the corresponding products are always in a ratio of about 1:1. Since these species have identical reactivity and structurally similar products, the products have been lumped in LISOPACOOH (a lump of ISOPAOOH and ISOPCOOH), LHC4ACCHO and LISOPACNO3. They are the only first generation products that are lumped, where the term first generation denotes the first long-lived species produced in

the oxidation chain. In summary, the first generation products from the OH-pathway in MIM2 are:

- Hydroperoxides: LISOPACOOH, ISOPBOOH and ISOPDOOH
- Carbonyls: LHC4ACCHO, MVK, MVKOH, MACR and HCOC5
- Diols: ISOPAHOH, ISOPBOH and ISOPDOH
- Alkyl nitrates: LISOPACNO3, ISOPBNO3 and ISOPDNO3

2.5 O₃-pathway

The ozonolysis of alkenes generates carbonyls and energetic Criegee biradicals (Atkinson and Arey (2003a)). The fate of such biradicals is described in Jenkin et al. (1997) as being a relaxation process that can yield significant amounts of OH. It consists mainly of decomposition to different products and of the production of a “thermalized” Criegee biradical. The branching ratios of such relaxation processes change according to the functional groups present and to the size of the molecule. OH is only produced in one of these decompositions, namely the hydroperoxide channel (Niki et al. (1987)). These thermalized biradicals in MCM are considered to react with H₂O, CO, NO, NO₂ and SO₂. For this, MIM2 follows the MCM protocol very closely. Since these relaxation reactions are very fast (higher than 1 s⁻¹) compared to the typical integration time step of 3-D models (≈30 min.), MIM2 assumes that all ozonolysis reactions directly yield the corresponding final products. The thermalized Criegee biradicals are assumed to react only with H₂O since this is the predominant fate under tropospheric conditions (Jenkin et al. (1997)).

2.6 The NO₃-pathway

For the oxidation of isoprene by NO₃ MIM2 follows MCM closely until LISOPACNO3 and NC4CHO are formed. Only the reaction of the peroxy radical NISOPO2 (from ISOP + NO3) with NO₃ is neglected. It is worth noting that this radical was represented in MIM by the lumped species ISON (see Sect. 3.6.1), being treated as a long-lived species and not like an RO₂. Finally, the peroxy radicals from this pathway are treated similarly to the ones from the OH-pathway.

2.7 Unsaturated C₅–C₄-products

The treatment of hydroperoxides, diols and alkyl nitrates was discussed above in Sect. 2.4. Except for two species being lumped (LISOPACOOH and LISOPACNO₃), their chemistry strictly follows MCM. Here we discuss the treatment of two other important C₄–C₅ groups.

2.7.1 Aldehydes

With respect to MACR (methacrolein) and its products like PAN, MIM2 follows MCM closely. The fate of the C₅- δ -hydroxy-carbonyls (LHC4ACCHO) is considered to be the average of the equally weighted reactions for HC4ACHO and HC4CCHO (MCM species). The OH-pathway for NC4CHO produces the lumped species LNISO₃, consisting of equal parts of NC4CO₃ (carboxylic RO₂) and C510O₂ (alkyl RO₂). The subsequent reactions result from averaging both reactivities and product yields.

2.7.2 Ketones

For the chemistry of MVK (methyl vinyl ketone) MIM2 does not neglect any products. The OH-addition to it results in the production of a lumped species, LHMVKABO₂, having the composition 0.3 HVMKAO₂ + 0.7 HVMKBO₂ (MCM species). A similar treatment is followed for MVKOH, and almost all the corresponding products are taken into account. However, a product of MVKOH photolysis, ALLYLOH (2-propen-1-ol), is neglected. The only C₅-ketone, HCOC₅, is treated like in MCM.

2.8 C₃–C₂-products

The chemistry of C₃–C₂ products in MIM2 is explicit and close to MCM. Species like methylglyoxal and hydroxyacetone are not lumped together with other species as was the case in MIM. New species like propene, nitrooxy acetone, glycolaldehyde, and glyoxal are present. In the case of propene the minor products of OH- and NO₃-addition, namely IPROPOLO₂ and PRONO3AO₂, are neglected since they behave similarly to the more abundant products. The peroxy acyl nitrate GLYPAN from glyoxal is neglected because it is found to be below 30 pmol/mol under all NO_x conditions studied.

Chapter 3

Mainz Isoprene Mechanism 2: Evaluation

3.1 Box model setup

The box model MECCA (Sander et al. (2005)) was used for this study. The model includes a kinetic preprocessor which automatically generates optimized Fortran90 code for the specific set of reactions. KPP-2.1 (Sandu and Sander (2006)), and the Rosenbrock 3rd order solver was used (Sandu et al. (1997)). From the comprehensive set of reactions, a subset of tropospheric gas-phase reactions was selected. Reactions of sulfur and halogen species were switched off in the model simulations. The box is considered to be 1 km long on each side and to be representative of the boundary layer. All the simulations start on 1st August 2000, at midnight and the latitude is set to 10° S, corresponding roughly to the Amazon forest. The relative humidity and the pressure are set to be 70% and 101 325 Pa respectively. A diurnal cycle for light and temperature was applied. The function used for the temperature cycle is a sinusoidal (Heard et al. (1998)) with values varying between 294 and 308 K and an average of 301 K:

$$T = 301 + 7 \times \sin\left(\frac{2\pi}{86400} \times t - 1.9635\right) \quad (3.1)$$

where t is the time in seconds. The photolysis rates from MCM v3.1 are used (Saunders et al. (2003)) for MCM, MIM and MIM2, while the solar zenith angle dependency used was the one included in MECCA. Only species that are not lumped in any of the mechanisms studied here were initialized with non-zero mixing ratios (see Table 3.1).

For simplicity the initialization does not change in any of the NO_x scenarios presented here. The isoprene flux was calculated using the equations given in Guenther

TABLE 3.1: Initial mixing ratios of species under the three scenarios here presented.

Species formula	initial mole fraction (mol mol ⁻¹)
H ₂ O	0.01851
O ₃	30 × 10 ⁻⁹
H ₂ O ₂	7 × 10 ⁻⁹
NH ₃	100 × 10 ⁻¹²
NO ₂	100 × 10 ⁻¹²
NO	10 × 10 ⁻¹²
HONO	40 × 10 ⁻¹⁴
HNO ₃	5.0 × 10 ⁻¹²
CH ₄	1.8 × 10 ⁻⁰⁶
HCHO	5.0 × 10 ⁻⁰⁹
CO	100 × 10 ⁻⁰⁹
CH ₃ OH	500 × 10 ⁻¹²
CH ₃ OOH	4.0 × 10 ⁻⁰⁹
HCOOH	350 × 10 ⁻¹²
CH ₃ C(O)O ₂ NO ₂ (PAN)	100 × 10 ⁻¹²
CH ₃ CO ₂ H	2.0 × 10 ⁻⁰⁹
CH ₃ CO ₃ H	1.5 × 10 ⁻⁰⁹
CH ₃ COCH ₂ OH	4.0 × 10 ⁻⁰⁹
CH ₃ COCHO	500 × 10 ⁻¹²
C ₅ H ₈ (isoprene)	2.0 × 10 ⁻⁰⁹

et al. (1995) and assuming an average photosynthetically active radiation (PAR) flux of 1000 $\mu\text{mol m}^{-2} \text{s}^{-1}$. The maximum isoprene flux reached at noon was 7.887×10^{11} molecule $\text{cm}^{-2} \text{s}^{-1}$. Guenther et al. (2006) present a more sophisticated calculation of the isoprene emission depending on many more parameters compared to the one presented in Guenther et al. (1995). However, the differences in global estimates are 67 Tg/yr, well below the uncertainty range of the estimates themselves. Moreover, for a box model evaluation of mechanisms for isoprene oxidation any emission function can be used. The use of such a function serves the purpose of having a diurnal cycle for the isoprene emission that is not far off from reality. The base NO flux was constant and equal to 3.33×10^9 molecule $\text{cm}^{-2} \text{s}^{-1}$. Three main NO_x scenarios were examined. One is the base emission scenario noted above and the other two are 10 and 100 times higher than the base emission rate, respectively. They will be referred to as, the low-, mid- and high-NO_x scenarios, respectively. Besides the isoprene and the NO_x emissions, no further emission or deposition of species was included in the simulations.

As can be seen in Figs. 3.1, 3.3 and 3.5, a comparison of three reduced mechanisms versus MCM is performed. These mechanisms are:

- MIM2 (this study)
- MIM (Pöschl et al. (2000)).
- MIMvK, which is MIM as implemented in Sander et al. (2005) and Jöckel et al. (2006). This version differs from the original one with the alkyl nitrate yield being increased from 4.4% to 12% as assumed by (von Kuhlmann et al. (2004)) based on (Sprenghether et al. (2002)) and with a few updates of the rate constants.

3.2 Oxidation pathways of isoprene and RO₂

The destruction of isoprene and all its peroxy radicals has been budgeted and the corresponding cumulative losses are shown in Table 3.2.

The most important oxidation pathway for isoprene is reaction with OH, ranging between ≈ 68 and 80% of the total loss depending on the NO_x mixing ratios. Reaction with O₃ is relatively more important in low-NO_x conditions ($\approx 31\%$). Finally, the reaction with NO₃ turns out to account for less than 1% of the total isoprene loss in unpolluted environments but it can exceed 10% in high-NO_x regimes.

The largest loss for the peroxy radicals in low-NO_x conditions is the reaction with HO₂ ($\approx 51\%$), while under high-NO_x conditions the reaction with NO predominates ($\approx 75\%$). Reactions with NO₃ are not very important under any of the conditions studied, though they can account for about 4% of the total loss under high-NO_x conditions. It is worth noting that the self- and cross-reactions (RO₂ + R'O₂) account for about 25% of the total loss in low-NO_x. This confirms the importance of such reactions in the oxidation of organics in the gas-phase as indicated previously by Madronich and Calvert (1990).

3.3 Low-NO_x regimes

3.3.1 MCM behaviour

In this scenario the NO emission rate was set to be 3.33×10^9 molecule cm⁻² s⁻¹. In Fig. 3.1 the mixing ratios of the most important tracers are shown. The ozone mixing ratio shows that the chemical system is close to the turning point between the O₃-producing (mid-NO_x) and O₃-depleting (low-NO_x) regimes. OH and isoprene have reached an approximate photostationary state after 5 days, with maximum values of about $6.5 \cdot 10^5$ molecule cm⁻³ and 6 nmol mol⁻¹, respectively.

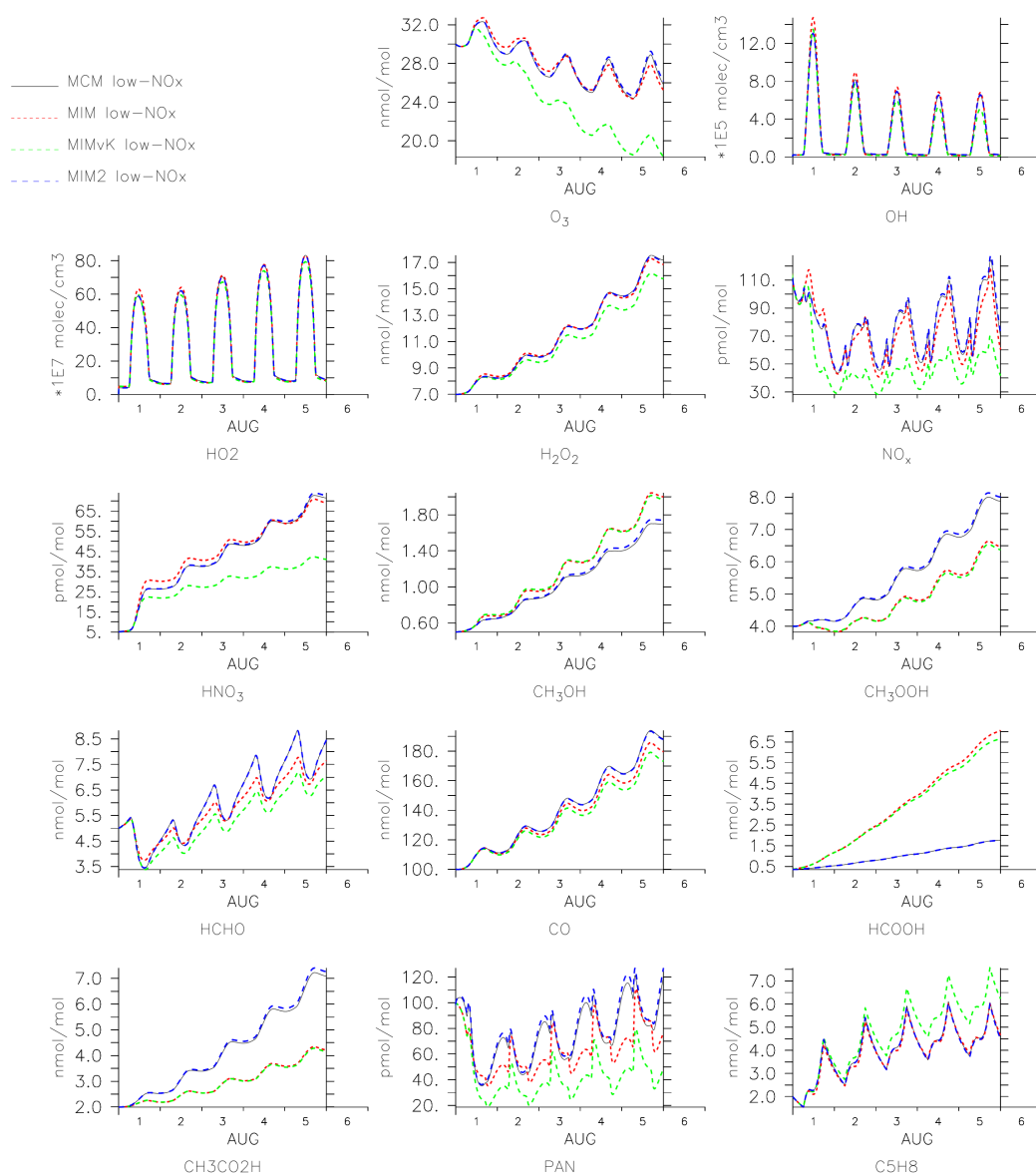
TABLE 3.2: Diurnal averages for the 5th day of simulation for the cumulative loss of isoprene and RO₂ (CH₃O₂ included) and the relative differences between MCM and MIM2 for selected species.

	low-[NO _x]	mid-[NO _x]	high-[NO _x]
scenario parameters			
NO emiss. (cm ⁻² s ⁻¹)	3.33 × 10 ⁹	3.33 × 10 ¹⁰	3.33 × 10 ¹¹
[NO _x]max (nmol mol ⁻¹)	0.128	0.765	5.066
Isoprene losses (%)			
L _{OH}	67.86	72.63	79.50
L _{O₃}	31.26	19.26	8.091
L _{NO₃}	0.8833	8.110	12.41
RO ₂ losses (%)			
L _{NO}	24.46	50.34	75.22
L _{HO₂}	50.51	35.97	16.78
L _{R^oO₂}	25.02	13.42	3.660
L _{NO₃}	<0.01	0.2678	4.338
average relative biases			
100*(MIM2-MCM)/MCM (%)			
O ₃	1.115	1.095	-0.6258
OH	1.388	1.834	4.400
HO ₂	-0.9017	-0.1166	4.482
H ₂ O ₂	-0.3620	-0.3668	0.5766
NO	-0.4443	-2.771	-150.1 ^a
NO ₂	2.422	1.240	2.125
HNO ₃	1.561	3.338	0.3348
CH ₃ OH	2.472	1.782	1.760
CH ₃ OOH	1.525	1.079	2.140
HCHO	0.07727	-0.8609	-0.8305
CO	-0.2780	-0.3393	-0.8868
HCOOH	-0.4829	-1.368	-1.665
CH ₃ CHO	2.377	-4.131	-5.217
CH ₃ CO ₂ H	2.312	1.961	1.929
PAN	5.574	3.436	2.890
HOCH ₂ CHO	8.901	-1.681	-2.993
GLYOX	-1.800	-0.8294	11.49
C ₃ H ₆	-0.6624	-2.563	-0.8083
NOA	1.073	2.015	2.600
ACETOL	-0.4158	0.4043	3.176
MGLYOX	5.285	2.793	3.166
MPAN	1.963	0.1996	-0.1643
MVK	0.1867	-1.471	-0.5412
MACR	-0.1962	-1.506	-1.714
ISOPBOH	0.9588	-0.3463	-0.1618
ISOPBOOH	-0.7308	-1.788	-0.8294
ISOPBNO ₃	0.3808	-1.932	-2.417
ISOPDOH	0.2964	-0.1322	-3.129
ISOPDOOH	-1.446	-1.643	-4.978
ISOPDNO ₃	-0.1476	-1.885	-3.888
NC ₄ CHO	2.569	-0.5616	-2.098
C ₅ H ₈	-1.137	-4.022	62.40 ^a

^a The value has little significance as it was found to be result of very small absolute biases at night when the concentrations of the tracer are close to zero.

3.3.2 MIM2 and MIM behaviour and biases

In Fig. 3.2 the biases relative to MCM for the species presented in Fig. 3.1 are shown. MIM2, unlike MIM, is mass-conserving with respect to carbon, as can be seen from the CO and HCHO mixing ratios. For instance, in MIM there is the following non-mass

FIGURE 3.1: Low-NO_x scenario: comparison of MCM, MIM, MIMvK and MIM2.

conserving reaction,



with a rate constant $k=10^{-10} \text{ cm}^3 \text{ molecule}^{-1} \text{ s}^{-1}$. In this reaction ISO₂H is a C₅-hydroperoxide and MACR reacts as a lumped C₄-carbonyl within the mechanism. Moreover, the ozonolysis of isoprene and MACR is not mass-conserving in MIM either. In these two reactions, product yields account for only 4.28 C atoms instead of 5, and 3.57 instead of 4, respectively. These are not the only reactions in MIM where carbon mass disappears. The contribution of isoprene oxidation to CO production in the atmosphere has been estimated by [Kanakidou and Crutzen \(1999\)](#) to be 330 Tg/yr, about 13.5%

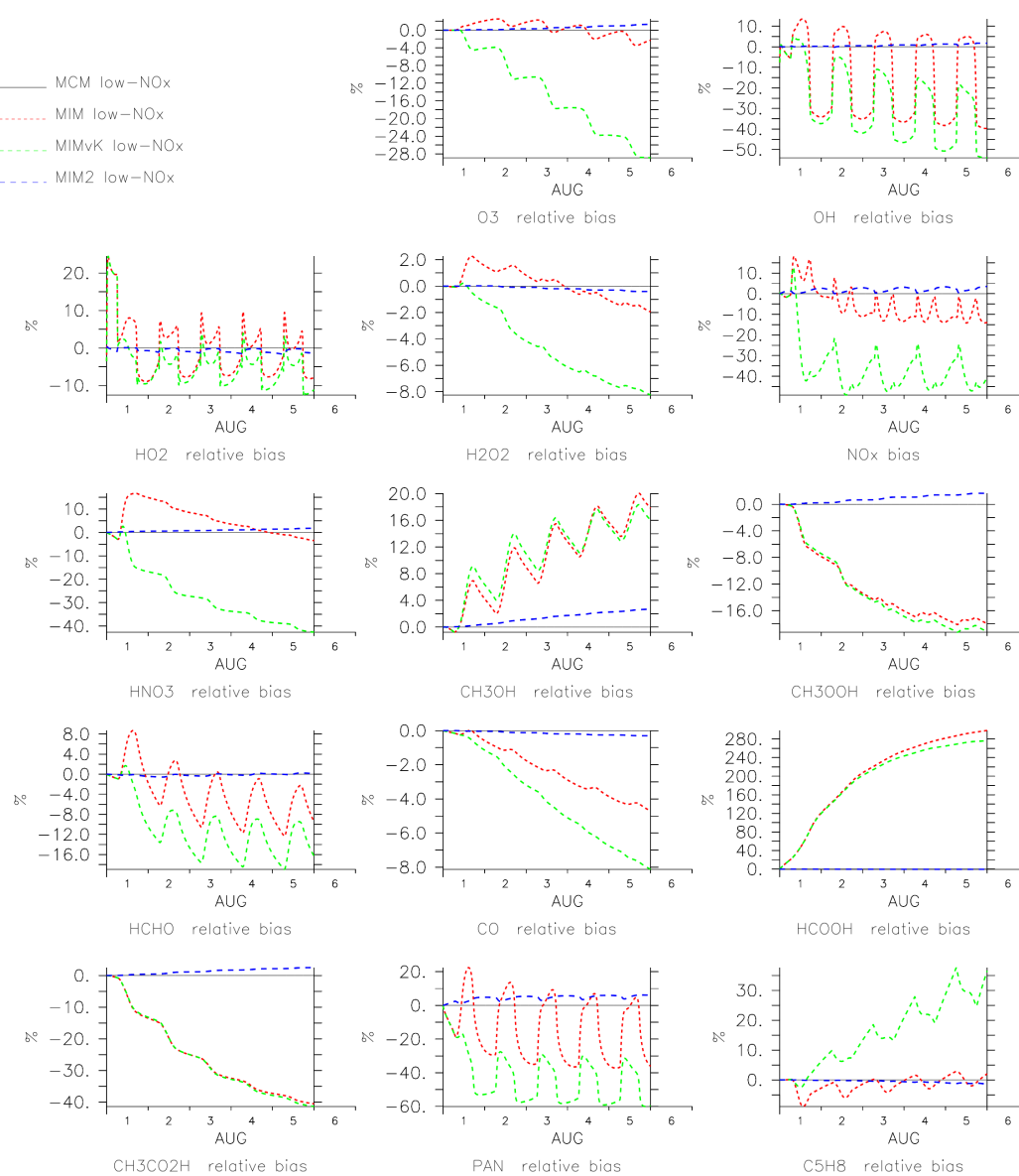
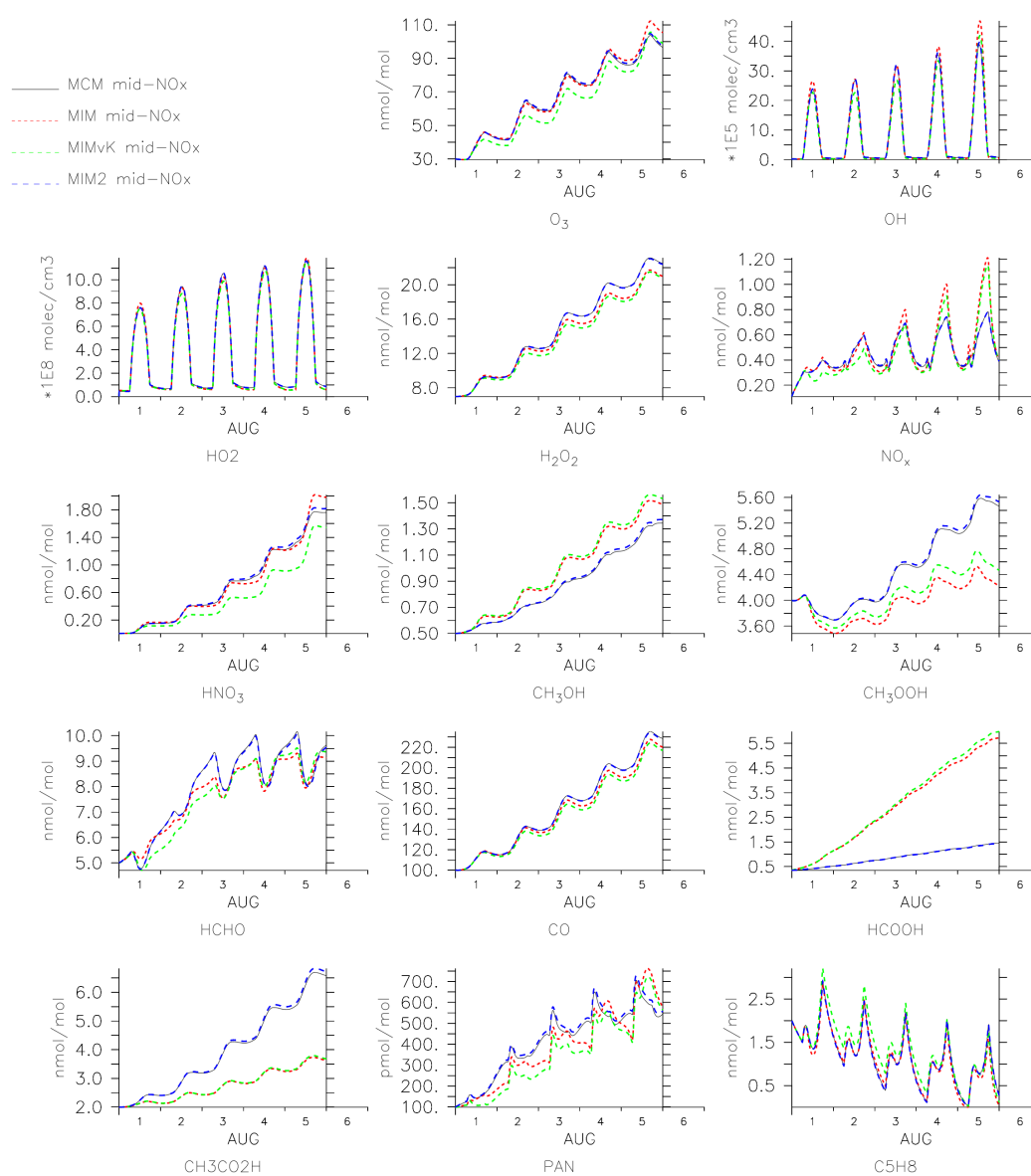


FIGURE 3.2: Low-NO_x scenario: relative biases, $100 \cdot (\text{mechanism} - \text{MCM}) / \text{MCM}$, of MIM, MIMvK and MIM2.

of the total estimated source. The MIM bias for CO grows steadily in absolute terms and reaches about -5% after a 5 day simulation while the MIM2 bias reaches only $\approx -0.02\%$. The CO-yield is thus higher in MIM2 compared to MIM. This might not hold in 3-D atmospheric model simulations because of dry deposition and scavenging. In fact, MIM2 differs remarkably from MIM with respect to the total alkyl nitrates and the hydroxy-peroxides from C₂ to C₅ (see Sect. 3.6). Such species are believed to be very soluble and reactive and can deposit efficiently with Henry's law coefficients in the range of $0.1 - 5 \cdot 10^5 \text{ M atm}^{-1}$ (Sander (1999), Shepson et al. (1996), Treves et al. (2000, and references therein)).

MIM neglects the formation of a few important species from isoprene oxidation: acetaldehyde (CH_3CHO), glycolaldehyde (HOCH_2CHO), glyoxal (CHOCHO), propene ($\text{CH}_3\text{CH}=\text{CH}_2$) and α -nitrooxy acetone ($\text{CH}_3\text{C}(\text{O})\text{CH}_2\text{OONO}_2$) (see Table 3.2 and Fig. A.1,A.2 and A.3 for MIM2 comparisons with MCM results). They are not considered, neither as single species, nor as part of lumped species. MIM2 drastically reduces the bias for species like formaldehyde (HCHO), peroxy acetyl nitrate (PAN), carbon monoxide (CO), acetic acid ($\text{CH}_3\text{C}(\text{O})\text{OH}$), formic acid (HCOOH) and methanol (CH_3OH) by the improved treatment of ozonolysis reactions, in particular the reaction $\text{ISOP} + \text{O}_3$ (see Sect. 2.5). From a simple budgeting (see Table 3.2), this latter reaction turns out to account for about 31% of the total destruction of isoprene in the low- NO_x scenario. It can be seen from Fig. 3.2 how these MIM biases for the above mentioned species increase over night. In particular, the large MIM bias for PAN (up to nearly -40%) is due to a much lower yield of CH_3CO_3 from the ozonolysis reactions. This yield from the isoprene ozonolysis is equal to 0.1 in MIM, versus 0.1575 in MIM2. These biases for MIM are all negative except for HCOOH and CH_3OH . The production of methyl peroxy radical (CH_3O_2) within MIM2 is essential to adequately reproduce the mixing ratios of methanol (CH_3OH) and methyl hydroperoxide CH_3OOH . The atmospheric production of CH_3OH through the permutation reactions of CH_3O_2 was estimated recently to be about 38 Tg/yr (Jacob et al. (2005), Millet et al. (2008b)). This amounts to nearly 16% of the total estimated global source, and MIM2 reduces the uncertainties in this term. The overestimation of CH_3OH in MIM is due to a too high CH_3O_2 yield from the ozonolysis reactions. On the other hand the CH_3OOH underestimation is due to the complete absence of CH_3O_2 production from the reactions of the C_5 -peroxy radicals and peroxides. These two reactions turn out to be important for CH_3OOH production because they take place mostly during daytime when the HO_2 concentration peaks. The production of CH_3O_2 in MCM takes place in the decomposition channel of the tertiary alkoxy radical ISOPBO that yields hydroxy-methyl vinyl ketone, MVKOH.

Unlike MIM, the MIM2 biases for the species in Fig. 3.2 are always lower than 6%. They often have constant sign and grow slowly. Overall the mechanism referred to as MIMvK performs very poorly in computing O_3 and isoprene under these conditions. This is due to the representation of the alkyl nitrates (see Sect. 3.6.1). The amount of NO_x that is sequestered by the alkyl nitrates is too high, so that OH and O_3 are reduced substantially. Such differences between MIMvK and MIM are not seen when the NO emissions are increased by a factor of 10, as discussed in the next section.

FIGURE 3.3: Mid-NO_x scenario: comparison of MCM, MIM, MIMvK and MIM2.

3.4 Mid-NO_x regimes

3.4.1 MCM behaviour

In this scenario the NO emission rate was set to be 3.33×10^{10} molecule $\text{cm}^{-2} \text{s}^{-1}$. In Fig. 3.3 the mixing ratios of the most important tracers are shown. The ozone and NO_x mixing ratios clearly show that the system is in the O₃-producing regime. The OH concentration keeps increasing and reaches values of about one order of magnitude higher than seen in the low-NO_x scenario (cf. Fig. 3.1). After 5 days, it peaks at about

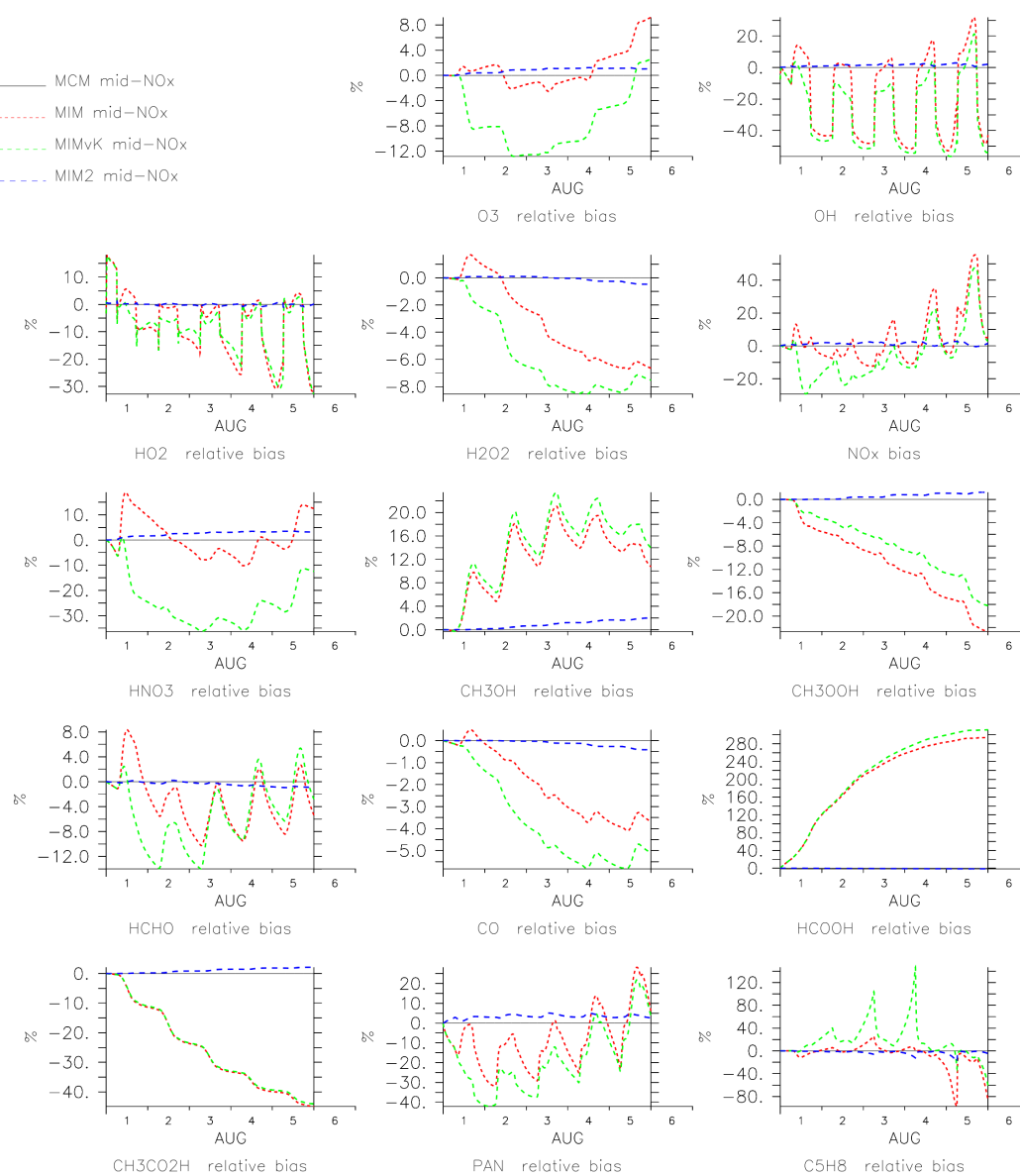


FIGURE 3.4: Mid-NO_x scenario: relative biases, $100 \cdot (\text{mechanism} - \text{MCM}) / \text{MCM}$, of MIM, MIMvK and MIM2.

$4 \cdot 10^6 \text{ molecule cm}^{-3}$. None of the species, except isoprene and HCHO, reach photostationary state. Compared to the low-NO_x scenario, both NO_x and PAN have a different diurnal cycle. Their mixing ratios do not have a secondary maximum shortly after midnight and continue to peak in the late afternoon and in the morning, respectively.

3.4.2 MIM2 and MIM behaviour and biases

Between the fourth and the fifth day of simulation time isoprene in MCM is depleted to nearly zero (see Fig. 3.3). Small differences in absolute terms between the different mechanisms are expected to result in quite large relative biases. For instance, when MCM computes isoprene concentrations very close to zero (during nighttime), both MIM and MIM2 give the largest relative biases with respect to isoprene itself (see Fig. 3.4). There is no clear tendency for the MIM2 average relative biases for all species to be better or worse for this scenario compared to the low-NO_x scenario (cf. Figs. 3.2 and 3.4). Even though the sign changes for some, they remain within the 5% range (see Table 3.2). The other two reduced mechanisms, MIM and MIMvK, show many biases similar to the biases in the low-NO_x scenario. What is striking, however, are the large biases with respect to OH, NO_x and PAN. The explanation lies in the differences regarding the organic nitrogen reservoirs in such mechanisms (see Sect. 3.6). The MIM bias for OH reaches +30% during daytime while for NO_x it reaches more than +50%. It is worth noting that in contrast to the low-NO_x scenario, the MIM relative bias for H₂O₂ starts to be substantial, reaching $\approx -7\%$. The H₂O₂-yield from ozonolysis of isoprene is 11% in MIM2 and 9% in MIM. Moreover, the ozonolysis of C₅- and C₄-carbonyls in MIM does not produce H₂O₂.

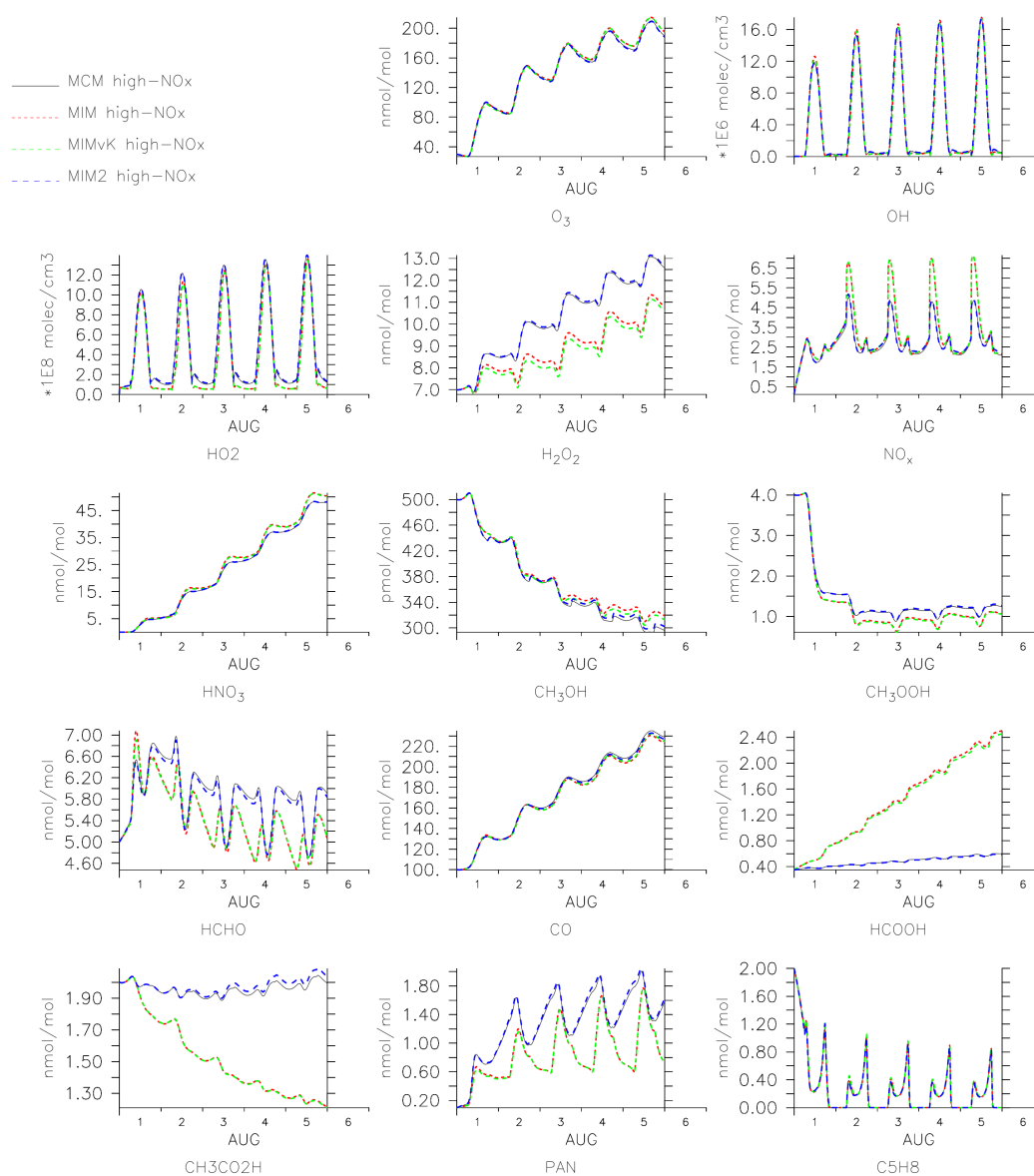
3.5 High-NO_x regimes

3.5.1 MCM behaviour

In this scenario the NO emission rate was set to 3.33×10^{11} molecule cm⁻² s⁻¹. In Fig. 3.5 the mixing ratios of the most important tracers are shown. O₃ is produced very efficiently, reaching 200 nmol mol⁻¹, and OH peaks with concentrations always higher than $1 \cdot 10^7$ molecule cm⁻³. PAN reaches values of 1.5 nmol mol⁻¹ and HCHO reaches photostationary state after 3 days simulation time. NO_x peaks in the morning at values around 5 nmol mol⁻¹ and a large part of the total nitrogen is stored as HNO₃, reaching a mixing ratio of more than 45 nmol mol⁻¹ at the end of the simulation. HCOOH and CH₃C(O)OH mixing ratios grow much less compared to the other NO_x scenarios.

3.5.2 MIM2 and MIM behaviour and biases

Under the high-NO_x regime both MIM and MIM2 show modest relative biases for O₃ being always within 1% (see Fig. 3.6).

FIGURE 3.5: High-NO_x scenario: comparison of MCM, MIM, MIMvK and MIM2.

As expected, MIM2 has a large average relative bias of -62.4% for isoprene and -150% for NO (see Table 3.2) that correspond, however, to small absolute biases when the mixing ratios are at night close to zero. Moreover, glyoxal shows a substantial average relative bias of about 11% mostly due to the lumping in the NO₃-pathway (see Table A.3). This bias grows significantly at night and becomes close to zero during the day (see Fig. A.3). In fact, the species LNISO3 is a lumped species representing two different kinds of RO₂, with one being alkyl and the other one acyl and having glyoxal and NOA as a reaction products, respectively. Besides isoprene, glyoxal and NO, there is no clear tendency for the MIM2 average relative biases for all other species to be better or worse for this scenario compared to the other NO_x scenarios (cf. Figs. 3.2, 3.4 and

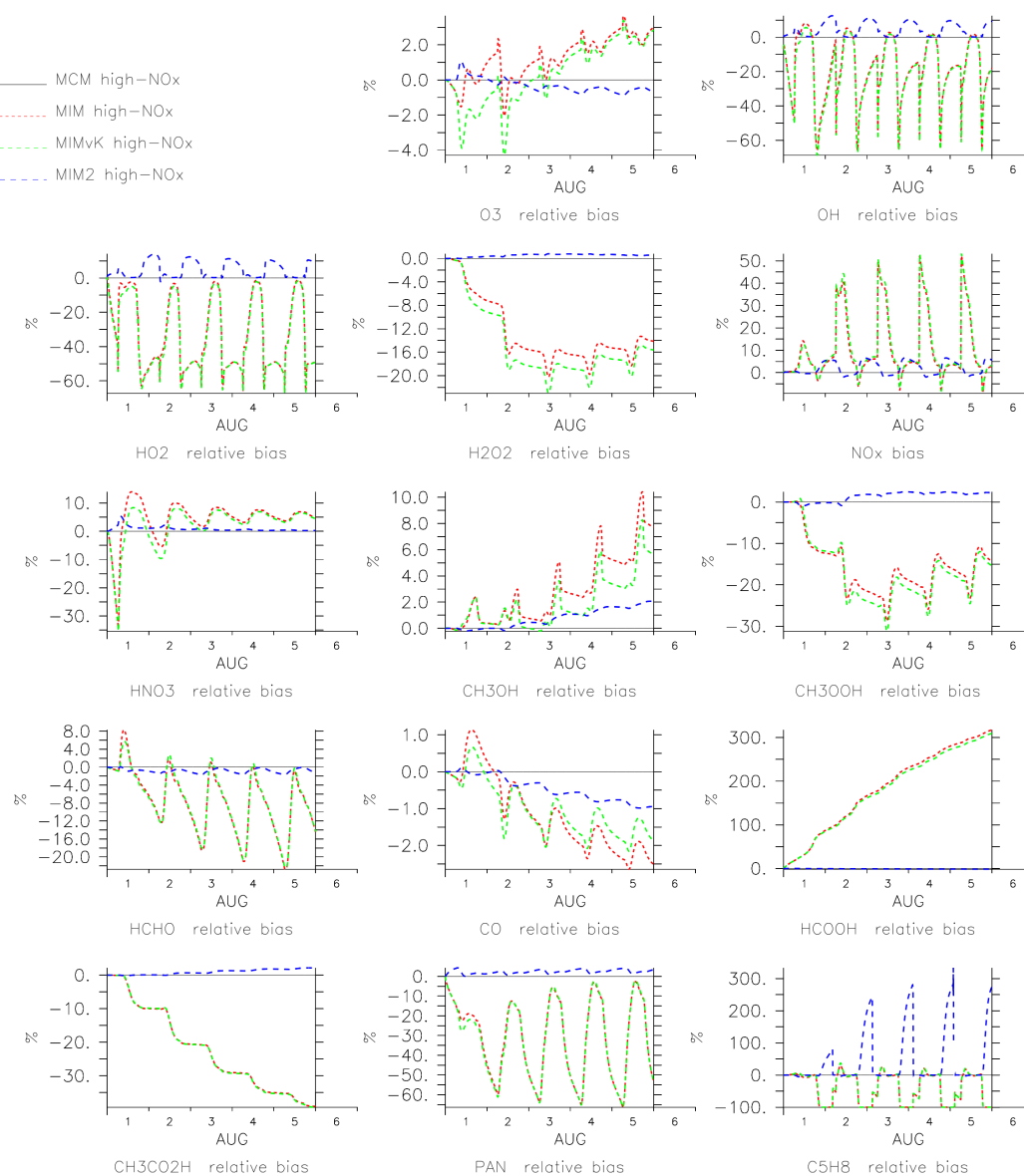
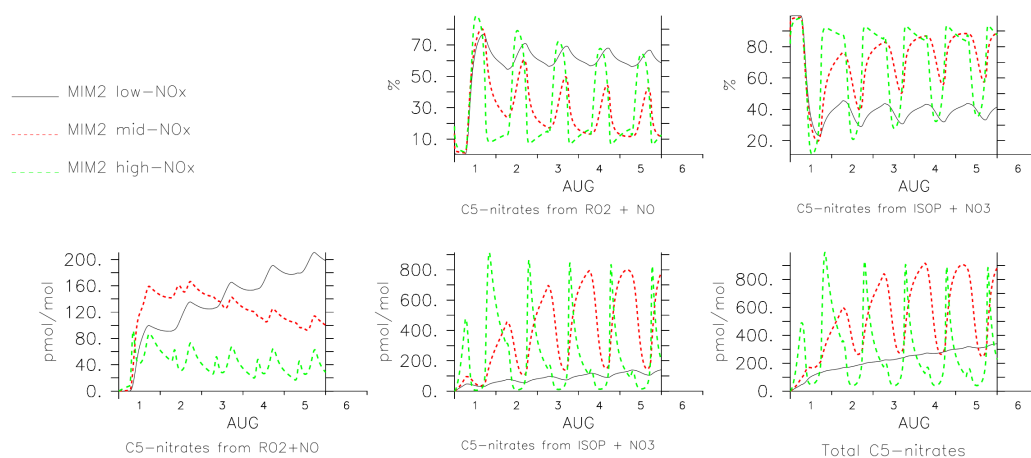


FIGURE 3.6: High-NO_x scenario: relative biases, $100 \cdot (\text{mechanism} - \text{MCM}) / \text{MCM}$, of MIM, MIMvK and MIM2.

3.6). The MIM relative bias for H₂O₂ becomes rather large, reaching $\approx -20\%$. Under such high-NO_x regimes, isoprene ozonolysis contributes little to the production of H₂O₂ because it accounts for only $\approx 8\%$ of the total isoprene destruction (see Table 3.2). The OH- and NO₃-pathways now account for $\approx 92\%$ of the isoprene destruction, while in the mid-NO_x and low-NO_x scenarios they account for ≈ 81 and 69% , respectively. The total yield of the C₅-carbonyls in the high-NO_x scenario is increased because they are not produced in the O₃-pathway. The ozonolysis of such species in MIM does not produce any H₂O₂.

FIGURE 3.7: Alkyl nitrates in MIM2 under different NO_x -regimes

3.6 Organic nitrogen and peroxides

3.6.1 Alkyl nitrates

There are eight alkyl nitrates included and they can be subdivided in three groups (see Table A.1). The first group includes three C_5 -alkyl nitrates produced by $\text{RO}_2 + \text{NO}$ reactions in the OH-pathway. One has an internal double bond (LISOPACNO3) and two have an external double bond (ISOPBNO3 and ISOPDNO3). The second group includes three alkyl nitrates produced by the NO_3 -pathway with NC4CHO and NISOPOOH having an internal double bond and LNISOOH with all carbon atoms being saturated. Finally, the third group includes two C_3 -alkyl nitrates. One is α -nitrooxy acetone (NOA), which is produced during the oxidation of the above mentioned alkyl nitrates. The other one is PR2O2HNO3 (see Table A.3), which is produced after the NO_3 -addition to propene. It is worth noting that one alkyl nitrate from the OH-pathway (LISOPACNO3) is produced in the permutation reaction of NISOPO2 in the NO_3 -pathway as well (see Table reftab:reactions). The chemistry of the alkyl nitrates in MCM and MIM2 is treated in a simplified manner. However, it is easily extendable, for example including ozonolysis reactions as in two recent models (Giacopelli et al. (2005), Horowitz et al. (2007)).

The mixing ratios of the MIM2 C_5 -alkyl nitrates are shown in Fig. 3.7 in the three different NO_x scenarios.

It can be seen that the relative distributions of the alkyl nitrates from the two pathways changes drastically with NO_x levels. In the low- NO_x scenario the C_5 -alkyl nitrates from the OH-pathway always dominate with respect to the ones from the NO_3 -pathway. In fact, they account for between 55–75% of the total C_5 -alkyl nitrates. As the system

changes towards the high-NO_x regimes, the diurnal cycles of C₅-alkyl nitrates become very pronounced. Under such conditions the C₅-alkyl nitrates from the NO₃-pathway start to dominate during nighttime, accounting for about 90% of the total nitrates. In two recent studies using very reduced isoprene oxidation mechanisms, it was estimated that the total fraction of the C₅-alkyl nitrates produced at night ranges from 50% to more than 60% (Horowitz et al. (2007), von Kuhlmann et al. (2004)). When MIM2 is implemented in a global atmospheric model, the C₅-alkyl nitrates from the two pathways are produced in roughly the same amounts (see Sect. 3.8). MIM considers only one C₅-alkyl nitrate (ISON) produced by both the OH- and NO₃-pathways. The peroxy radical that should result from the addition of NO₃ to isoprene is assumed to go directly into ISON, which has the properties of a long-lived species. In fact, this lumped species in MIM reacts with OH, yielding hydroxyacetone and nitroxyacetaldehyde (called NALD in MIM). The rate constant assigned to this reaction is $k = 1.3 \cdot 10^{-11} \text{cm}^3 \text{molecule}^{-1} \text{s}^{-1}$, being a factor between 3 and 9 lower than the actual rate constants for the single isomers that ISON represents. The rate constant for that reaction is artificial and was used by Pöschl et al. (2000) to strongly tune MIM to the MCM results. Moreover, the species NALD, and called in NO3CH2CHO in MCM, is actually a product of 1,3-butadiene and 2-methylbut-3-en-2-ol oxidation. Furthermore, we note that in such a reaction there is no release of NO₂ as for the alkyl nitrates resulting from the OH-pathway. We note that the treatment of the alkyl nitrates in MCM is also to an extent simplified. Overall this causes MIM to accumulate too much nitrogen in the alkyl nitrates (relative bias up to 900% in high-NO_x scenario), delaying considerably the release of NO₂ down the oxidation chain. Since MIM2 considers eight alkyl nitrate species, it is a very appropriate tool to constrain the chemistry of alkyl nitrates with field data and an atmospheric chemistry model like in Horowitz et al. (2007). In that study their model was found to fit the field data the best with a 4% yield of alkyl nitrates from the reaction of isoprene peroxy radicals with NO. By contrast, MCM was found to match chamber data experiments with an average yield of 10% from such reactions (Pinho et al. (2005)). The MIM2 relative biases for NOA are very small as well. By contrast, we show in Figs. 3.8–3.10 MIM computing large relative biases either for the alkyl nitrates or for NOA (compared to NALD from MIM). The chemistry and the physical properties, such as solubility, of the C₅-alkyl nitrates and NOA are rather different, with the former ones having a double bond and an hydroxy group and the latter with none of these. Hence, the interplay between the chemistry, deposition and transport is expected to be non-negligible in a 3-D atmospheric chemistry model.

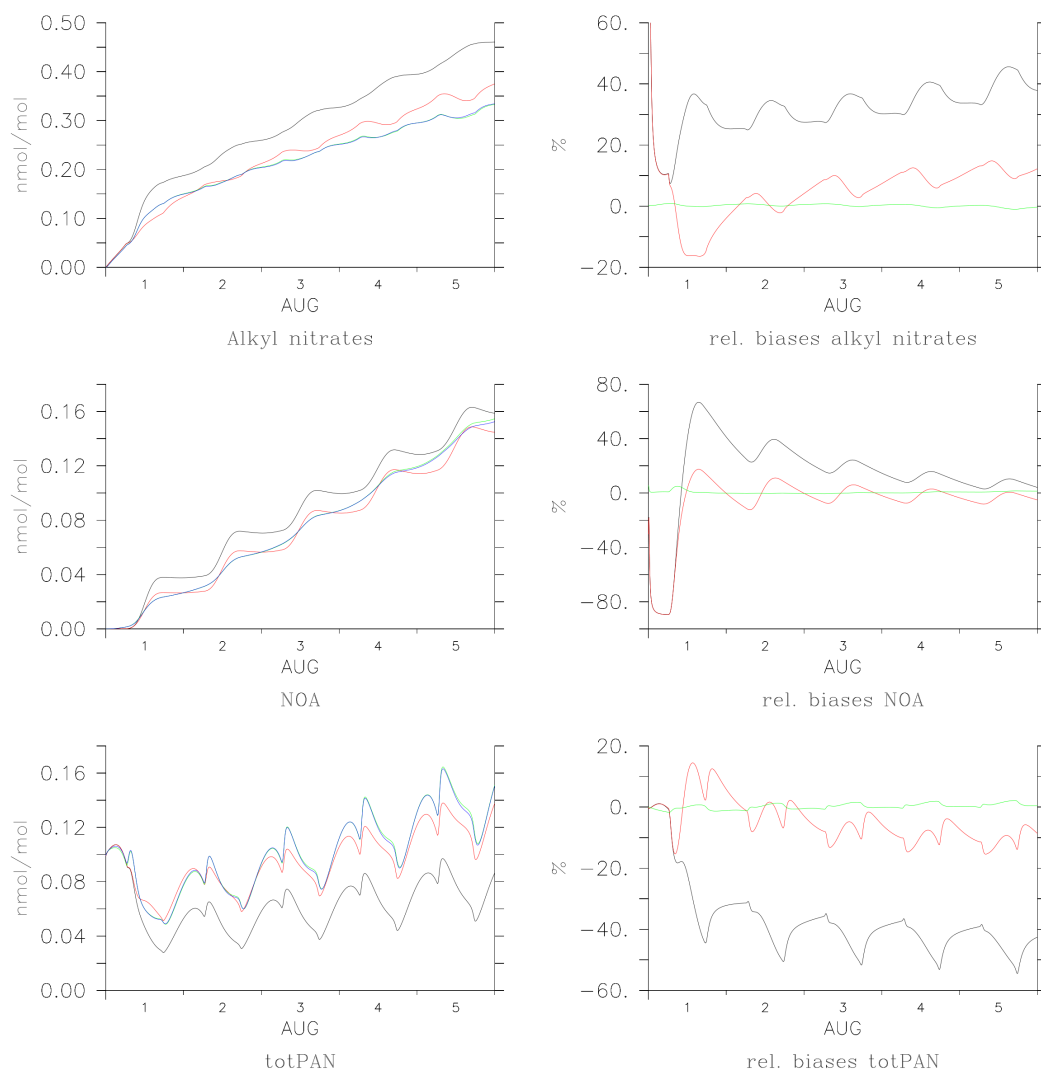


FIGURE 3.8: Nitrogen reservoirs in low- NO_x scenario. In all the plots the actual mixing ratios of each species are presented with MIMvK (black line), original MIM (red line), MIM2 (blue line) and MCM (green line). The alkyl nitrates shown here are the sum of all alkyl nitrates except NOA (shown separately).

3.6.2 Peroxy acyl nitrates

PAN and its homologues have the general formula $\text{RC}(\text{O})\text{OONO}_2$, and the isoprene mechanism in MCM considers 11 of them. MIM2 considers four peroxy acyl nitrates. In the low- NO_x scenario the MIM2 relative bias for the total peroxy acyl nitrates is in the 5% range, while in the other two NO_x scenarios it reaches values as low as -15% (Figs. 3.8–3.10). In all cases the largest deviations from the MCM results occur during nighttime when temperatures favour the formation of $\text{RC}(\text{O})\text{OONO}_2$. This indicates a lower capacity of the reduced mechanism to store nitrogen in this reservoir.

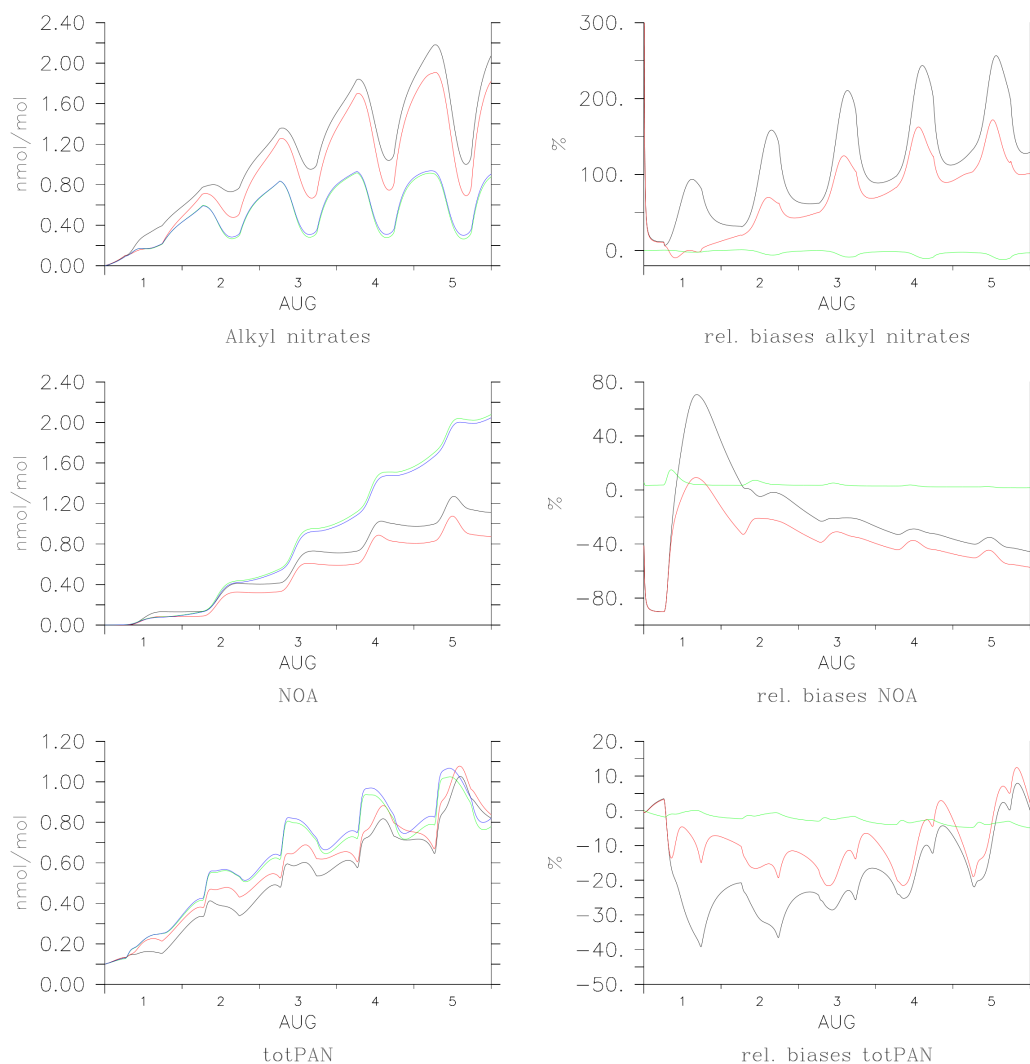


FIGURE 3.9: Nitrogen reservoirs in mid- NO_x scenario. In all the plots the actual mixing ratios of each species are presented with MIMvK (black line), original MIM (red line), MIM2 (blue line) and MCM (green line). The alkyl nitrates shown here are the sum of all alkyl nitrates except NOA (shown separately).

3.7 $\text{C}_2\text{--C}_5$ peroxides

Comparisons of the higher organic peroxides from the reduced mechanisms are shown for all NO_x scenarios considered here (see Figs. 3.11–3.13). Large MIM2 biases are computed only for the high- NO_x conditions. They originate from the nighttime chemistry that is simplified in MIM2, neglecting an important sink for the peroxy radicals, namely its reaction with NO_3 radicals (see Sect. 3.5.2). Clearly the biases grow during nighttime when NO_3 mixing ratios are non-negligible, while during daytime they decrease substantially.

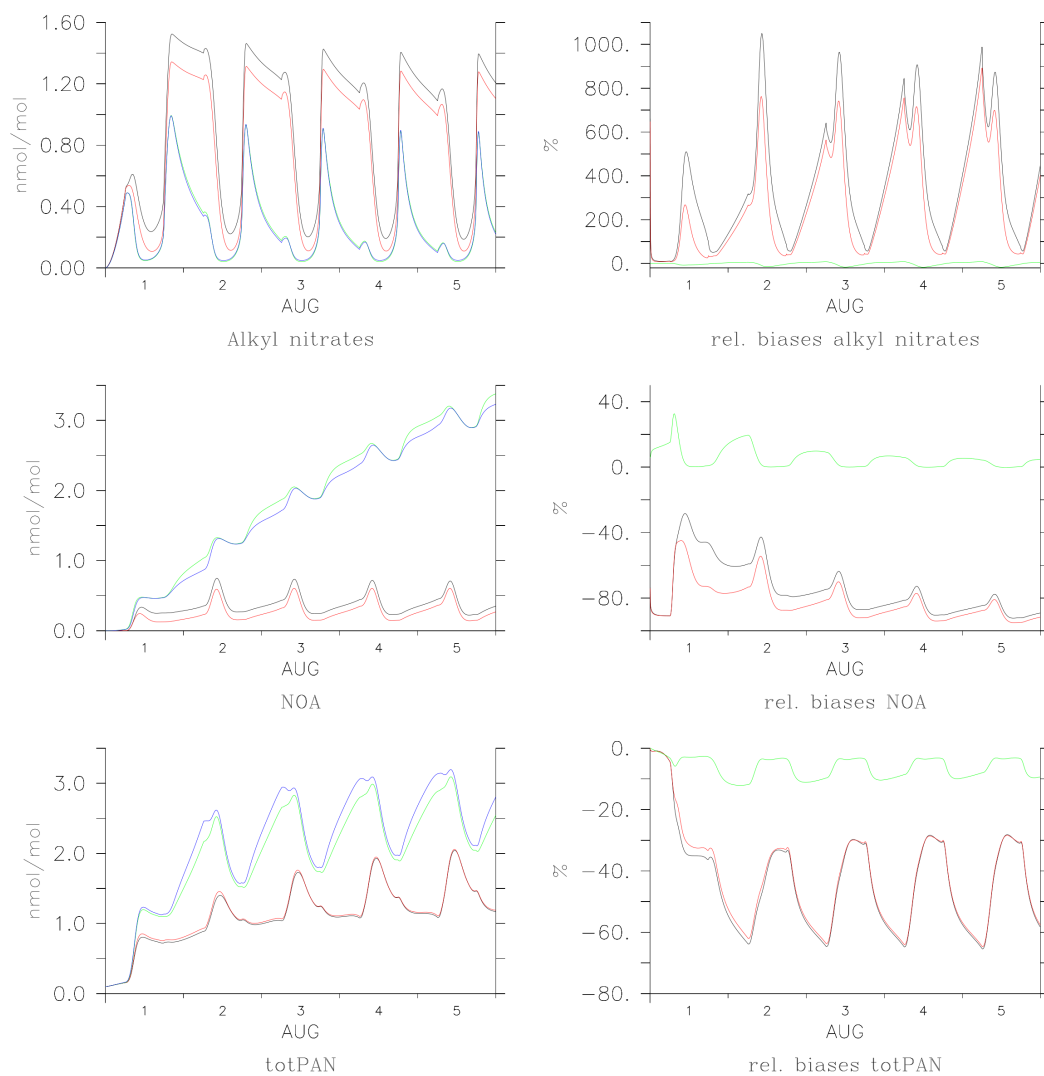


FIGURE 3.10: Nitrogen reservoirs in high- NO_x scenario. In all the plots the actual mixing ratios of each species are presented with MIMvK (black line), original MIM (red line), MIM2 (blue line) and MCM (green line). The alkyl nitrates shown here are the sum of all alkyl nitrates except NOA (shown separately).

3.8 Impact on the global scale

3.9 Implementation in a global model

The focus of this section is on the differences between 3-D simulations with MIM2 and with the mechanism referred to here as MIMvK, used in a recently established global atmospheric chemistry model (Jöckel et al. (2006)). The total isoprene emission in the simulations for the year 2005 was 566.7 Tg/yr of isoprene, equivalent to 500 Tg(C)/yr. The model setup is described in more detail in Butler et al. (2008). All the tested

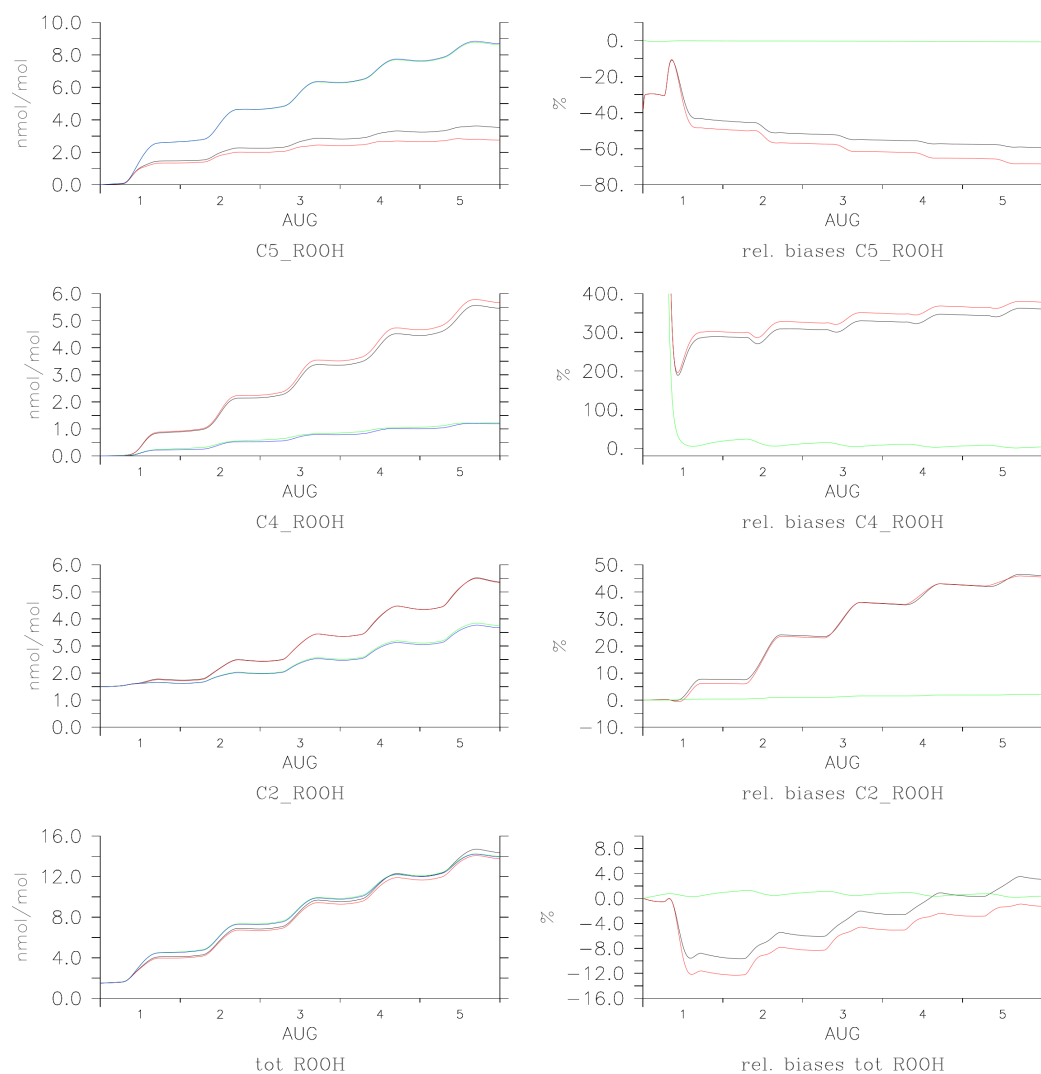


FIGURE 3.11: Organic peroxides other than CH_3OOH for all four mechanisms in this study under low- NO_x conditions. In all the plots the actual mixing ratios of each species are presented with MIMvK (black line), original MIM (red line), MIM2 (blue line) and MCM (green line). C_3 -peroxides are not shown because MIM and MIMvK do not have any.

mechanisms were budgeted and the product yields per molecule of isoprene estimated. The contribution of each pathway to the isoprene oxidation was calculated to be 84% for OH, 11% for O_3 and 5% for NO_3 , globally. Pfister et al. (2008) estimated similar contributions being 80% for OH, 15% for O_3 and 5% for NO_3 . The product yields of isoprene in global models are subject to uncertainties due to assumptions regarding dry and wet deposition of the relative intermediates, as well as other contributing factors such as emissions and transport. Note that a few minor updates to MIM2 were made after this global run was completed, but these should have negligible effects on the results presented here in this section.

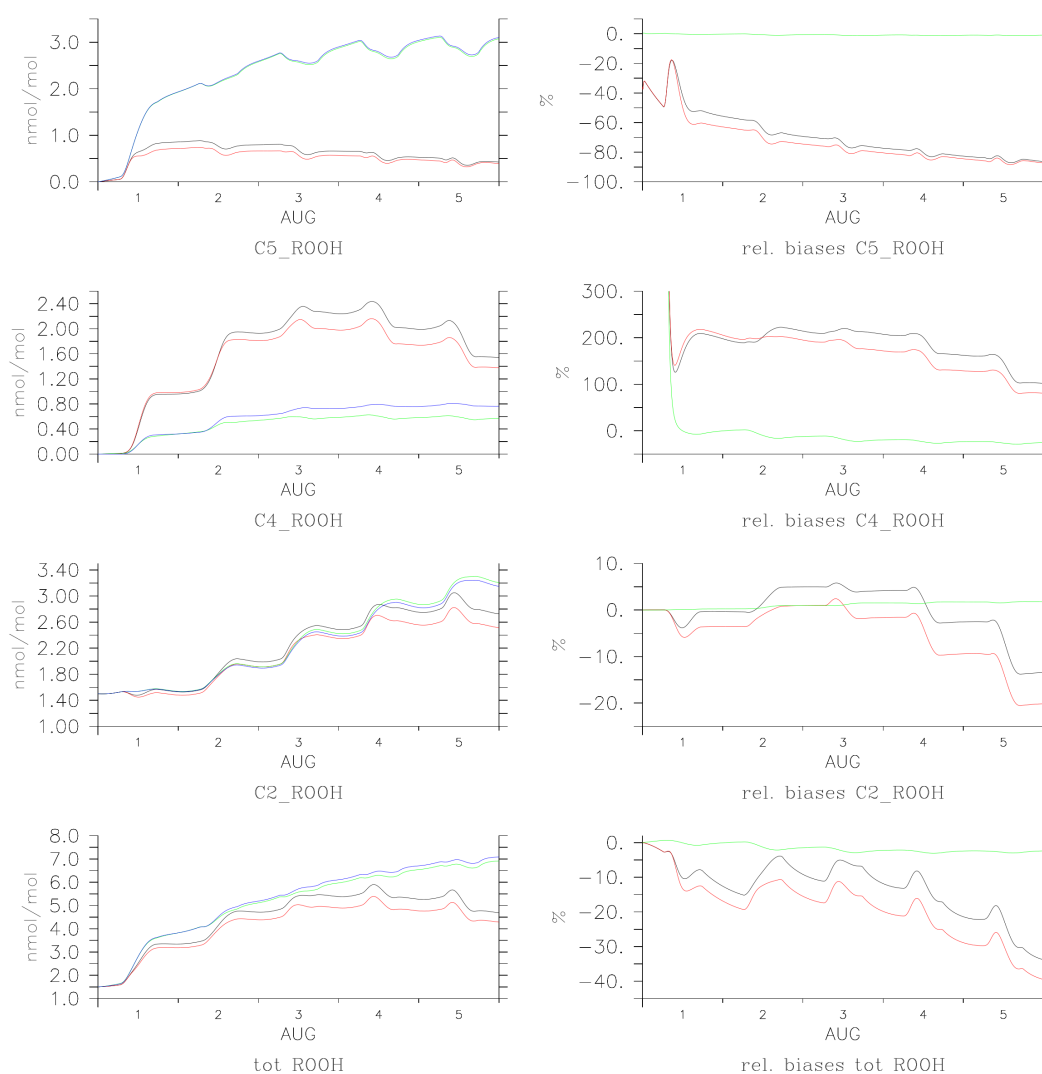


FIGURE 3.12: Organic peroxides other than CH₃OOH for all four mechanisms in this study under mid-NO_x conditions. In all the plots the actual mixing ratios of each species are presented with MIMvK (black line), original MIM (red line), MIM2 (blue line) and MCM (green line). C₃-peroxides are not shown because MIM and MIMvK do not have any.

3.10 OH and isoprene

The seasonal relative differences for OH and isoprene between the MIM2 and MIMvK isoprene mechanisms are presented in Fig. 3.14. The reduction in isoprene mixing ratios in MIM2 is expected to improve the model-measurement agreement over a region like Amazonia, in which models have traditionally overestimated isoprene mixing ratios by about a factor of 3 (von Kuhlmann et al. (2004)). For this reason such models have been implemented in the past with isoprene emission strengths in the range 215–350 Tg(C)/yr, well below the range of 424–530 Tg(C)/yr calculated by different models (Guenther et al.

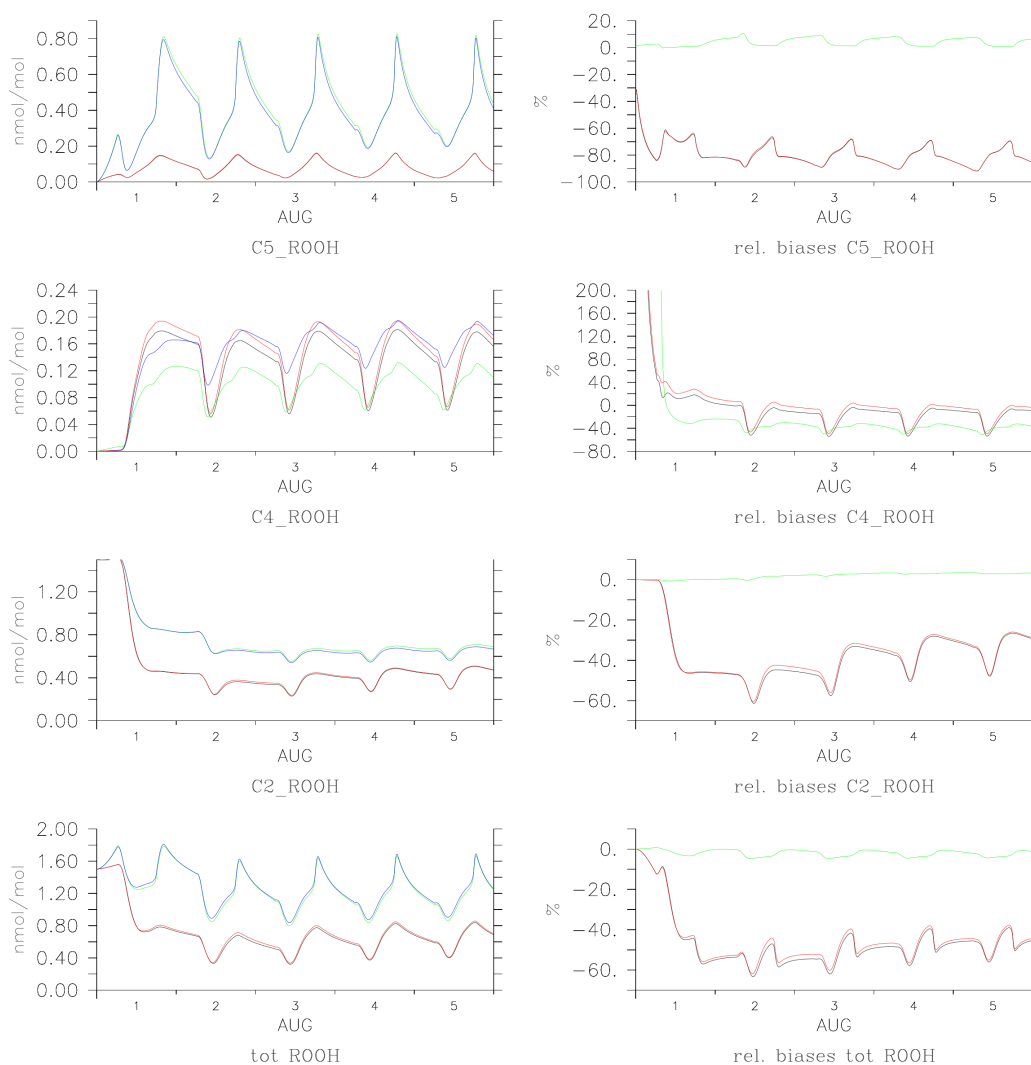


FIGURE 3.13: Organic peroxides other than CH_3OOH for all four mechanisms in this study under high- NO_x conditions. In all the plots the actual mixing ratios of each species are presented with MIMvK (black line), original MIM (red line), MIM2 (blue line) and MCM (green line). C_3 -peroxides are not shown because MIM and MIMvK do not have any.

(1995, 2006), Lathière et al. (2006), Müller et al. (2008). The overall increase in OH and the decrease in isoprene mixing ratios, however, are not enough to match the observations which were made during the GABRIEL campaign (Lelieveld et al. (2008)). A more in-depth discussion of the model-measurement comparison during this campaign for OH, isoprene and many other intermediates is presented in Butler et al. (2008).

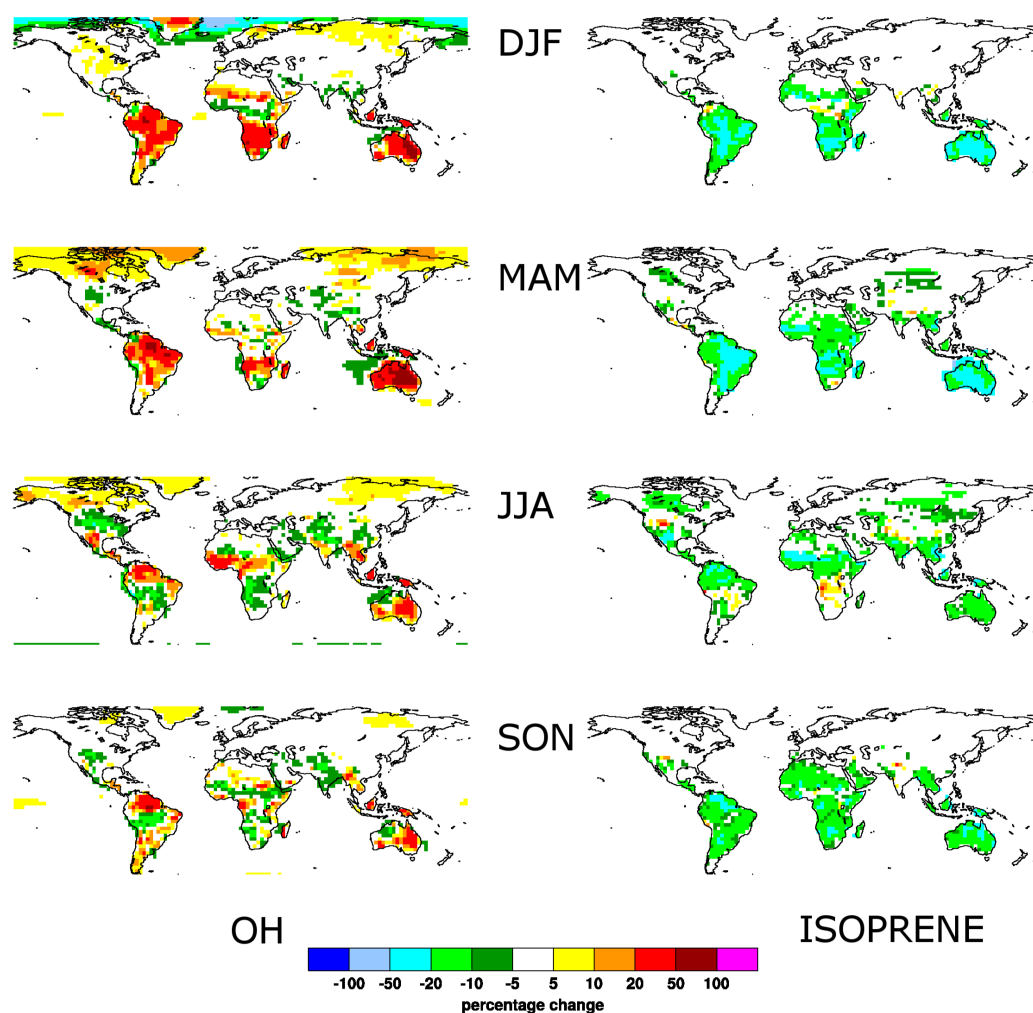


FIGURE 3.14: Seasonal relative change $100 \cdot (\text{MIM2} - \text{MIMvK}) / \text{MIMvK}$ for OH (left panel) and isoprene (right panel).

3.11 New species

There are many important species in MIM2 that are either new (compared to MIM) or not lumped anymore. We discuss the relevance of the chemical production of three new species with respect to their atmospheric budgets.

3.11.1 Glyoxal

The total yield of glyoxal in our 3-D simulation is estimated to be 7.0% and results in a chemical production only from isoprene oxidation of 33.83 Tg/yr. Recently, [Myriokefalitakis et al. \(2008\)](#) calculated a total global production of 56 Tg/yr, of which 39.2 Tg/yr (70%) is from the oxidation of biogenic VOC. The main contributors were isoprene and

monoterpenes with global annual emissions of 501 Tg/yr and 244 Tg/yr, respectively. However, satellite retrievals show that global atmospheric chemistry models underestimate the glyoxal annual mean total column where terpene emissions are the strongest (Myriokefalitakis et al. (2008), Wittrock et al. (2006)).

3.11.2 Propene

Propene ($\text{CH}_2=\text{CHCH}_3$) is produced with yields of 12.75% from ozonolysis of isoprene and of 50% from the photolysis of MVK (Atkinson et al. (2006)). In MCM and MIM2 its yield from MVK photolysis is 60%. In a recent study by Pozzer et al. (2007) the parameterized emission from vegetation was 2.15 Tg/yr with all off-line sources amounting to 9.94 Tg/y (A. Pozzer, personal communication). The total yield of propene in the 3-D simulation is estimated to be 2.7%, resulting in a chemical production of 9.451 Tg/yr. Moreover, judging from Pozzer et al. (2007), this chemical source of propene is expected to substantially improve the representation of its diurnal cycle and its vertical distribution compared to observations.

3.11.3 Acetaldehyde

The total yield of acetaldehyde is 2% and the chemical production from isoprene oxidation amounts to 7.33 Tg/yr. It is produced in the ozonolysis of MVK and the oxidation of propene. According to our simulations isoprene oxidation can account for about 5 to 10% of the large missing global source of acetaldehyde of 80–160 Tg/yr inferred by Singh et al. (2001).

3.12 Incorporation of new experimental results

Lelieveld et al. (2008) first proposed that the current understanding of isoprene chemistry under low- NO_x conditions is not well understood yet. To date, NO_x -free experimental studies of isoprene reactions have been sparse and difficult. In fact, under these conditions the major oxidation products are the hydroperoxides that have low volatilities and are labile. The current MCM isoprene chemistry reflects the experimental knowledge that was available at the time of Jenkin et al. (1998), and has not been significantly updated since then. Therefore, we show here the impact of some recent experimental results on a simulation under the low- NO_x scenario. This highlights one of the major advancements of MIM2: unlike in MIM (and other highly lumped reduced mechanisms), the implementation of such changes in MIM2 is very straightforward.

The modifications consist of:

- 1) elimination of the species MVKOH (1-hydroxybut-3-en-2-one), since [Benkelberg et al. \(2000\)](#) found no evidence for its formation from isoprene oxidation.
- 2) implementation of the degradation of the methyl vinyl radical from MACR oxidation ([Orlando et al. \(1999\)](#)).
- 3) adoption of the product yields for the first peroxy radicals of isoprene as recently estimated by [Paulot et al. \(2009a\)](#). Two minor isomers yield MVK and MACR as products. Therefore, their yields are added to the those of ISOPBO2 and ISOPDO2. The modified yields 0.3, 0.424, 0.276 for LISOPACO2, ISOPBO2 and ISOPDO2, respectively.
- 4) adoption of the corresponding (see point 3) alkyl nitrate yields from the $\text{RO}_2 + \text{NO}$ reactions. For the externally and internally double bonded isomers the yields are 0.057 and 0.24, respectively.
- 5) inclusion of the new results on the $\text{RO}_2 + \text{HO}_2$ reactions for which OH has been found to often be a product ([Dillon and Crowley \(2008\)](#), [Hasson et al. \(2004\)](#), [Jenkin et al. \(2007\)](#)). For the acyl and β -keto peroxy radicals we used OH yields of 0.50 and 0.15, respectively. These yields are taken from [Dillon and Crowley \(2008\)](#) which is the only study in which OH was detected. The branching ratios of the radical terminating channels were then re-scaled so that the total yield was unity.

The results of the modified MIM2 are shown in Fig. 3.15.

For most species the deviations from MIM2 become significant after two days. An increase in the OH concentration of about 15% at noon appears to be the result of the non-radical terminating branches of the $\text{RO}_2 + \text{HO}_2$ reactions. The isoprene mixing ratio decreases by roughly the same amount. Hydroperoxides like H_2O_2 and CH_3OOH increase by about 8%. O_3 is found to change to a small extent (1-2%). Interestingly, the mixing ratios of the two dicarbonyls, glyoxal and methyl glyoxal, increase by more than 20%. This should significantly reduce the underestimation of glyoxal over pristine tropical forest by models ([Myriokefalitakis et al. \(2008\)](#)). The MVK mixing ratio increases by more than 10% while MACR decreases by about 8%. The average alkyl nitrate yield for the $\text{RO}_2 + \text{NO}$ reactions of the OH-pathway is slightly increased from 10% to about 11%. However, the total mixing ratio of the alkyl nitrates with 5 carbon atoms decreases by more than 15% already after the second day. These changes are mainly due to increases in OH mixing ratios.

Though the changes in species abundances indicated above are significant, they are still insufficient to explain the high HO_x levels measured during the GABRIEL campaign ([Lelieveld et al. \(2008\)](#)). New insights in the low- NO_x chemistry of isoprene are needed.

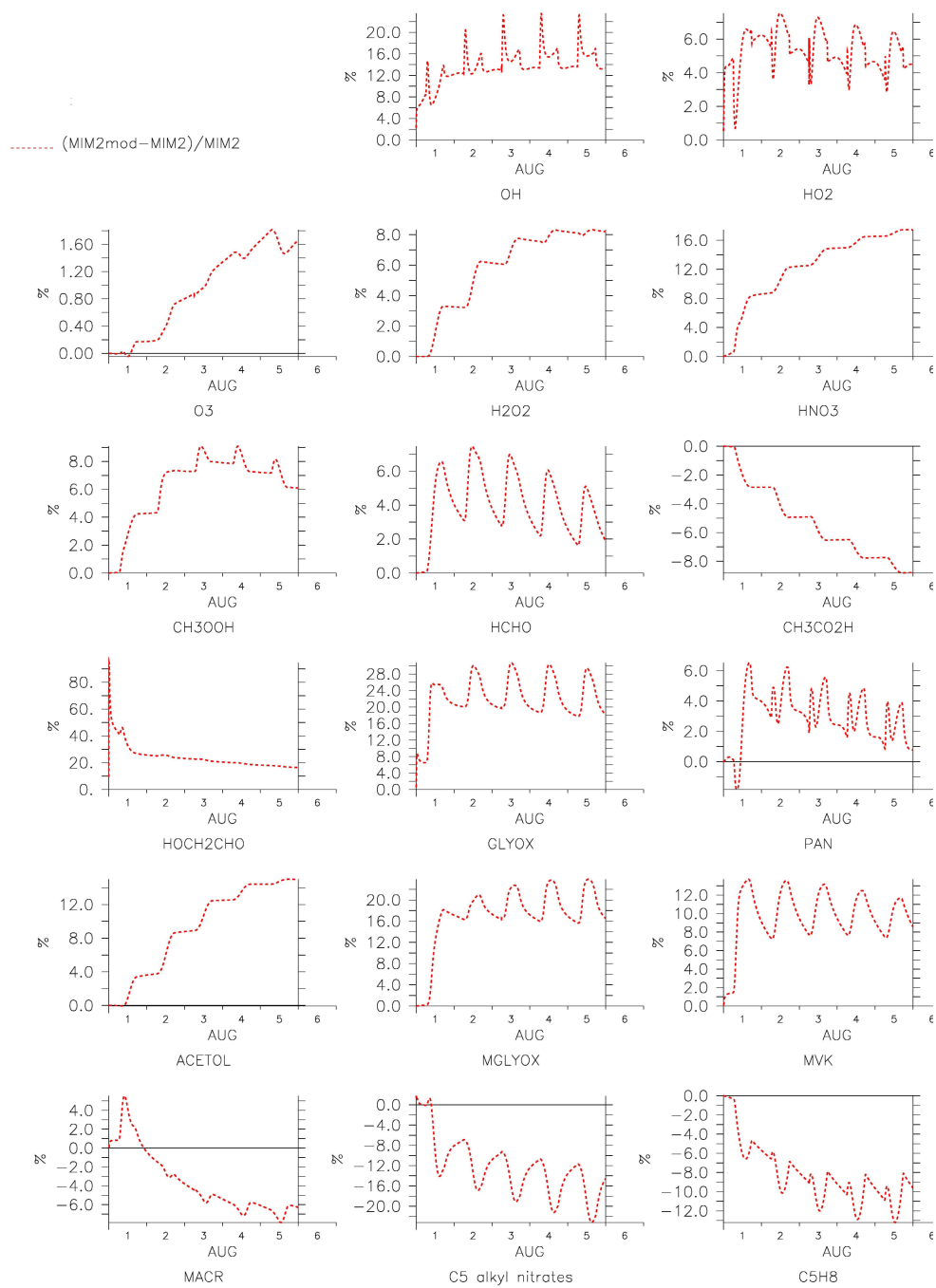


FIGURE 3.15: Relative differences of the modified MIM2 for some major species under the low-NO_x scenario.

To a significant extent they involve new decomposition pathways of peroxy radicals and hydroperoxides from isoprene oxidation (see Chapters 4 and 5).

Chapter 4

Development of a new detailed isoprene oxidation mechanism

4.1 Motivation

During a field campaign in a pristine tropical environment with intense vegetation very high concentrations of HO_x were measured (Butler et al. (2008), Lelieveld et al. (2008), Martinez et al. (2008)). These results are in contrast with model results. In fact, observed OH in the boundary layer was up to 8-9 times higher than the global model output using MIM2. The discrepancy was found to be positively correlated with isoprene concentrations when a box model with the MCM constrained by measurements was used (Kubistin et al. (2008)). For isoprene mixing ratios above 1 ppb, the ratio of observed-to-modelled OH mixing ratio was in the range of 4 to 20 (see Fig. 4.1).

In these environments, isoprene is the largest sink for OH in the boundary layer and the average OH concentration was found to be $5 \cdot 10^6 \text{ molec cm}^{-3}$. The model/observation discrepancy under low-NO_x conditions for HO_x is well known (Ren et al. (2008), Tan et al. (2001)). Previously, it has been hypothesized that unknown very reactive terpenes exist that are co-emitted with isoprene and react quickly with ozone to give OH (Di Carlo (2004), Goldstein et al. (2004), Kurpius and Goldstein (2003)). Despite the potential of this hypothesis to explain the measurements in the canopy (Goldstein and Galbally (2007)), supporting evidence has not been provided. Furthermore, the emission rate and the efficiency of escaping the canopy of these hypothesized VOCs are too low to be able to explain the discrepancies for observed HO_x in the boundary layer.

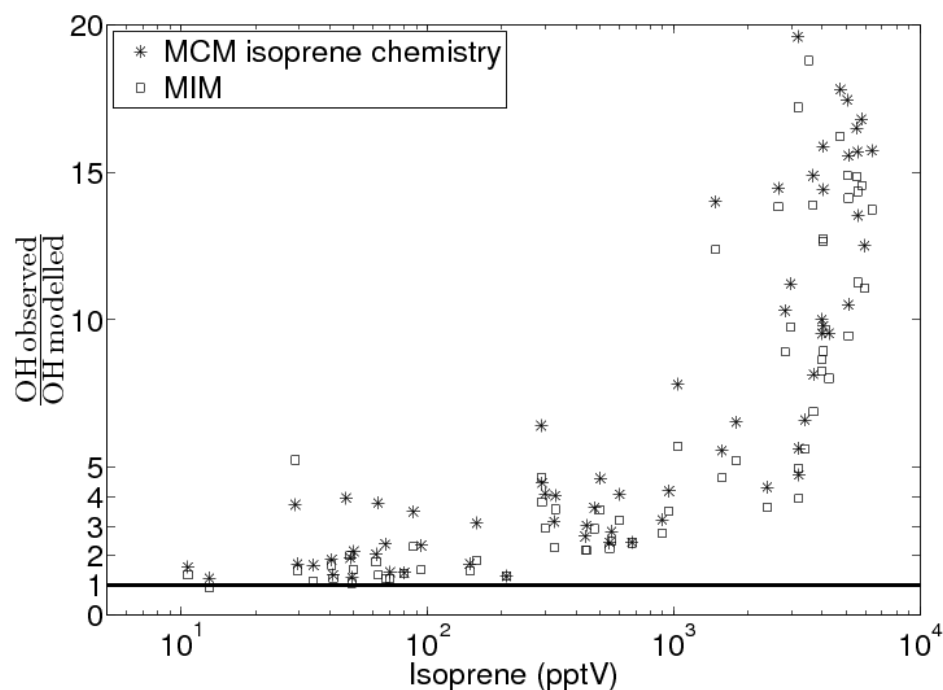


FIGURE 4.1: Ratio of observed to modelled OH mixing ratio during the GABRIEL campaign as a function of isoprene mixing ratio (Kubistin et al. (2008)).

Therefore, I approach the problem from a different angle. I question whether isoprene oxidation under low-NO_x regimes really constitutes a large OH sink, as currently assumed in models. I examine one state-of-the-art model for isoprene oxidation. In light of new experimental results, which have appeared in the literature in the last ten years, many assumptions and reactions I find to be obsolete. This chapter describes efforts to extend and update a detailed isoprene mechanism that is widely used in the atmospheric chemistry community. In Chapter 5 I evaluate this extended mechanism with a focus on the OH-recycling pathways.

4.2 Strategy

4.2.1 Starting point

The Master Chemical Mechanism v3.1 (MCM) for isoprene is taken as the starting point for the extended mechanism (Jenkin et al. (1997), Saunders et al. (2003)). The MCM has been described in Chap. 2 with respect to the MIM2 development. Its results have also been shown for box model simulations under three different NO_x scenarios (see Chap. 3). In summary, MCM implements available experimental data and makes use of

Structure Activity Relationships (SARs) for estimating the rate coefficients and reaction products.

4.2.2 Development directions

High OH levels under low-NO_x regimes imply that the oxidation by OH dominates the isoprene degradation (see Sec. 4.3). However, the generation of unsaturated products is significant under these conditions and their reactions with O₃ are revisited (see Sec. 4.4). Hence, the mechanism development is mainly focused on the reaction of organic compounds with OH and O₃.

In general, new IUPAC recommendations are adopted when available (Atkinson et al. (2006)). Newer recommendations for single reactions can be accessed at the website: <http://www.iupac-kinetic.ch.cam.ac.uk/>. When experimental data are lacking, either new or extended Structure Activity Relationships (SARs) are used to estimate both reaction rate coefficients and branching ratios of reactions.

4.3 Reactions with OH

4.3.1 SAR formalism

Based on relatively few experimental data, R. Atkinson developed and tested a simple method to estimate the reaction rate coefficients of OH with organic compounds in the gas phase (Kwok and Atkinson (1995) and references therein). According to this formulation, the rate coefficient is the sum of the ones for H-abstraction and OH-addition to the double bonds and aromatic rings. In this case, I can:

$$k_{OH,total} = k_{OH,abs} + k_{OH,add}$$

How these terms are calculated is described in the next two sections. Even though the MCM v3.1 uses the last update of R. Atkinson to the SAR (Atkinson (2000)), I will compare my newly derived SARs to Kwok and Atkinson (1995) that, unlike the update, is publicly available.

4.3.2 OH-addition to double bonds

OH radicals add to double bonds to form hydroxyalkyl radicals. The reaction coefficient is determined by the functional groups that are bound to the carbon atoms participating in that double bond. Because of the nature of these reactions, the OH radical has two

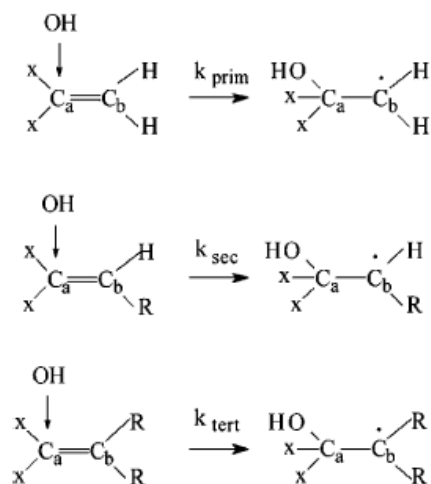


FIGURE 4.2: Site specific addition of OH to different double bonds. The reactions are ordered according to the increasing stability of the resulting organic radicals, from primary to tertiary (Peeters et al. (2007)).

possible sites to add. If the unsaturated molecule being considered is asymmetric with respect to the double bond, OH addition to one of the two carbon atoms is expected to be preferred. Experimental data on both rate coefficients and branching ratios for major compounds like isoprene (see Sec.4.3.9.2) and methacrolein (see Sec.4.3.9.1) are available. However, many products of isoprene oxidation have not been studied yet and a SAR is needed to estimate their reactivity.

Peeters et al. (2007) recently developed a site-specific SAR for polyalkenes at 298 K. It was established that $k_{\text{OH,add}}$ can be approximated well by the sum of individual rate constants that depend solely on the stability of the alkyl radicals being formed (see Fig. 4.2). In fact, from quantum mechanical calculations it is known that the OH first forms a π complex with the alkene through a barrierless association reaction. The electron density of the pre-reactive π complex is affected by the substituents. These substituents affect the energy of the (late) transition states that bring to the radicals. The substituents that affect the energy of one transition state do not affect significantly the energy of the second possible one. For each double bond there are two transition states and their relative energies (stabilities) affect the branching ratios of radical production from OH-addition.

This means that the following simple formula for non-conjugated polyalkenes ¹ can be used:

$$k_{OH,add} = p k_{prim} + s k_{sec} + t k_{tert}$$

where p , s and t are the number of possible primary, secondary and tertiary radicals that can be formed from OH addition and k_{prim} , k_{sec} and k_{tert} from Peeters et al. (2007) are listed in Tab. 4.1.

The present SAR shows that the OH addition that forms the most stable alkyl radical is also the fastest. Hence, one does not need to make any additional assumptions about the branching ratios. This SAR is only for alkenes that do not include functional groups. However, many oxygenated unsaturated compounds arise from isoprene oxidation. In fact, functional groups like $>C=O$ and $-CH_2OH$ that are next to double bonds affect the rate of OH addition. Therefore, I extend the SAR by Peeters et al. (2007) following the approach of Atkinson (1987) that make use of “group substituents factors”. I assume that each substituent does not affect the branching ratios of the addition and calculate these factors as ratios of the well known rate constants of the compound bearing the “substituent” and of its associated parent alkene (Atkinson and Arey (2003a)). For instance, the substituent factor for the group $CH_3C(=O)$ is calculated taking the rate constants of methyl vinyl ketone and propene. Substituent factors are needed only for groups other than H or alkyl groups. For an alkene of formula $XCH=CYZ$ the SAR is:

$$k_{OH,add} = F_a(X)F_a(Y)F_a(Z)(k_{sec} + k_{tert})$$

where the F_a are the substituents factors for the group X, Y and Z.

All parameters used for predicting OH addition are shown in Tab. 4.1. Because of the lack of data I assume that all substituents bearing the hydroperoxidic group ($-OOH$) have the same factors as the corresponding ones bearing the hydroxy group ($-OH$). This extended SAR has not been fully evaluated yet and future modifications are not excluded.

4.3.3 H-abstraction by OH

OH radicals can also abstract H atoms from organic molecules to form H_2O and R^\bullet alkyl radicals. Making use of the latest IUPAC recommendations I built a SAR very similar to the one by Kwok and Atkinson (1995). For a compound with the general formula XCH_2CHYCH_2Z the total abstraction reaction rate is estimated in the following manner:

¹An alkene that does not bear two or more alternating double bonds.

TABLE 4.1: Site-specific rate constants and group substituent factors of the extended SAR for OH addition to double bonds and comparison with Kwok and Atkinson (1995) (KA95). k are for 298 K and 1 bar and expressed in $\text{cm}^3 \text{molec}^{-1} \text{s}^{-1}$ and F_a is unitless.

Parameters	KA95	this study	source ^a
k_{prim}	–	0.45×10^{-11}	0.5 k_{ethene}
k_{sec}	–	3.00×10^{-11}	0.5 $k_{2-butene}$
k_{tert}	–	5.50×10^{-11}	0.5 $k_{2,3-dimethyl-2-butene}$
$k_{prim} + k_{sec}$	2.63×10^{-11}	3.45×10^{-11}	
$k_{prim} + k_{tert}$	5.14×10^{-11}	6.05×10^{-11}	
$k_{sec} + k_{tert}$	8.69×10^{-11}	8.50×10^{-11}	
$F_a(-C(O)CH_3)$	0.90	0.76	$k_{MVK}/k_{propene}$
$F_a(-CHO)$	0.34	0.31	$\frac{k_{methacrolein}^{add}}{k_{2-methylpropene}}$
$F_a(-C(O)OONO_2)$	–	0.56	$k_{MPAN}/k_{2-methylpropene}$
$F_a(-CH_2OH)$	1.6	1.7	$k_{2-propene-1-ol}/k_{propene}$
$F_a(>CHOH)$	1.6	2.2	$k_{1-pentene-3-ol}/k_{1-pentene}$
$F_a(>C(OH)-)$	1.6	2.2	$\frac{k_{3-methylbut-1-en-3-ol}}{k_{3,3-dimethyl-1-butene}}$
$F_a(-CH_2ONO_2)$	0.47	0.64 ^b	$\frac{k_{O_2NOCH_2C(CH_3)=CHCH_2OH}}{F_a(-CH_2OH) k_{2-methyl-2-butene}}$

^a k_{prim} , k_{sec} and k_{tert} are taken from Peeters et al. (2007), the k for the oxygenated alkenes are taken from the IUPAC recommendations and the k for the simple alkenes are taken from Atkinson and Arey (2003a)

^b Taken from Paulot et al. (2009a)

$$k_{OH,abst} = k_{OH,C^1} + k_{OH,C^2} + k_{OH,C^3}$$

where C^1 , C^2 and C^3 are the carbon atoms from left to right in the formula and each term of the previous equation is expressed as:

$$\begin{aligned} k_{OH,C^1} &= F(-X) F(-CHYR) k_s \\ k_{OH,C^2} &= F(-CH_2X) F(-CH_2Z) F(-Y) k_t \\ k_{OH,C^3} &= F(-CHYR) F(-Z) k_s \end{aligned}$$

where k_s and k_t are the rate coefficients specific for secondary and tertiary H atoms, respectively. The substituent factors (F) are analogues to the ones in the SAR for OH addition. It is assumed that $F(-CH_3)$ is 1 and the substituent factors for all other groups are calculated relative to it. The details of the SAR and its comparison to Kwok and Atkinson (1995) are shown in Tab. 4.2.

The abstraction of H atoms from the hydroxy group is assumed to have the rate coefficient of the following reaction as recommended by IUPAC.

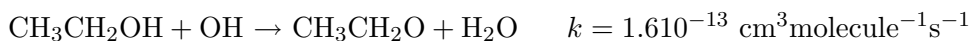


TABLE 4.2: Parameters of the new SAR for H abstraction by OH and comparison with the one by Kwok and Atkinson (1995) (KA95). k_p , k_s and k_t are the rate constants for the $-\text{CH}_3$, $-\text{CH}_2-$ and $> \text{CH}-$ groups. They are given for 298 K and 1 bar and expressed in $\text{cm}^3 \text{molec}^{-1} \text{s}^{-1}$ and F is unitless.

Parameters	KA95	this study	source ^a
k_p	1.36×10^{-13}	1.24×10^{-13}	$1/2k_{\text{ethane}}$
k_s	9.34×10^{-13}	8.42×10^{-13}	$k_{\text{propane}} - k_{\text{ethane}}$
k_t	1.94×10^{-12}	1.75×10^{-12}	$k_{2\text{-methylpropane}} - 3/2k_{\text{ethane}}$
$F(-\text{CH}_3)$	1.00	1.00 ^b	
$F(-\text{CH}_2-)$	1.23	1.23 ^b	
$F(> \text{CH}-)$	1.23	1.23 ^b	
$F(> \text{C} <)$	1.23	1.23 ^b	
$F(=\text{O})$	8.70	8.15	$\frac{k_{\text{CH}_3\text{CHO}+\text{OH}\rightarrow\text{CH}_3\text{CO}}}{k_t}$
$F(-\text{C}(=\text{O})\text{R})$	0.75	0.73	$\frac{k_{\text{CH}_3\text{COCH}_3}}{k_{\text{ethane}}}$
$F^{\text{sec}}(-\text{OH})$	3.50	3.44	$\frac{k_{\text{CH}_3\text{CH}_2\text{OH}+\text{OH}\rightarrow\text{CH}_3\text{CHOH}}}{k_s}$
$F^{\text{tert}}(-\text{OH})$	3.50	2.68	$\frac{k_{2\text{-propanol}} - 2k_p - k_{\text{ROH}+\text{OH}\rightarrow\text{RO}}}{k_{2\text{-methylpropane}} - 3k_p}$
$F^{\text{sec}}(-\text{OOH})$	–	18.13	$\frac{F^{\text{sec}}(-\text{OH}) k_{\text{CH}_3\text{OOH}+\text{OH}\rightarrow\text{CH}_2\text{OOH}}}{k_{\text{CH}_3\text{OH}+\text{OH}\rightarrow\text{CH}_2\text{OH}}}$
$F^{\text{tert}}(-\text{OOH})$	–	14.12	$\frac{F^{\text{tert}}(-\text{OH}) F^{\text{sec}}(-\text{OOH})}{F^{\text{sec}}(-\text{OH})}$
$F(-\text{CH}_2\text{OH})$	1.23	1.29	$\frac{k_{\text{CH}_3\text{CH}_2\text{OH}+\text{OH}\rightarrow\text{CH}_2\text{CH}_2\text{OH}}}{k_p}$
$F^{\text{t}}(-\text{CH}_2\text{OH})^{\text{c}}$	–	0.53	$\frac{k_{\text{HOCH}_2\text{CHO}+\text{OH}\rightarrow\text{HOCH}_2\text{CO}}}{k_t F(=\text{O})}$
$F(-\text{CHO})$	0.75	0.55	$\frac{k_{\text{HOCH}_2\text{CHO}+\text{OH}\rightarrow\text{HOCHCHO}}}{k_p F_s(\text{OH})}$
$F(-\text{COOH})$	0.74	1.67	$\frac{k_{\text{CH}_3\text{COOH}+\text{OH}\rightarrow\text{CH}_2\text{COOH}}}{k_p}$
$F(-\text{ONO}_2)$	0.04	0.04 ^b	
$F(-\text{CH}_2\text{ONO}_2)$	0.20	0.20 ^b	
$F^{\text{sec}}(\text{allyl})$	1	3.6 ^d	

^a the k for the simple alkanes are taken from Atkinson and Arey (2003a) and k for the oxygenated saturated compounds are taken from the IUPAC recommendations

^b not updated and taken from Kwok and Atkinson (1995)

^c in cases the group $-\text{CH}_2\text{OH}$ is attached to aldehydic carbons

^d calculated using the results by Vereecken and Peeters (2001)

Finally, the H abstraction from methyl groups ($-\text{CH}_3$) and vinyl groups ($-\text{CH}=\text{CH}_2$) is usually neglected because the rate constants are very low. For a methyl group attached to a general alkyl my SAR estimates a group rate constant of $1.5 \cdot 10^{-13} \text{ cm}^3 \text{ molecule}^{-1} \text{ s}^{-1}$. In the mechanism H abstraction from methyl groups is considered only for the reactions of OH with CH_3OH and CH_3OOH , for which the experimental values recommended by IUPAC are used.

TABLE 4.3: Comparison of predicted (this study and Kwok and Atkinson (1995)) with experimental rate constants (k_{OH}) for selected organic compounds at 298 K and 1 bar. k_{OH} is expressed in $\text{cm}^3\text{molecule}^{-1}\text{s}^{-1}$.

Compound	$k_{OH}^{exp.}$	err.(%) KA95	err.(%) new SAR
HOCH ₂ CHO	8.0×10^{-12} a	166	16.4
HCOCHO	9.7×10^{-12} a	161	62
CH ₃ CH ₂ CH ₂ OH	5.8×10^{-12} a	-6	-12
CH ₃ C(=O)CH=CH ₂ (MVK)	2.0×10^{-11} a	19	31.5
CH ₃ CH ₂ CH ₂ CHO	2.4×10^{-11} a	-4.6	-20
(CH ₃) ₂ COHCH=CH ₂	6.3×10^{-11} a	-32	21
HOCH ₂ CH=C(CH ₃)CH ₂ ONO ₂	9.5×10^{-11} b	-27	8
HOCH ₂ CH=C(CH ₃)CHO	1.1×10^{-10} b	-38	19

^a recommended by IUPAC

^b from isoprene whose k_{OH} was experimentally estimated by Paulot et al. (2009a)

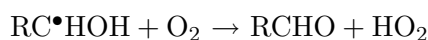
4.3.4 Reaction with OH: measurements vs. predictions

A comparison of the SAR's predictions with the experimental rate constants for selected compounds is shown in Tab. 4.3. A clear improvement is seen for C₅ unsaturated multi functional compounds from isoprene. Contrary to the old SAR, there is a tendency for the new one to overestimate the k_{OH} of these species. Overall the new SAR performs better mainly for two reasons. The first one is obviously the fact that it has been built with the most recent data available. The second is the reliance on a recent SAR for OH addition that makes use of both recent experimental and quantum chemistry data.

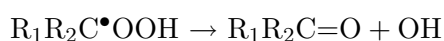
H-abstraction for isoprene is predicted to be negligible (Atkinson et al. (1989)). Isoprene undergoes almost entirely OH-addition because of its two conjugated double bonds. I have not shown the SARs parameters for structures having conjugated double bonds since isoprene is the only compound in the mechanism of such kind. Furthermore, its reaction with OH has been well studied and the IUPAC recommends a rate constant of $1.0 \times 10^{-10} \text{ cm}^3\text{molecule}^{-1}\text{s}^{-1}$. Both my new SAR and the one by Kwok and Atkinson (1995) fit well the IUPAC value, estimating similar values of 1.05 and $0.955 \times 10^{-10} \text{ cm}^3\text{molecule}^{-1}\text{s}^{-1}$. The temperature-dependent expression for its rate constant recommended by IUPAC is used in this mechanism.

4.3.5 Alkyl radicals

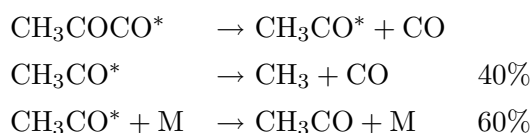
Both abstraction and addition by OH produce alkyl radicals (R^\bullet). They generally react with O_2 with high pseudo-unimolecular rate constants of ($k \cdot [O_2] > 1 \times 10^7 s^{-1}$). α -hydroxy radicals ² undergo the following general reaction:



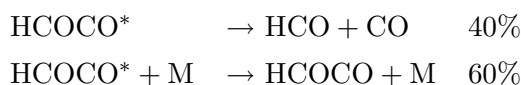
The most common fate of alkyl radicals is the exothermic O_2 -addition to form excited peroxy radicals (RO_2^*). Their fate is discussed in Sec. 4.3.6. In some cases, even if thermalized, RO_2 is unstable enough to undergo fast decomposition before other reactions can take place. One case is the thermal decomposition of α -hydroperoxy radicals promptly giving OH back as predicted by Vereecken et al. (2004):



The other case involves the acyl radicals ($R_1R_2R_3CCO$). When they are produced by H abstraction they have excess energy because of the exothermicity of such reactions. According to Baeza-Romero et al. (2007) the CH_3COCO^* radical, resulting from reaction of methyl glyoxal with OH, has an excess energy of about 30 kcal mol^{-1} . This energy is sufficient for the radical to lose CO fragments in the following way:



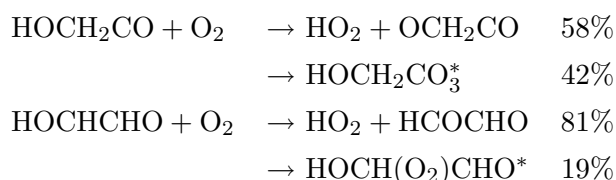
The energized α -dicarbonyl radical ($HCOCO^*$) from the reaction of glyoxal with OH has also been shown to decompose promptly to CO and HCO (Niki et al. (1983), Orlando and Tyndall (2001)). In these studies it is stated that unimolecular decomposition competes with the reaction with O_2 . However, in light of the study by Baeza-Romero et al. (2007), it is more likely that decomposition competes with collisional stabilization instead. Therefore, I assume that at 298 K and 933 mbar



Then the HCO and HCOCO radicals reacts with O_2 to give $HO_2 + CO$ and $HCOCO_3^*$ (Sec. 4.3.6.4), respectively.

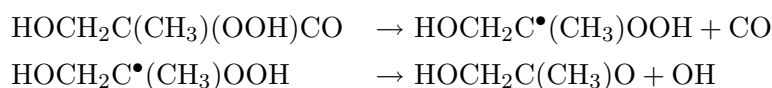
²Greek letters are used to specify the relative position of a functional respect to another. Denoting with α the carbon atom bearing the reference functional group, the other carbon atoms next to it are denoted as β , γ , δ etc., progressively.

Reaction of glycoaldehyde with OH and decomposition of alkoxy radicals from isoprene produce the acyl radical HOCH_2CO^* . It has been predicted to have a too slow decomposition under atmospheric conditions (Mereau et al. (2001)). Butkovskaya et al. (2006a) confirmed this arguing that the slow HCHO formation was incompatible with decomposition. After collisional stabilization, reaction with O_2 takes place yielding significant amounts of HO_2 . Butkovskaya et al. (2006a) also determined the fate of the second alkyl radical HOCHCHO from glycolaldehyde oxidation. These two alkyl radicals undergo H-abstraction and addition by O_2 with following branching ratios:



The product OCH_2CO of the first reaction decomposes to HCHO and CO. The excited peroxy radicals $\text{HOCH}_2\text{CO}_3^*$ and $\text{HOCH}(\text{O}_2)\text{CHO}^*$ undergo decomposition as described in Sec. 4.3.6.5 and 4.3.6.6, respectively. Similar mechanistic insights have also been determined in the reaction of hydroxyacetone with OH (Butkovskaya et al. (2006b)).

Another important excited radical is $\text{HOOCH}_2\text{CO}^*$. It is produced during the oxidation of acetaldehyde and the decomposition of the Criegee intermediate $\text{CH}_3\text{CH}=\text{O}^+-\text{O}^-$ (see Sec. 4.4). The same radical with similar excess energy is also produced by H abstraction of HOOCH_2CHO , a species that is not considered by the MCM. Kuwata et al. (2003, 2005) calculated that $\text{HOOCH}_2\text{CO}^*$ undergoes unimolecular decomposition quantitatively producing $\text{HCHO} + \text{CO} + \text{OH}$. The effect of hydroxy and hydroperoxy groups has also been studied for acyl radicals. Mereau et al. (2001) studied the radical $(\text{CH}_3)_2\text{C}(\text{OH})\text{CO}$ and predicted a loss of CO with a 78% yield. Kuwata et al. (2005) studied the fate of $\text{HOOCH}(\text{CH}_3)\text{CO}^*$ originating from vinoxy radicals + O_2 . Even in this case the quantitative unimolecular decomposition yielding OH was predicted. Compared to $\text{HOOCH}_2\text{CO}^*$, the presence of the methyl group lowered the decomposition energy barrier by $1.7 \text{ kcal mol}^{-1}$. The acyl radical from the hydroperoxide of methacrolein bears two alkyl groups and one HOO-group and therefore decomposition is likely to take place:

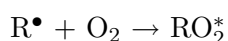


Hence, I assume that both $\text{R}_1\text{R}_2\text{C}(\text{OH})\text{CO}$ and $\text{R}_1\text{R}_2\text{C}(\text{OOH})\text{CO}$ radicals decompose by losing a CO, with the latter ones producing α -hydroperoxy radicals that in turn decompose yielding OH and a ketone.

4.3.6 Excited RO₂ radicals

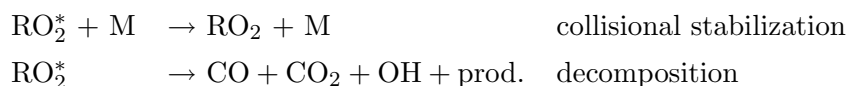
4.3.6.1 General atmospheric fate

Under atmospheric conditions most of the R• radicals react quantitatively with O₂ in the following manner:



where RO₂* is the excited peroxy radical.

The reaction is highly exothermic and it leads to the formation of excited peroxy radicals. The excess energy is in the range of 33-37 kcal mol⁻¹ (Clifford et al. (1998)). This energy must be dissipated in one way or another. In fact, they can either undergo collisional stabilization or decomposition.

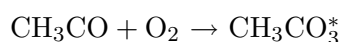


The competition between the two processes is obviously a function of density and less of temperature. At constant temperature, as pressure decreases the branching ratio of the decomposition becomes more important for RO₂* that forms during the oxidation of acetaldehyde (see Sec. 4.3.6.2). In the oxidation of glycolaldehyde, a decrease in temperature results in an increase of the fraction of excited radicals undergoing decomposition (see Sec. 4.3.6.6 and 4.3.6.5).

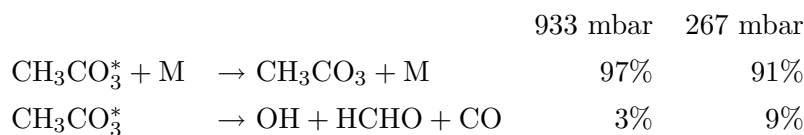
In the past years some experimental studies have shown how decomposition is an important pathway for RO₂ having 2 or 3 carbon atoms. Often this decomposition produces OH radicals. Peroxy radicals with 4 and 5 C atoms are unlikely to undergo decomposition. In the case of isoprene + OH, their formation is significantly less exothermic, 19-24 kcal mol⁻¹, than regular alkyl + O₂ reactions (Lei et al. (2001)). The low exothermicity of the reaction and the bigger size of such radicals make collisional stabilization the fastest process under tropospheric conditions. In the next section the relatively new chemistry of some major C₂-C₃ products of isoprene oxidation is discussed.

4.3.6.2 CH₃CO₃* radical

Oxidation of acetaldehyde with OH and decomposition of major alkoxy radicals from isoprene produce the acetyl radical, CH₃CO. In the atmosphere this radical undergoes the following reaction:



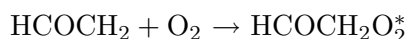
The atmospheric fate of the resulting excited intermediate has been determined in a few experimental studies ([Blitz et al. \(2002\)](#), [Butkovskaya et al. \(2004\)](#), [Carr et al. \(2008\)](#), [Tyndall et al. \(1997\)](#)). [Carr et al. \(2008\)](#) studied these reactions as function of pressure measuring OH directly with He as bath gas. At 300 K they determined the following branching ratios:



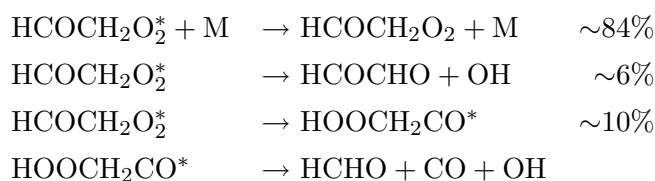
For the present purposes I adopt the branching ratios at 933 mbar pressure as a good approximation for the ones at 1 bar.

4.3.6.3 HCOCH₂O₂^{*} radical

This excited peroxy radical is produced by the reaction between O₂ and vinoxy radicals:



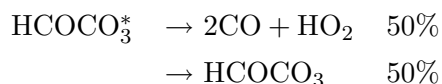
Vinoxy radical is in turn produced in the reaction of acetaldehyde with O and in the decomposition of a Criegee intermediate (see Sec.4.4). Based on previous experimental studies by [Gutman and Nelson \(1983\)](#) and [Zhu and G.Johnston \(1995\)](#), [Butkovskaya et al. \(2004\)](#) implemented the fate of this radical in a mechanism for the oxidation of acetaldehyde at 267 mbar. This included two channels for the decomposition with a combined yield of 38%. However, [Kuwata et al. \(2003\)](#) give theoretically a decomposition yield of 58% and 25% at 200 and 1 bar, respectively. Even though at 267 mbar the yields from the two studies differ significantly, it seems reasonable to use the yield of [Butkovskaya et al. \(2004\)](#) scaled by the reduction from 267 to 1000 mbar calculated by [Kuwata et al. \(2003\)](#). Therefore, I implemented the following branching at 1 bar pressure:



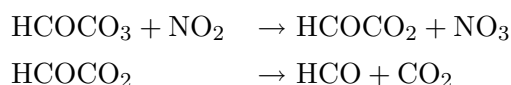
The excited radical HOOCH₂CO^{*} decomposes to give HCHO + CO + OH (see Sec. 4.3.5).

4.3.6.4 HCOCO₃^{*} radical

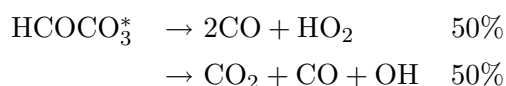
This radical is formed from the reaction of O₂ with the thermalized HCOCO radical. The latter can be formed in two ways. The first is by decomposition of multifunctional alkoxy radicals from isoprene oxidation. The second and most important way is by the reaction of HCOCHO with OH. This reaction produces an energetic HCOCO^{*} radical that to a large extent is collisionally stabilized (see Sec. 4.3.5). At 298 K and 933 mbar, Niki et al. (1983) and Orlando and Tyndall (2001) determined its fate to be:



In that study no PAN-like compound from the reaction HCOCO₃ + NO₂ could be detected and the following reactions were assumed:

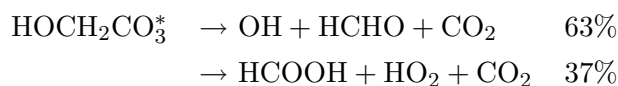


Unlike Orlando and Tyndall (2001), Feierabend et al. (2008) studied the reaction of glyoxal with OH monitoring the latter by direct detection. They could determine a 30% maximum OH-reformation varying pressure (max. 267 mbar) and 21% O₂). This number is very similar to the branching ratio of the CO₂-forming channel (Orlando and Tyndall (2001)). Therefore, I consider it very likely that OH is produced together with CO₂. I assume that under atmospheric conditions the HCOCO₃^{*} radical is not collisionally stabilized and undergoes a complete decomposition following the mechanism:



4.3.6.5 HOCH₂CO₃^{*} radical

Butkovskaya et al. (2006a) explained the fate of this excited peroxy radical looking at the O₂-adducts that are formed with two conformers of the HOCH₂CO radicals. They estimated HOCH₂CO₃^{*} radicals complete decomposition with the two following channels:



4.3.6.6 HOCH(O₂)CHO^{*} radical

The HOCH(O₂)CHO^{*} is produced during the OH-initiated oxidation of glycolaldehyde and the decomposition of some alkoxy radicals and the Criegee intermediate HOCH₂CH=O⁺O⁻

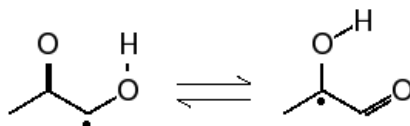
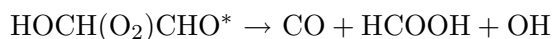


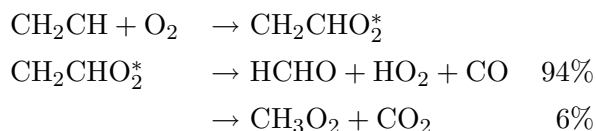
FIGURE 4.3: Tautomeric equilibrium between the two forms for the radical from the reaction of OH with hydroxyacetone.

(4.4.2.4). [Butkovskaya et al. \(2006a\)](#) inferred its fate to involve a 1,4-H shift followed by decomposition:



4.3.6.7 Vinyl peroxy radical ($\text{CH}_2=\text{CHO}_2^*$)

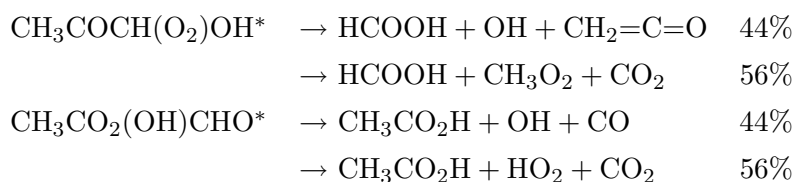
This radical comes from the degradation of acrolein ($\text{CH}_2=\text{CHCHO}$) and the photolysis of MVK (Sec. 4.5.3). Its fate is represented according to the results of [Feng and Wang \(2002\)](#) and Orlando (pers. comm.):



4.3.6.8 $\text{CH}_3\text{COCH(O}_2\text{)OH}^*$ and $\text{CH}_3\text{CO}_2(\text{OH})\text{CHO}^*$ radicals

The reaction of hydroxyacetone with OH produces the alkyl radical $\text{CH}_3\text{COC}^*\text{HOH}$. This radical can exist in two tautomeric forms³ that equilibrates very quickly (see Fig. 4.3). Therefore, reaction with O_2 produces two excited peroxy radicals. Their chemistry has been determined by [Butkovskaya et al. \(2006b\)](#) as producing formic and acetic acid along with some OH. Their fate is presented below:

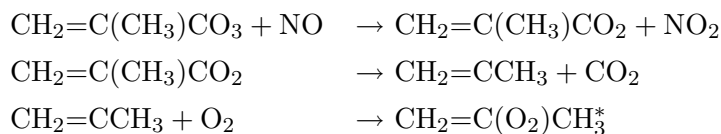
³Tautomerism - the existence of two or more chemical compounds that are capable of facile inter-conversion, in many cases merely exchanging a hydrogen atom between two other atoms, to either of which it forms a covalent bond. Unlike other classes of isomers, tautomeric compounds exist in mobile equilibrium with each other, so that attempts to prepare the separate substances usually result in the formation of a mixture that shows all the chemical and physical properties to be expected on the basis of the structures of the components ([Encyclopaedia Britannica](#)).



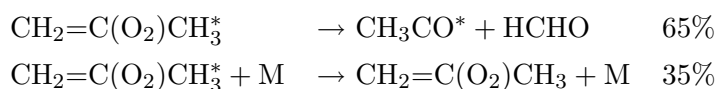
An analogy is assumed for C₃ radicals for which the CH₃- is substituted by HOCH₂-, HOOCH₂ and HCO-. In light of many experimental results it seems likely that C₄ and C₅ excited peroxy radicals do not undergo such decomposition but rather fast stabilization.

4.3.6.9 Methyl vinyl peroxy radical (CH₃C(O₂)=CH₂^{*})

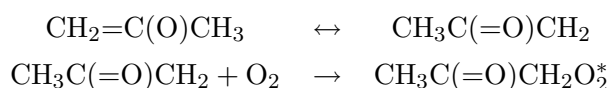
This alkyl radical is originated by loss of CO₂ from the acyl RO₂ of methacrolein (see Sec. 4.3.9.1). The mechanism of its formation and degradation is given below (Orlando et al., 1999).



The way the resulting RO₂^{*} radicals dissipate the excess energy has also been inferred. About 65% is by decomposition. The remaining 35% is thought to be either another decomposition or a collisional stabilization. However, the second decomposition proposed is unlikely to happen because of the higher number of atoms that makes the stabilization easier as in the case of RO₂^{*} from glycolaldehyde and hydroxy acetone oxidation (Sec. 4.3.6). Therefore, the degradation mechanism is likely to be the following.



where CH₂=C(O₂)CH₃ undergoes the standard reactions of stabilized RO₂ and the species CH₃CO^{*} decomposes into CH₃ + CO because it is produced in vibrationally hot state. The fate of the corresponding alkoxy radical (CH₂=C(O)CH₃) is understood by writing its second and more important resonance structure ⁴, CH₃C(=O)CH₂, that is a closer representation of its actual structure. This resonance form turns out to be the same alkyl radical from the reaction of acetone with OH.



⁴Theory of resonance - in chemistry, theory by which the actual normal state of a molecule is represented not by a single valence-bond structure but by a combination of several alternative distinct structures. The molecule is then said to resonate among the several valence-bond structures or to have a structure that is a resonance hybrid of these structures ([Encyclopaedia Britannica](#)).

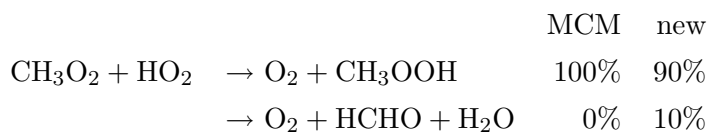
Finally, the species CH_3CO^* is produced in vibrationally hot state and decomposes into $\text{CH}_3 + \text{CO}$.

4.3.7 Stabilised RO_2

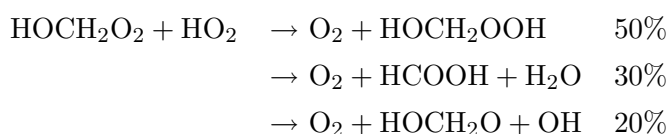
4.3.7.1 Reaction with HO_2

Until recently, $\text{RO}_2 + \text{HO}_2$ reactions were thought only to be radical terminating reactions yielding stable products. Some experimental studies have shown that the reaction between RO_2 and HO_2 is often a radical propagating reaction. In fact, alkoxy radicals along with OH are produced in significant fractions. Below I describe the new branching ratios for the reactions of some important peroxy radicals.

[Elrod et al. \(2001\)](#) studied the reaction of methyl peroxy radical (CH_3O_2) with HO_2 and found a 10% yield of HCHO. They also found this yield to increase as the temperature decreases reaching about 30% at 218 K. This new channel is expected to significantly modify the modeled HCHO mixing ratios and to accelerate the HO_x production due to photolysis of HCHO itself. The two channels are described below.

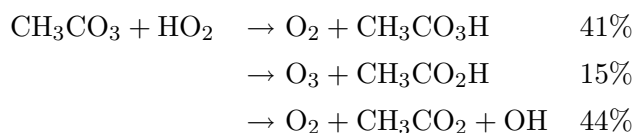


The reaction of HOCH_2O_2 with HO_2 at 296 K was recently studied by [Jenkin et al. \(2007\)](#). OH and formic acid (HCOOH) were found to be produced with a 20% and 50% yield, respectively. A complete description of all the channels is presented below.



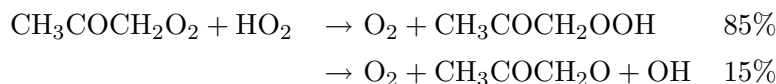
where the radical HOCH_2O reacts with O_2 to give $\text{HCOOH} + \text{HO}_2$.

The reaction of peroxy acetyl radical (CH_3CO_3) with HO_2 was investigated in great detail by three studies ([Dillon and Crowley \(2008\)](#), [Hasson et al. \(2004\)](#), [Jenkin et al. \(2007\)](#)). Contrary to previous knowledge, OH was found to be the major product (44%). The reaction undergoes three channels described as:



where CH_3CO_2 decomposes to CH_3 and CO_2 .

The reaction of acetoxy radical ($\text{CH}_3\text{COCH}_2\text{O}_2$) with HO_2 was recently studied by [Hasson et al. \(2004\)](#), [Jenkin et al. \(2007\)](#) and [Dillon and Crowley \(2008\)](#). Only two channels were identified:



In light of the experimental results presented above, I apply a structure-reactivity analogy for all RO_2 produced in the oxidation of isoprene. In particular, I assume that RCO_3 and RCOCH_2O_2 peroxy radicals react with HO_2 in the same way as CH_3CO_3 and $\text{CH}_3\text{COCH}_2\text{O}_2$, respectively. However, due to the large size of the mechanism being developed, the formation of many $\text{C}_{4-5}-\text{RCO}_2\text{H}$ has often been neglected.

4.3.7.2 Reaction with NO

The reaction rates as estimated by the MCM protocol ([Saunders et al. \(2003\)](#)) are maintained. These reactions mostly convert peroxy to alkoxy radicals. Often other products such as alkyl nitrates are produced in which the NO radical adds to the RO_2 molecule. The MCM makes use of a well established method (a SAR) to determine the branching ratio of these two channels. Recently, new alkyl nitrates yields from the first peroxy radicals from isoprene, MVK and MACR have been estimated in a very detailed chamber study ([Paulot et al. \(2009a\)](#)). These yields have been determined to be significantly different from the ones used in the MCM. For instance, the internally double bonded RO_2 from OH addition to isoprene has been estimated to yield about 24% of alkyl nitrate in the reaction with NO. For the same species MCM assigns a much lower yield of 8.9%. On the other hand, the externally double bonded RO_2 have a alkyl nitrate yield of 6.7% was estimated. However, the total average alkyl nitrate yield from [Paulot et al. \(2009a\)](#) and MCM are 11.7 and 10% , respectively. Furthermore, the MCM does not consider any alkyl nitrate deriving from MACR and only one isomer of alkyl nitrate from MVK with a 1.7% yield. [Paulot et al. \(2009a\)](#) reports alkyl nitrate yields of 15 and 11% for MACR and MVK, respectively. Hence, these higher and new alkyl nitrate yields are adopted.

The MCM treatment of the unsaturated C_5 -nitrates neglects OH-addition to double bonds is considered. Instead, only OH abstraction is considered leading to a 100% NO_2 -recycling in one-step. This has important consequences for the NO_x recycling efficiencies in isoprene chemistry under polluted regimes ([Ito et al. \(2009\)](#)). [Paulot et al. \(2009a\)](#) also gained mechanistic information about the fate of these alkyl nitrates establishing that OH addition is the dominant pathway. This implies a much lower NO_x recycling efficiency (55%) in comparison to MCM (100%). However, this new chemistry is beyond

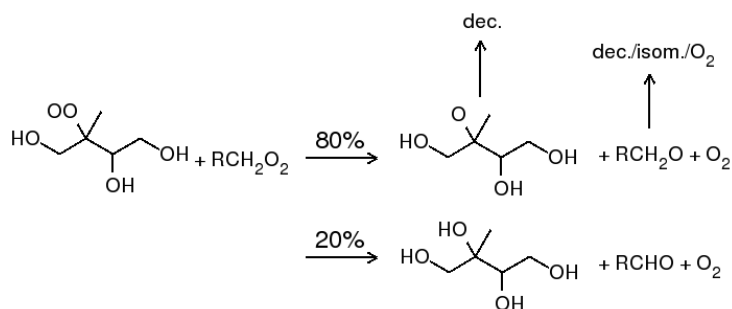


FIGURE 4.4: Example of homogeneous gas-phase production of tetrols in isoprene oxidation involving reactions between peroxy radicals.

the scope of this study and will be implemented in the future in order to study the ozone production due to isoprene in polluted environments.

4.3.7.3 Reaction with other RO₂ and NO₃

The reactions with other peroxy radicals and with nitrate radical are treated following the MCM protocol (Saunders et al. (2003)). Applying the development protocol to the RO₂ from isoprene hydroperoxides led to the production and treatment of tetrols⁵ that were recently measured in the atmosphere (Claeys et al. (2004a,b)). Heterogeneous reaction mechanisms involving organic aerosols have been proposed by Edney et al. (2005) and Böge et al. (2006b). The homogeneous gas-phase mechanism here developed involves reactions of RO₂ bearing 3 hydroxy groups with all other peroxy radicals. For one of the four possible C₅-RO₂ the tetrol is produced with a 20% yield as described in Fig. 4.4.

4.3.7.4 Peroxy ring-closure

Under very low-NO_x regimes peroxy radicals have a lifetime of about $1 - 3 \times 10^{-2} s^{-1}$ against the traditional reactions with NO, HO₂ and RO₂. For these conditions, Vereecken and Peeters (2004) predicted that some unsaturated RO₂ from terpenes may undergo a non-traditional peroxy ring-closure. The mechanism is the intramolecular version of the

⁵Compounds bearing four hydroxy groups (-OH).

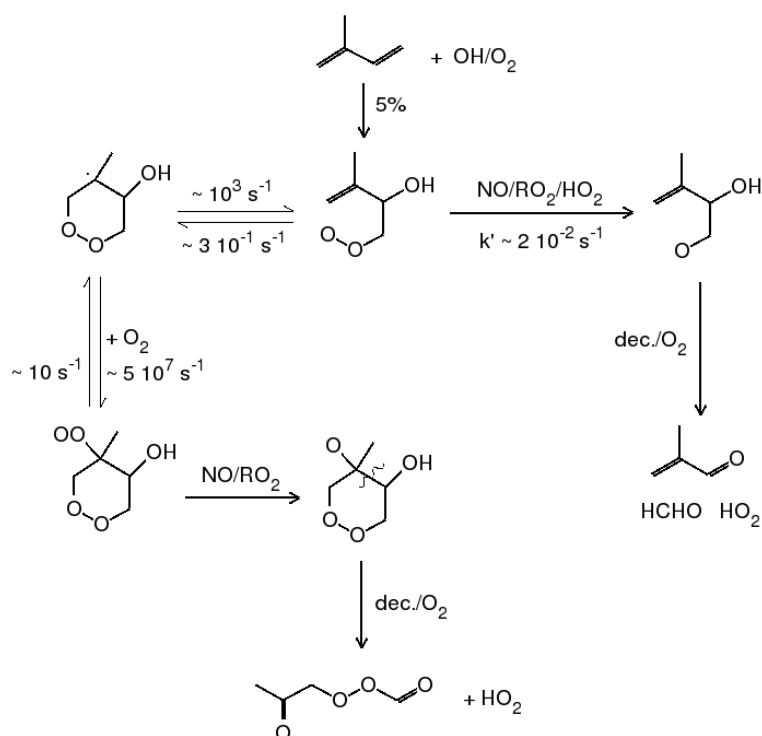


FIGURE 4.5: Competition between peroxy ring-closure and reactions with other radicals for one isomer of the peroxy radicals from isoprene under very low-NO_x. Numbers close to arrows are the (pseudo-)unimolecular rate constants for the reactions indicated.

RO₂ addition to double bonds that are well-known from cool-flame combustion science (Stark (1997, 2000)). This non-traditional route has been successfully used in developing the oxidation mechanism of α -pinene, whereby acetone yields could be better explained (Capouet et al. (2004), Vereecken et al. (2007)). Among the first isoprene RO₂, two isomers can undergo such peroxy ring-closure. Its competition with the traditional pathways is shown in Fig. 4.5 for one peroxy radical. Soon after the peroxy ring-closure, very fast reaction with O₂ takes place forming an heterocyclic RO₂. The mechanism for the subsequent chemistry has been developed. The fate of the resulting heterocyclic alkoxy radical has been predicted with the help of the SAR described in the next section (Sec. 4.3.8).

4.3.8 Fate of alkoxy radicals RO[•]

The alkoxy radicals can usually undergo reaction with O₂, decomposition and isomerization. The last reaction is competitive only if the radical forms a 6-membered ring while abstracting an H atom (1,5 H-shift). This is the case for C₄ radicals. The reactions are illustrated each with their respective frequencies in Fig.4.6 for a particular alkoxy radical. The competition of the three reactions determines the number of NO to NO₂ conversions

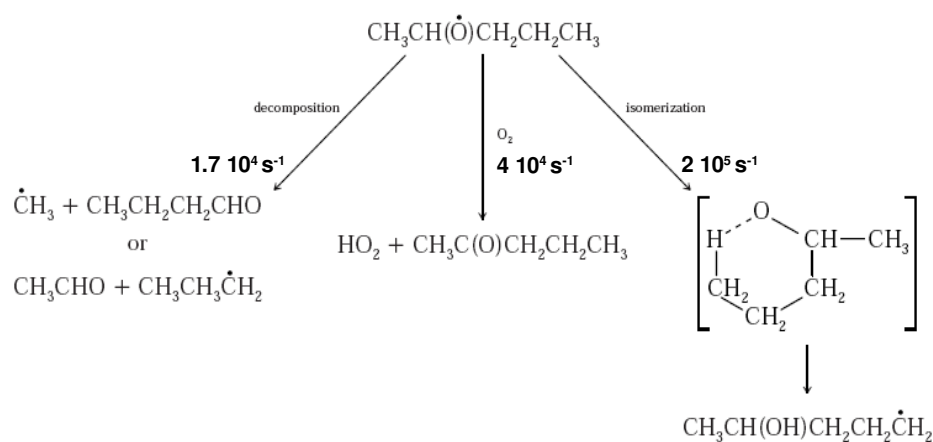


FIGURE 4.6: General fate of alkoxy radicals from VOC oxidation (Atkinson, 1997a). The reaction frequencies shown are for atmospheric conditions at 298 K and 1 bar.

in the atmospheric oxidation of organic molecules. However, this competition takes place only for radicals which are produced with little or no excess energy. This is not the case for alkoxy radicals resulting from $\text{RO}_2 + \text{NO}$ reactions (Sec. 4.3.7.2). In fact, these reactions are calculated to be exothermic by ca. 11 kcal mol^{-1} (Mereau et al. (2000)), which is higher than decomposition barriers for all β -hydroxy and many other oxygenated RO^\cdot species. Such activated radicals undergo prompt decomposition to significant extents prior to thermalization. For instance, Orlando et al. (2000) calculated that 80% of the acetonoxo radicals $\text{CH}_3\text{C}(=\text{O})\text{CH}_2\text{O}^\cdot$ from $\text{CH}_3\text{C}(=\text{O})\text{CH}_2\text{O}_2 + \text{NO}$ reactions have sufficient energy to decompose promptly under tropospheric conditions. In the same study the decomposition barrier was also estimated to be lower than $7.5 \text{ kcal mol}^{-1}$. Furthermore, Johnson et al. (2004) proposed a SAR to estimate the fraction of alkoxy radicals from $\text{RO}_2 + \text{NO}$ reactions that are activated and undergo prompt decomposition. However, in most cases decomposition also dominates the fate of thermalized alkoxy radicals. Given the focus of my development for low- NO_x regimes, I treat the alkoxy radicals as being all thermalized. Discrimination of activated and thermalized ones will be subject of development in the near future. In order to estimate the dominant fate of the alkoxy radicals I make use of SARs. For the reactions with O_2 and the isomerization I make use of the updated SARs by Atkinson (2007). The rate constants for these two processes do not vary much with changing molecules. However, the frequency for decomposition

of alkoxy radicals can vary a lot and ranges from $< 1s^{-1}$ to $10^{12} s^{-1}$. Therefore, it is critical to make good estimates of these rates. For the decomposition I use the SAR developed by [Peeters et al. \(2004\)](#) and extended by L. Vereecken for the hydroperoxy (-OOH) and nitro (-ONO₂) groups (L. Vereecken, pers. comm.). This SAR estimates the activation energy for the β C-C fission with the relationship:

$$E_b(kcal/mol) = 17.5 - 2.1 \cdot N_\alpha(alk) - 3.1 \cdot N_\beta(alk) \\ - 7.5 \cdot N_{\alpha,\beta}(-OH) - 8.0 \cdot N_\beta(=O) - 12 \cdot N_\alpha(=O) \\ - 9.5 \cdot N_{\alpha,\beta}(-OOH) - 3.1 \cdot N_\alpha(-ONO_2) - 2.7 \cdot N_\beta(-ONO_2)$$

where N is the number of substituents of one kind in position α or β relative to the alkoxy and “alk” stands for alkyl group.

If $E_b \leq 7kcal/mol$ then a correction must be applied:

$$E'_b = E_b + 0.027 \cdot (9 kcal/mol - E_b)^2$$

To calculate the rate coefficient one needs to put the value of E_b in the following formula:

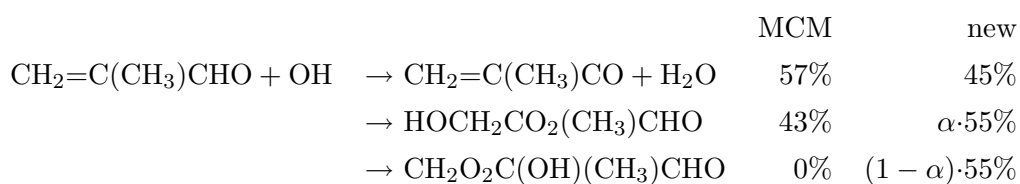
$$k(s^{-1}) = 1.8 \cdot 10^{13} \exp(-E_b/RT)$$

The SAR for the decomposition confirms experimental results that contradict the MCM for the fate of the alkoxy radical HOCH₂CO(CH₃)CH=CH₂ from isoprene. In MCM this radical is named ISOPBO and is predicted to lose a methyl group with a 25% yield of a species named MVKOH (HOCH₂COCH=CH₂). However, [Benkelberg et al. \(2000\)](#) determined that the detection of MVKOH was an erroneous identification of a peak obtained with a mass spectrometer. Therefore, HOCH₂CO(CH₃)CH=CH₂ very likely decomposes yielding 100% of MVK and HCHO.

4.3.9 Reaction of OH with major compounds

4.3.9.1 Methacrolein

The OH-initiated oxidation of methacrolein under high-NO_x has been studied in detail by [Orlando et al. \(1999\)](#). However, the mechanistic results of this valuable study have not been incorporated in MCM yet. The branching ratios in MCM and [Orlando et al. \(1999\)](#) are compared:



where $\alpha < 1$.

Using the site-specific SAR (Sec. 4.3.2) α is estimated to be about 0.92. Furthermore, [Orlando et al. \(1999\)](#) gave a lower bound of 0.85 for α . The degradation of $\text{CH}_2\text{O}_2\text{C}(\text{OH})(\text{CH}_3)\text{CHO}$ should produce the radical CH_3COHCHO . Subsequent reaction with O_2 produce methylglyoxal with a 85% yield (Sec. 4.3.6.8). The alkoxy radical from $\text{HOCH}_2\text{CO}_2(\text{CH}_3)\text{CHO}$ is predicted to yield hydroxyacetone and methyl glyoxal in a 66:34 ratio. However, the uncertainties of the SAR make this calculated ratio not robust. On the other hand, I can assume the 8% yield of methyl glyoxal ([Tuazon and Atkinson \(1990b\)](#)) to be only from the internal OH addition. Under high- NO_x , [Paulot et al. \(2009a\)](#) determined a 15% alkyl nitrate yield. Using these data and assumptions together I can calculate the branching ratio α :

$$(1 - \alpha) \cdot Y_{MGLYOX}^{CH_3COHCHO} \cdot (1 - Y_{ROONO_2}) = Y_{MGLYOX}^{MACR} \Rightarrow \alpha = 0.89$$

It follows that the hydroxyacetone yield (only from $\text{HOCH}_2\text{CO}_2(\text{CH}_3)\text{CHO}$ degradation) is $0.89 \cdot 0.55 \cdot (1 - 0.15) = 0.42$, consistent with $45 \pm 5\%$ estimated by [Tuazon and Atkinson \(1990b\)](#) and [Orlando et al. \(1999\)](#).

4.3.9.2 isoprene

Under daylight conditions, isoprene oxidation is initiated by OH to a very large extent. Its reaction with OH has little activation energy and the relative rate constant at 298 K is $1 \times 10^{-10} \text{ cm}^3 \text{ molec}^{-1} \text{ s}^{-1}$, close to the kinetic limit⁶. OH-addition to its double bonds is the dominant pathway with H-abstraction being negligible ([Atkinson et al. \(1989\)](#)). The latter one is not considered by nearly all oxidation mechanisms in use. The first isoprene products to be considered should be hydroxy alkyl radicals. However, under the widely accepted assumption that stable RO_2 are produced, they are not explicitly represented and assumed to undergo fast O_2 addition. The MCM considers only four isomeric RO_2 , though eight are possible (see Fig. 4.7). In this work the RO_2 production branching ratios from isoprene + OH is taken from the recent detailed study under high- NO_x conditions ([Paulot et al. \(2009a\)](#)). However, due to limitations of time I treat the six structural isomers⁷, for which the relative product yields are shown in Fig. 4.7. Two of these structural isomers can be present in two stereoisomers⁸ E and Z. Although [Paulot](#)

⁶The kinetic limit for a bimolecular reaction can be estimated making use of the collision frequency from the kinetic theory of gases. For a barrierless reaction ($E_a = 0$), every collision should result in a reactive event. Thus, at 298K and 1 atm, molecules having a radius of 0.2nm and molecular weight of 50 gmol^{-1} would react with a rate constant $k = 2.51 \times 10^{-10} \text{ cm}^3 \text{ molec}^{-1} \text{ s}^{-1}$ ([Finlayson-Pitts and Pitts, Jr. \(2000\)](#))

⁷In structural isomers, the atoms and functional groups are joined together in different ways.

⁸In stereoisomers the bond structure is the same, but the geometrical positioning of atoms and functional groups in space differs.

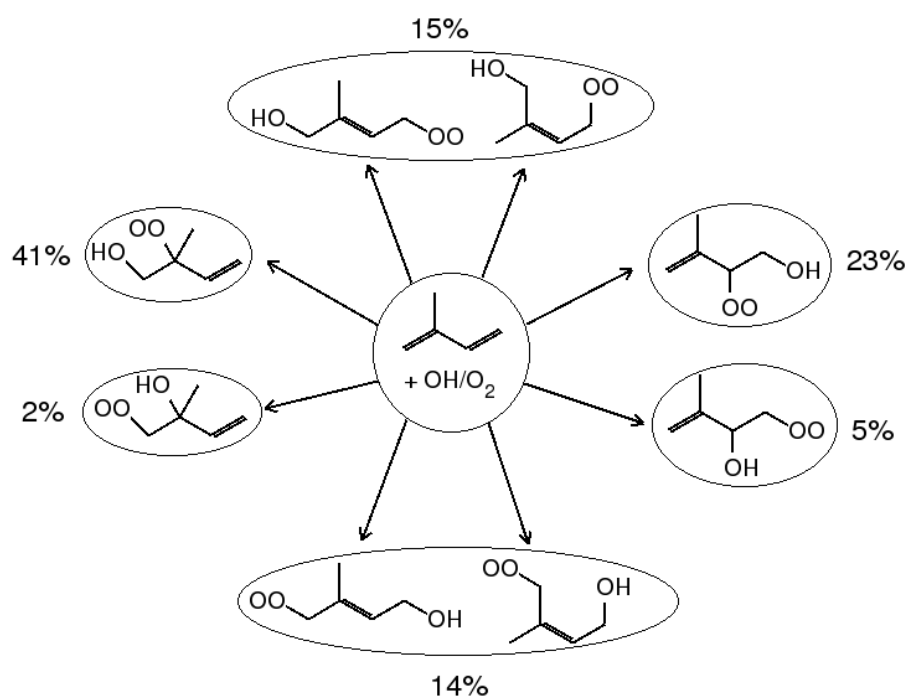


FIGURE 4.7: OH addition to isoprene, subsequent O₂ addition and RO₂ with relative yields for each isomer taken from Paulot et al. (2009a). The two pairs of RO₂ in the upper and lower part of the graph are geometric isomers and treated in the mechanism as single species.

et al. (2009a) established experimentally the E and Z isomers undergo very different pathways, their chemistry should not be crucial in explaining the high OH-recycling mechanisms and I, therefore, maintained the MCM treatment. Implementation of the new chemistry for these geometric RO₂ isomers will be implemented at a later stage. The six RO₂ here considered and their relative alkoxy radicals are treated according to the latest SARs as described in Sec. 4.3.7 and 4.3.8.

4.4 Reactions of O₃ with unsaturated VOC

4.4.1 General mechanism

The atmospheric reactions of O₃ with VOC bearing double bonds has been reviewed recently (Johnson and Marston (2008)). As shown in Fig. 4.8, they go through a [3+2] cycloaddition of ozone to the double bond to form a primary ozonide (POZ). This reaction is highly exothermic (48-60 kcalmol⁻¹) and this excess energy is retained within the adduct, leading to a very rapid decomposition of the POZ to a carbonyl and a diradical compound called Criegee intermediate. When the alkene is asymmetric

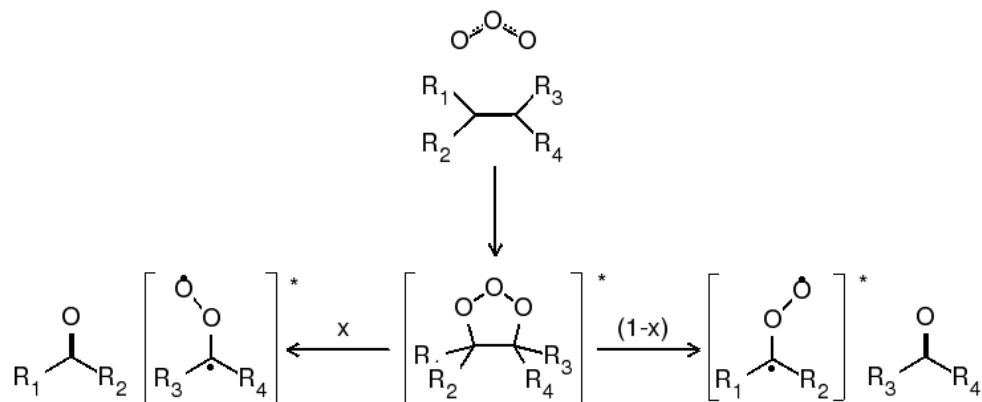


FIGURE 4.8: General mechanism of ozonolysis. The diradical species are the Criegee intermediates. R_i ($i = 1, 4$) can be either an alkyl radical or a H atom.

two channels for the POZ decomposition are possible. The Criegee intermediates are excited and very short-lived. They are usually represented as diradicals although having most of the times a more zwitterionic character (see Fig. 4.9a). The diradical and the zwitterionic form are used here interchangeably. These intermediates can exist as two conformers⁹ (Fig. 4.9b), *syn* and *anti*, that do not interconvert because the C-O bond has a significant π character (double bond). The conformation of the Criegee intermediates is very important in determining their fate (see Sec. 4.4.2).

4.4.2 Fate of Criegee intermediates

4.4.2.1 General

Criegee intermediates have a rather complex fate which involves other short-lived intermediates. They can undergo either collisional stabilization or decomposition. The latter can go *via* the “hot acid” and “hydroperoxide” channel (see Fig. 4.10). Whether one channel or the other is preferred depends critically on the size, the availability of H atoms to migrate to the external O atom and the conformation. For instance, the $\bullet\text{CH}_2\text{OO}\bullet$

⁹One of a set of stereoisomers, each of which is characterized by a conformation corresponding to a distinct potential energy minimum (IUPAC Goldbook).

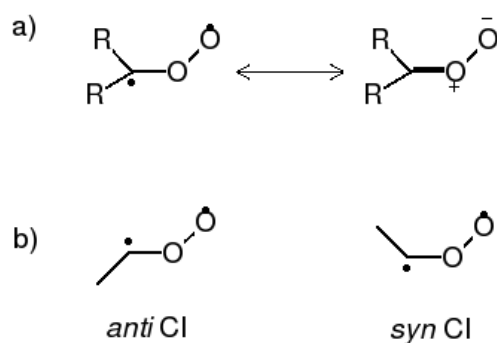


FIGURE 4.9: Criegee intermediates. a) Resonance between the diradical and the zwitterionic form. b) The conformers *syn* and *anti*.

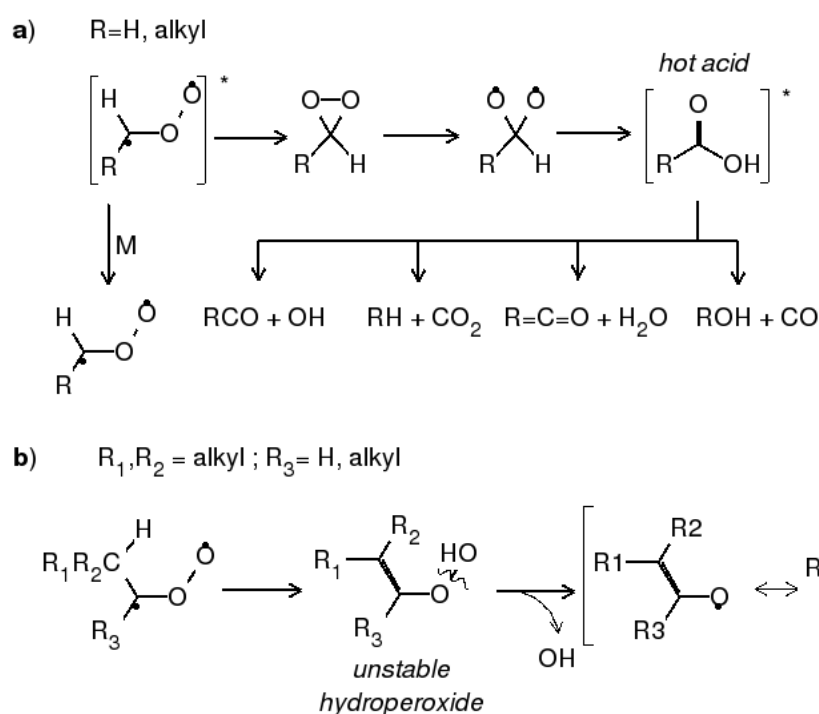


FIGURE 4.10: Possible fates of Criegee intermediates that are *anti* monosubstituted conformers (a) and *syn* monosubstituted and disubstituted conformers (b).

and *anti* monosubstituted Criegee intermediates decompose solely *via* the “hot acid” channel or under go stabilisation (see Fig. 4.10a). Instead, *syn* monosubstituted or disubstituted Criegee intermediates decompose *via* the “hydroperoxide” channel. This channel was first proposed by Niki et al. (1987) and has been corroborated by more than 20 years of research (Johnson and Marston (2008) and references therein). Recently,

time-resolved studies of OH formation from ozonolysis gained valuable mechanistic insights (Kroll et al. (2001a,b)). At atmospheric pressure OH yields were consistent with previously reported yields only at reaction times of around 1 s^{-1} , indicating the involvement of stabilized Criegee intermediates in the OH formation. The key intermediate appears to be an α, β unsaturated hydroperoxide, either excited or thermalized, that decompose producing OH and a vinoxy radical (see Fig. 4.10b). Kuwata et al. (2003) calculated that the O-O bond in vinyl hydroperoxide has a dissociation energy ($D(\text{O-O})$) of about 20 kcalmol^{-1} compared to the one of CH_3OOH being about 45 kcalmol^{-1} . The significant difference lies in the resonance stabilization of the resulting vinoxy radical. Interestingly, using the low $D(\text{O-O})$ in the expression for the thermal decomposition of CH_3OOH (Baulch et al. (2005)), I estimate that vinyl hydroperoxide has slightly less than 1 s lifetime under atmospheric conditions. Recently, Nguyen et al. (2009) calculated for a vinyl hydroperoxide from β -pinene ozonolysis that $D(\text{O-O})$ is less than 17 kcalmol^{-1} . I consider these unsaturated hydroperoxides explicitly in the mechanism. Since their lifetime is likely always less than 1 s^{-1} , I let them decompose all at the same rate with a rate constant $k = 6. \times 10^{14} \exp(-20000/(1.986 T))$. It is interesting to note that OH-initiated oxidation of MACR (Sec. 4.3.9.1) and photolysis of MVK and MACR (Sec. 4.5.3) also lead to vinyl hydroperoxides through production of vinyl radicals.

As a guide, I follow the SAR by Rickard et al. (1999) for the fate of Criegee intermediates. The SAR assumes that OH is produced *via* the “hydroperoxide” channel with a 100% efficiency, with the exception of $\bullet\text{CH}_2\text{OO}\bullet$. Consequently, $(\text{CH}_3)_2\text{COO}\bullet$ and *syn*- $\text{CH}_3\text{CHOO}\bullet$ should always give OH radicals, while *anti*- $\text{CH}_3\text{CHOO}\bullet$ should not. Assuming that the *syn* and *anti* are always produced in a 1:1 ratio, the OH yields for generic Criegee intermediates $\text{R}_1\text{R}_2\text{CHOO}$ and RCHOO are 1 and 0.5, respectively. However, I integrate this SAR with the last recommendations by IUPAC. In the next sections the fate of many specific Criegee intermediates is illustrated.

4.4.2.2 $\bullet\text{CH}_2\text{OO}\bullet$

The simplest Criegee intermediate cannot decompose *via* the “hydroperoxide” channel. Compared to MCM, the three channels have similar branching ratios. It is worth noting that the latest recommended OH yield is slightly higher.

	MCM	new
$[\bullet\text{CH}_2\text{OO}\bullet]^* + \text{M} \rightarrow \bullet\text{CH}_2\text{OO}\bullet$	0.37	0.37
$[\bullet\text{CH}_2\text{OO}\bullet]^* \rightarrow \text{CO} + \text{H}_2\text{O}$	0.50	0.47
$\rightarrow \text{HO}_2 + \text{CO} + \text{OH}$	0.13	0.16

4.4.2.3 $\text{CH}_3\dot{\text{C}}\text{HOO}\bullet$

It comprises both the *anti* and the *syn* conformers. The first one decomposes *via* the “hot acid” channel. The latter one is assumed to entirely rearrange to give the unstable hydroperoxide $\text{CH}_2=\text{CHOOH}$ and give OH and vinoxy radical. Below its detailed fate is shown.

		MCM	new
$[\text{CH}_3\dot{\text{C}}\text{HOO}\bullet]^* + \text{M}$	$\rightarrow \text{CH}_3\dot{\text{C}}\text{H}_2\text{OO}\bullet$	0.18	0.16
$[\text{CH}_3\dot{\text{C}}\text{HOO}\bullet]^*$	$\rightarrow \text{CH}_4 + \text{CO}_2$	0.125	0.15
	$\rightarrow \text{CH}_3 + \text{HO}_2 + \text{CO}_2$	0.125	-
	$\rightarrow \text{CH}_3 + \text{CO} + \text{OH}$	0.57	-
	$\rightarrow \text{CH}_2=\text{CHOOH}$	-	0.50
	$\rightarrow \text{CH}_2\text{CO} + \text{H}_2\text{O}$	-	0.06
	$\rightarrow \text{CH}_3\text{OH} + \text{CO}$	-	0.09
	$\rightarrow \text{CH}_3\text{CO} + \text{OH}$	-	0.04

The MCM has actually three different kinds of excited $[\text{CH}_3\dot{\text{C}}\text{HOO}\bullet]^*$. For comparison I took the one that was closer to the SAR by Rickard et al. (1999) that is used by the MCM as stated by Saunders et al. (2003). I find, however, the inconsistency between the SAR and the MCM treatment regarding the “hydroperoxide” channel set to have a branching ratio of 0.57 in the latter. Taking into account the fate of the decomposition products, the new effective OH yield is about 0.59, that is very similar to the yield in MCM.

4.4.2.4 $\text{HOCH}_2\dot{\text{C}}\text{HOO}\bullet$

This intermediate is produced from the ozonolysis of C_5 unsaturated β -hydroxy compounds. Its fate is shown below.

		MCM	new
$[\text{HOCH}_2\dot{\text{C}}\text{HOO}\bullet]^* + \text{M}$	$\rightarrow \text{HOCH}_2\dot{\text{C}}\text{HOO}\bullet$	0.18	0.16
$[\text{HOCH}_2\dot{\text{C}}\text{HOO}\bullet]^*$	$\rightarrow \text{CH}_3\text{OH} + \text{CO}_2$	0.125	0.15
	$\rightarrow 2\text{HO}_2 + \text{HCHO} + \text{CO}_2$	0.125	-
	$\rightarrow \text{HCHO} + \text{CO} + \text{HO}_2 + \text{OH}$	0.57	-
	$\rightarrow \text{HOCH}=\text{CHOOH}$	-	0.50
	$\rightarrow \text{CH}_3\text{OH} + \text{CO}$	-	0.15
	$\rightarrow \text{HOCH}_2\text{CO} + \text{OH}$	-	0.04

The formation of HOCHCO , analogous of chetene, is neglected and its branching ratio assigned to the channel producing $\text{CH}_3\text{OH} + \text{CO}$. The unsaturated hydroperoxide

HOCH=CHOOH decomposes giving OH and the radical HOCHCHO. The latter produces OH with a 19% yield after reacting with O₂ (see Sec. 4.3.6.6). Considering the fate of the other products I estimate a new effective OH yield of about 0.61.

4.4.2.5 HCO•CHOO•

This intermediate is produced from the ozonolysis of C₅ unsaturated β-hydroxy compounds. Its fate is shown below.

	MCM	new
[HCO•CHOO•]* + M → HCO•CHOO•	0.18	0.16
[HCO•CHOO•]* → HCHO + CO ₂	0.125	0.15
→ 2HO ₂ + HCHO + CO ₂	0.125	-
→ 2CO + HO ₂ + OH	0.57	-
→ HOOCH=CHO	-	0.50
→ HCOOH + CO	-	0.15
→ HCOCO + OH	-	0.04

4.4.2.6 HOOCH₂•CHOO•

This intermediate is produced from the ozonolysis of a C₅ unsaturated hydroperoxide (see Sec. 4.4.5) and is not considered in MCM. Assuming the branching ratios for [CH₃•CHOO•]* to be a good approximation, I implemented the following reactions.

[HOOCH ₂ •CHOO•]* + M → HOOCH ₂ •CHOO•	0.16
[HOOCH ₂ •CHOO•]* → CH ₃ OOH + CO ₂	0.15
→ HOOCH=CHOOH	0.50
→ HOOCH=CO + H ₂ O	0.06
→ HOCH ₂ OOH + CO	0.09
→ HOOCH ₂ CO + OH	0.04

The unsaturated hydroperoxide HOOCH=CHOOH decomposes giving glyoxal and 2 OH. Considering the fate of the other products I estimate an effective OH yield of about 1.14.

4.4.2.7 HOCH₂•C(OO•)CH₃

According to the SAR by Rickard et al. (1999), both conformers of R₁R₂CHOO (*anti* and *syn*) decompose *via* the “hydroperoxide” channel giving OH. The mechanism is illustrated in Fig. 4.11. It is worth noting that the product of the *anti* conformer is a

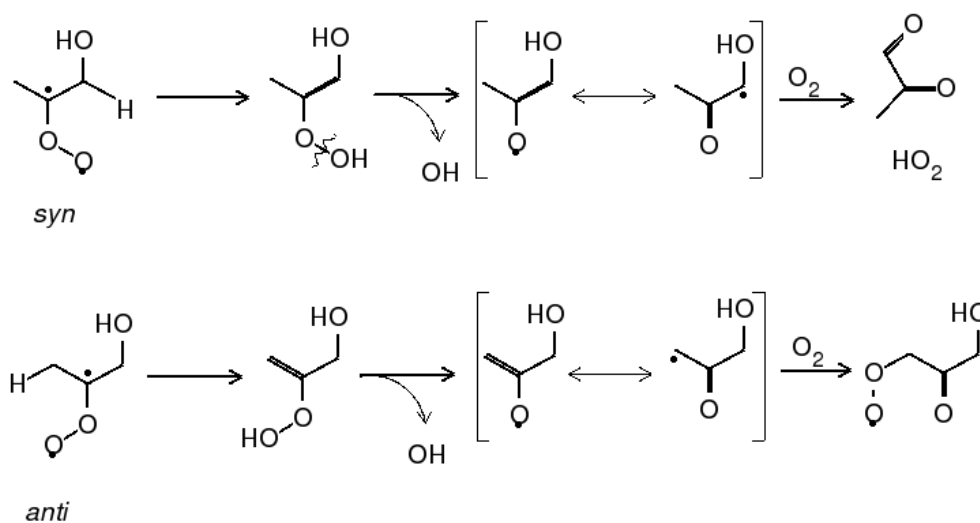


FIGURE 4.11: Quantitative decomposition of a simple Criegee intermediate.

β -keto RO₂ whose further degradation results in significant OH production. In contrast, the MCM treatment is inconsistent with its own development protocol (Saunders et al. (2003)) considering an 11% yield of the stabilised Criegee intermediate and the rest (89%) methylglyoxal as if only *syn* conformers were produced.

4.4.2.8 HOOCH₂C(OO•)CH₃

This Criegee intermediate results from the ozonolysis of a C₅ unsaturated hydroperoxide that is not considered in the MCM. I developed the mechanism for the decomposition of both conformers (se Fig. 4.12). It can be seen that HOOCH₂C(OO•)CH₃ decomposition is predicted to give OH with a 1.5 yield. Normally, the OH yields from Criegee intermediates are below or equal to unity. The potential implications of this very OH yield are discussed in Sec. 4.4.5.

4.4.2.9 HCO•C(OO•)CH₃

This Criegee intermediate is produced from the ozonolysis of MACR and a C₅ hydroxy carbonyl. Omitting the intermediate species likely involved in the decomposition, its fate can be described as follow.

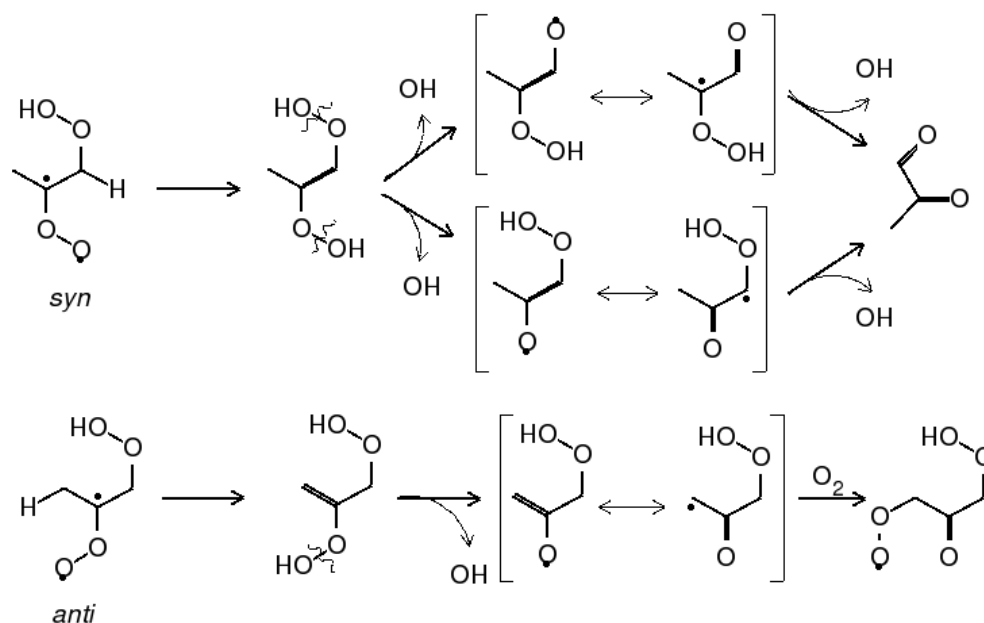
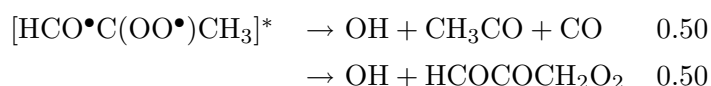


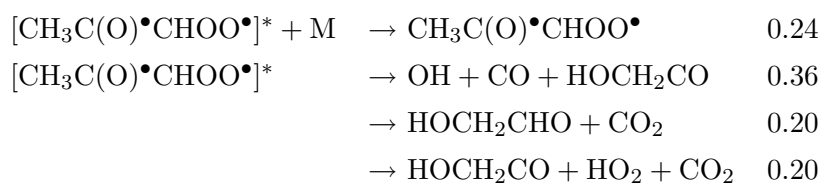
FIGURE 4.12: Decomposition of a Criegee intermediate from ozonolysis of an isoprene hydroperoxides. The *syn* and *anti* conformers have final OH yields of 2 and 1, respectively.



Thus an OH yield of 1 is predicted. However, the degradation of the other products (CH_3CO and $\text{HCOCOCH}_2\text{O}_2$) leads to additional OH production. Comparison with the MCM is not meaningful because the MCM has two “ad hoc” intermediates whose fate is inconsistent with the MCM development protocol (Saunders et al. (2003)).

4.4.2.10 $\text{CH}_3\text{C}(\text{O})\bullet\text{CHOO}\bullet$

In isoprene oxidation the species $\text{CH}_3\text{C}(\text{O})\bullet\text{CHOO}\bullet$ is produced only in the ozonolysis of MVK. This Criegee intermediate cannot undergo the usual “hydroperoxide” channel for the lack of H atoms allowing a 1,5-H shift. I find the MCM treatment of this intermediate to be a good guess of its fate. It can be described as below.



Considering further OH production in the reaction $\text{HOCH}_2\text{CO} + \text{O}_2$ (26%), an effective OH yield of about 0.51 is estimated for the present Criegee intermediate.

4.4.3 Fate of stabilised Criegee Intermediates

As shown above, Criegee intermediates are stabilized by collisions to a significant extent. The *syn* conformers undergo likely decomposition, either thermal or prompt, *via* the “hydroperoxide” channel as explained in Sec. 4.4.2.1. The *anti* conformers are precluded this pathway and undergo bimolecular reactions. The atmospheric fate of the stabilized Criegee intermediates have been investigated in a number of studies (Hasson et al. (2001a,b, 2003), Neeb et al. (1997), Sauer et al. (1999) and references therein). The most important bimolecular reaction in the atmosphere is the reaction with H_2O . A remarkable finding was that the sole product of $\bullet\text{CH}_2\text{OO}\bullet$ is hydroxymethyl hydroperoxide (Neeb et al. (1998)). This is in contrast with the MCM that considers the formation of HCOOH and $\text{HCHO} + \text{H}_2\text{O}_2$. Neeb et al. (1997) studied the fate of the stabilized $\bullet\text{CH}_2\text{OO}\bullet$ and $\text{CH}_3\bullet\text{CHOO}\bullet$ with H_2O . I assume that intermediates with analogous structure to the latter have the same branching ratios for each channel. With the exception of C_4 Criegee intermediates, the fate of stabilized Criegee intermediates, not decomposing *via* the “hydroperoxide” channel, is illustrated below.

		MCM	new
$\bullet\text{CH}_2\text{OO}\bullet + \text{H}_2\text{O}$	$\rightarrow \text{HOCH}_2\text{OOH}$	0	1
	$\rightarrow \text{HCHO} + \text{H}_2\text{O}_2$	0.375	0
	$\rightarrow \text{HCOOH} + \text{H}_2\text{O}$	0.625	0
$\text{R}\bullet\text{CHOO}\bullet + \text{H}_2\text{O}$	$\rightarrow \text{RCH(OH)OOH}$	0	0.15
	$\rightarrow \text{RCHO} + \text{H}_2\text{O}_2$	0.375	0.77
	$\rightarrow \text{RCOOH} + \text{H}_2\text{O}$	0.625	0.08

4.4.4 Branching ratios and rate constants

In order to predict the decomposition of the POZ I use again the SAR by Rickard et al. (1999). The branching ratios for three differently substituted alkenes are shown in Fig. 4.13. They can be rationalized looking at stability of the radical species of each channel. A channel producing a more stable radical, e.g. a tertiary radical, should be favoured in comparison to other one producing a less stable radical, e.g. a secondary radical. This SAR by Rickard et al. (1999) was based on old IUPAC recommendations regarding Criegee intermediates and developed to predict OH yield for alkene ozonolysis. However, the IUPAC recommendations about the OH yields changed slightly. A fundamental assumption is that the chemistry of oxygenated unsaturated compounds from

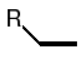
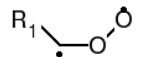
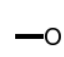
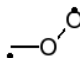
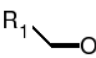
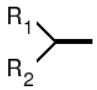
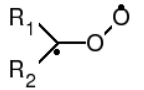
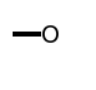
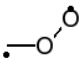
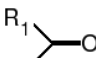
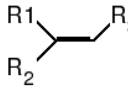
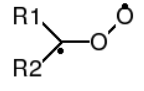
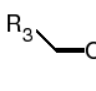
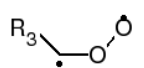
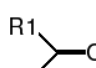
Alkene	Criegee intermediate	Carbonyl	Branching ratio
			0.57
			0.43
			0.67
			0.33
			0.73
			0.27

FIGURE 4.13: Branching ratios for ozonolysis of generic alkenes.

isoprene oxidation can be reasonably well approximated by this SAR for alkenes. The reason for that is the presence of heteroatoms that can alter the stability of the radicals forming. Furthermore, this SAR is not for conjugated dienes like isoprene. In this case I continue the MCM treatment of isoprene ozonolysis because it accurately reproduces the experimentally available data (Atkinson (1997b)). Substituents around the double bonds affect the rate constants modifying the bonding and anti-bonding molecular orbitals. I maintain the MCM rate constants unless new specific IUPAC recommendations are made. New ozonolysis reactions involving unsaturated C₅ hydroperoxides, diols and hydroxy alkyl nitrates are considered. The rate constants of the parent alkenes are taken representing likely a lower limit. In fact, the substituent group HOCH₂- has the tendency to enhance the rate constant with respect to the parent alkene (Grosjean and Grosjean (1994)). The predicted chemistry for the two internally double bonded C₅ hydroperoxides is described in Sec. 4.4.5.

4.4.5 Unsaturated hydroperoxides

The ozonolysis of many C₅ unsaturated isoprene oxidation products is not considered in MCM. Applying the SAR described above led to a notable discovery. All alkenes and many oxygenated analogues have OH yields to be lower than one. However, the Criegee

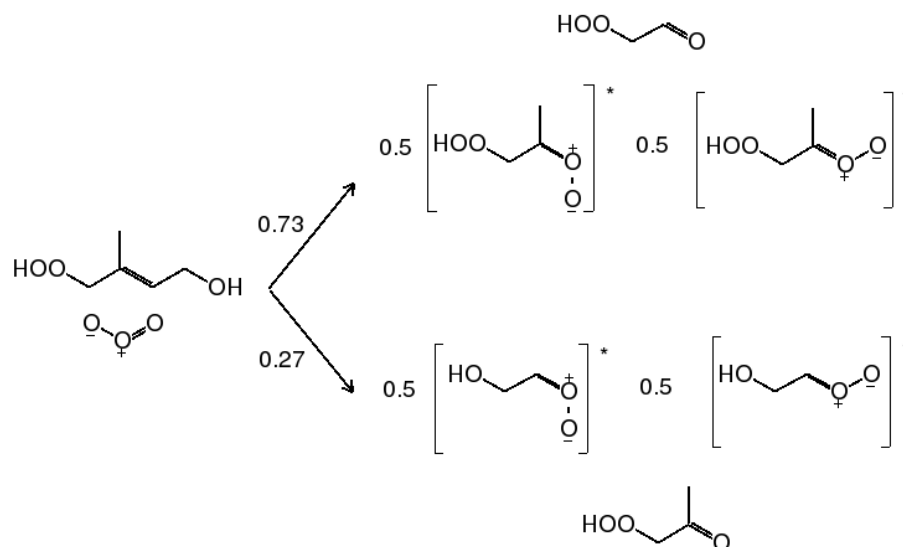


FIGURE 4.14: Ozonolysis of one internally double bonded hydroperoxide for which the total OH yield is estimated to be higher than one (see text).

intermediates from internally double bonded hydroperoxides contain $-\text{CH}_2\text{OOH}$ groups that provide an additional source of OH radicals during their decomposition (see Sec. 4.4.2.1). The best example is shown in Fig. 4.14. The C₃ Criegee intermediate in this case is predicted to produce 1.5 OH by decomposition. Considering the branching ratio, this channel alone may yield 1.1 OH. When the OH production from the other channel is accounted for, a total OH yield of about 1.3 is predicted. Such high OH yields may be important in explaining recent findings of elevated non-stomatal O₃ losses within the forest canopy (Goldstein et al. (2004), Kurpius and Goldstein (2003)). The radiation intensity in canopies is usually reduced causing a higher O₃/OH ratio compared to above-canopy conditions. Reactions with O₃ with unsaturated hydroperoxides may be important in sustaining OH levels and protecting plants from O₃ damages. In Sec. 5.1.4 hypothesis is tested.

4.5 Photolysis reactions

4.5.1 PAN

The photolysis of PAN and PAN-like compounds is not very important in the lower troposphere. In fact, it starts to become important above about 7 km altitude. In all models it is represented with one channel that yields its precursors. However, [Harwood et al. \(2003\)](#) found that there is a second channel in which the precursors are not formed and that is a net sink of PAN. The new IUPAC recommendation for PAN at 308 nm, compared to the MCM assumption, is:

		MCM	IUPAC
$\text{CH}_3\text{C}(\text{O})\text{OONO}_2 + h\nu$	$\text{CH}_3\text{CO}_3 + \text{NO}_2$	100%	60%
	$\text{CH}_3\text{CO}_2 + \text{NO}_3$	0%	40%

The branching ratios are used for PAN and its homologues.

4.5.2 Glycolaldehyde

The IUPAC recommendations regarding glycolaldehyde photolysis have not been updated since 2002. Meanwhile two recent studies appeared in the literature shedding more light on the relative importance of thermodynamic possible channels. [Magneron et al. \(2005\)](#) detected OH directly and estimated that a 7% branching ratio for the channel that produces OH and CH_2CHO . [Karunanandan et al. \(2007\)](#) obtained complementary information on the other channels. Combining the results of the studies the photolysis of glycolaldehyde can be described as follows.

		MCM	this work
$\text{HOCH}_2\text{CHO} + h\nu$	$\rightarrow \text{HOCH}_2 + \text{HCO}$	100%	83%
	$\rightarrow \text{OH} + \text{CH}_2\text{CHO}$	-	7%
	$\rightarrow \text{CH}_3\text{OH} + \text{CO}$	-	10%

By analogy, the photolysis of species like $\text{CH}_3\text{CHOHCHO}$ are implemented taking the branching ratios for HOCH_2CHO as a first-order approximation.

4.5.3 Methyl vinyl ketone and methacrolein

The current IUPAC recommendations for MVK photolysis are significantly different from the MCM as detailed below.

TABLE 4.4: Number of reactions and species for the MCME mechanism and comparison to the other ones considered in this study.

Mechanism	Species	Reactions
MIM	15 ^a	44
MIM2	68 ^a	199
MCM	180 ^a	595
MCME	≈ 850	≈ 3800

^a Note that only C₂–C₅ species have been taken into account.

	MCM	IUPAC
CH ₃ COCH=CH ₂ + <i>hν</i> → CH ₂ =CHCH ₃ + CO	50%	60%
→ CH ₃ CO ₃ + HCHO + CO + HO ₂	50%	-
→ CH ₃ CO + CH ₂ =CH	-	20%
→ CH ₂ =CHCO + CH ₃	-	20%

The branching ratios for the propene producing channel are similar. The second MCM channel is to be considered an approximation of the channel producing CH₃CO and CH₂=CH radicals. In fact, the main degradation products under high-NO_x of these radicals are CH₃CO₃, HCHO, CO and HO₂ (see Sec. 4.3.6.2 and 4.3.6.7). However, a significant amount of OH can be produced during the reactions these alkyl radical undergo.

Regarding MACR photolysis, quantitative information about reaction channels are scarce (Raber and Moortgat (1995)). I take, therefore, the MCM channels and substitute one channel with the more appropriate production of methyl vinyl radical whose atmospheric fate is described in Sec. 4.3.6.9.

	MCM	this work
CH ₂ =C(CH ₃)CHO + <i>hν</i> → CH ₃ CO ₃ + HCHO + CO + HO ₂	50%	-
→ CH ₂ =CCH ₃ + CO + HO ₂	-	50%
→ CH ₂ =C(CH ₃)CO + HO ₂	50%	50%

According to Pinho et al. (2005), the photolysis frequencies as used in the MCM are lowered by a factor of 0.12 and 0.168 for MACR and MVK, respectively.

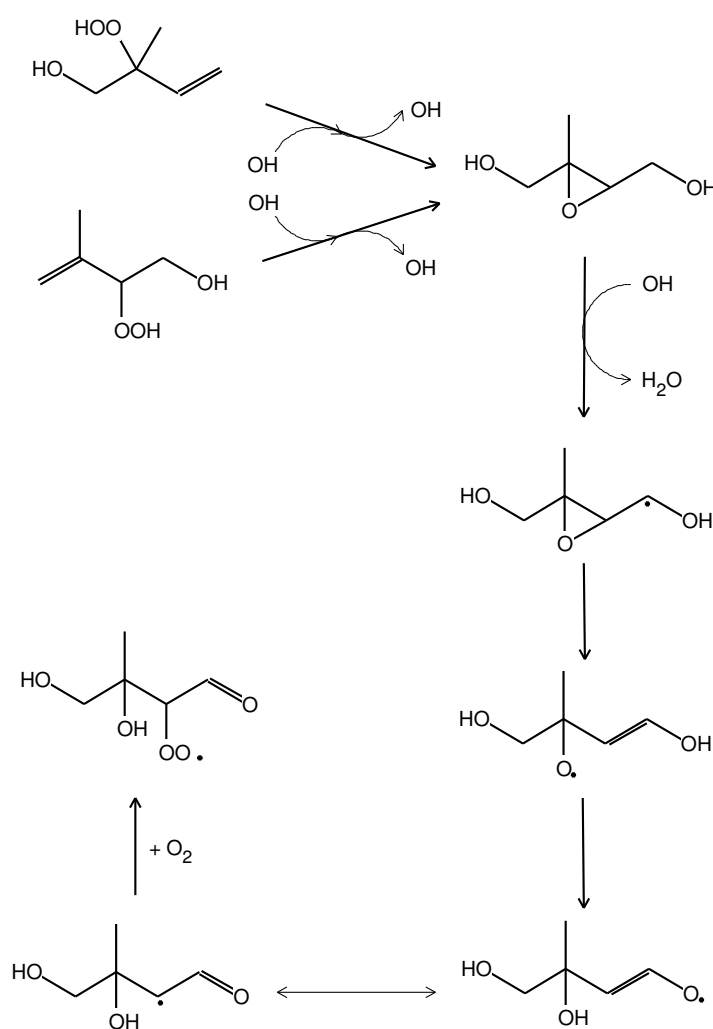


FIGURE 4.15: A general representation of epoxide formation from β hydroperoxide alkyl radicals above a tropical pristine forest.

4.6 MCM extended

4.6.1 Version 1

The update and substantial extension of the MCM mechanism for isoprene described in this chapter has led to the development of a highly explicit oxidation mechanism, called MCME v1, in which many intermediates are treated. New pathways have been included and new SAR for the OH- and O_3 -pathway have been developed. The new mechanism conserves mass with respect with carbon and has about 850 species and 3800 reactions.

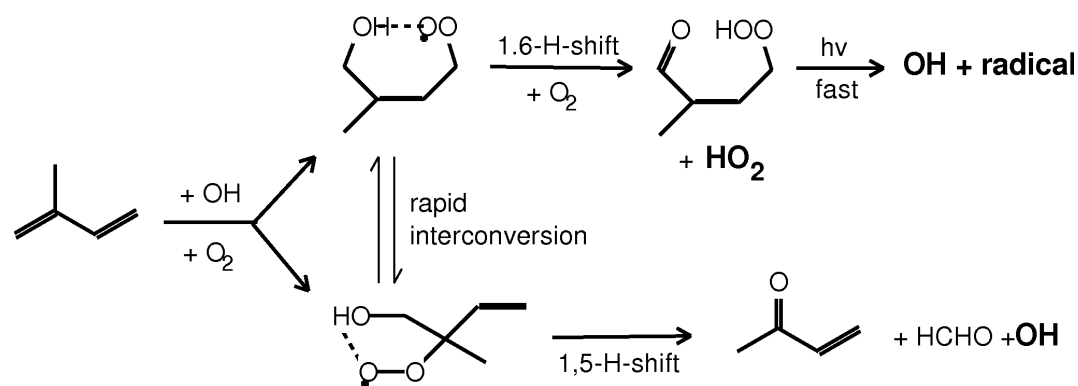


FIGURE 4.16: 1,5- and 1,6-H-shifts for isoprene derived peroxy radicals as proposed by Peeters et al. (2009).

A comparison with MCM and the two reduced mechanisms MIM and MIM2 is shown in Tab. 4.4.

4.6.2 Version 2

The first version of MCME is highly explicit and allows inclusion of new oxidation routes with relatively little effort. This made it possible in the framework of this thesis to include two recently published breakthroughs (Paulot et al. (2009b), Peeters et al. (2009)), adding about 20 reactions. These breakthroughs encompass three new efficient routes for the recycling of both OH and HO₂. They are briefly described below.

Unexpected epoxide formation (Paulot et al. (2009b))

NO_x-free experiments on isoprene oxidation in the CALTECH environmental chamber have revealed the production of epoxydiols. The likely formation route is the reaction of unsaturated hydroperoxides with OH that form an excited alkyl radical with a –OOH group in the β position (Fig. 4.15). The ring closure and the simultaneous OH elimination should be a process faster than O₂ addition to form RO₂. This mechanism is known in combustion chemistry, and according to calculations, a tertiary β-OOH alkyl radical in thermal equilibrium is estimated to undergo ring closure with an activation energy of about 14 kcal/mol at a frequency of about 600 s⁻¹ at 298 K (Wijaya et al. (2003, and references therein)). However, in isoprene oxidation the epoxide precursor is formed with about 30 kcal/mol excess energy. Therefore, prompt ring closure and OH elimination is expected. The resulting epoxydiol reacts with OH with a rate constant of 1.5 10⁻¹¹. The chemistry of products is unknown and a tentative mechanism is drawn in Fig. 4.15.

H-shifts and fast ROOH photolysis (Peeters et al. (2009))

Theoretical calculations have been carried out on potentially important H-shifts which isoprene related RO₂ can undergo. A very efficient 1,6-H-shift ($k_{298} > 1 \text{ s}^{-1}$) has been identified for Z geometric isomers of 1-hydroxy-4-peroxy radicals (see Tab. 4.16). The resulting alkoxy radical will readily react with O₂ leading to the production of HO₂. The stable product, an unsaturated carbonyl hydroperoxide, has been estimated to photo-dissociate with a $J = 3 \cdot 10^{-4} \text{ s}^{-1}$ that under atmospheric conditions results in about 100% OH radical generation. Furthermore, 1,5-H-shifts for β -hydroxy RO₂ from isoprene, methacrolein and methyl vinyl ketone have been estimated to be competitive with the standard RO₂ sinks under pristine conditions.

In the next chapter (Chapter 5) both versions of MCME are evaluated against MCM in a box model under a variety of case scenarios and against field data from the GABRIEL campaign (Lelieveld et al. (2008)).

Chapter 5

Enhanced isoprene oxidation

5.1 Unconstrained simulations

5.1.1 Simulation parameters

The two versions of MCME are compared to MCM with a box model setup similar to the one used for the MIM2 evaluation (see Sec. 3.1). However, many more species are initialized since all mechanisms compared here are explicit. The full list of initialized species is shown in Tab. 5.1. It can be seen from the table that, unless NO emissions are prescribed, the simulations are NO_x-free. In order to make the evaluation more representative of tropical boundary layer conditions, the photolysis frequencies have been increased with $J(O^1D)_{max} \approx 7 \cdot 10^{-5} s^{-1}$. The maximum isoprene flux in the simulations is about $4 \cdot 10^9$ molecule cm⁻² s⁻¹. No dry deposition is taken into account and therefore species like H₂O₂, O₃ and NO_x eventually reach very high and unrealistic mixing ratios.

5.1.2 Case 1: NO_x-free boundary layer

A substantial fraction of the global isoprene emission occurs in the southern tropics where NO mixing ratios are below 60 pmol/mol (Emmons et al. (1997), Müller et al. (2008), Torres and Buchan (1988)). After being emitted, most of isoprene is oxidized in the continental boundary layer. Therefore, the first set of simulations is for conditions representative of a boundary layer above a pristine tropical forest. The results for the most important species is shown in Fig. 5.1. Each mechanism significantly differs from the other two. As expected, the highest HO_x concentrations are computed by MCMEv2. At noon of the 2nd model day the OH (HO₂) concentration is 7 (1.8) times higher than

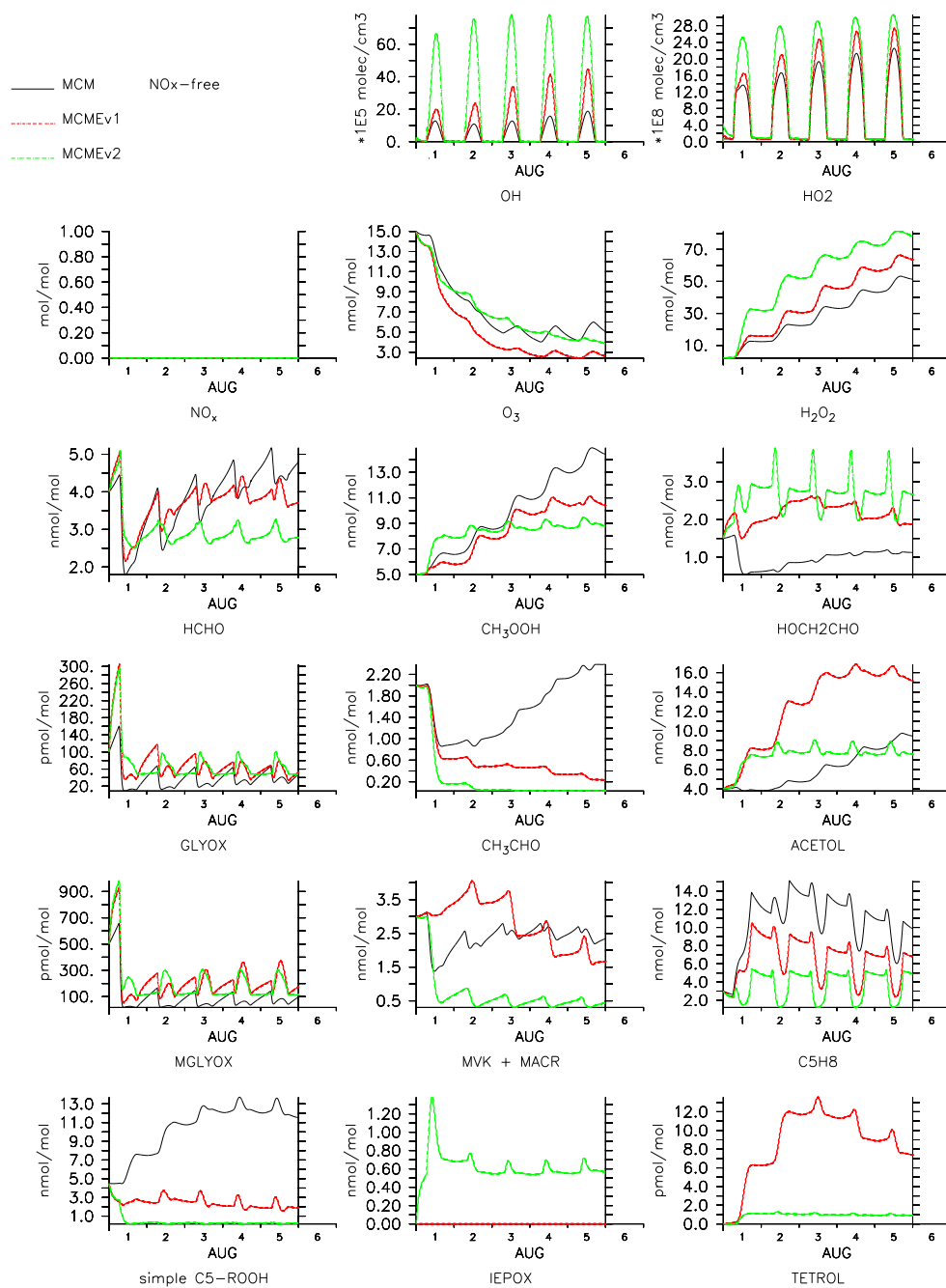


FIGURE 5.1: Comparison of MCME v1 and v2 with MCM for a NO_x-free boundary layer.

TABLE 5.1: Initial mixing ratios of species under the three scenarios here used.

Species formula	initial mole fraction (mol mol ⁻¹)
H ₂ O	0.01851
O ₃	15 × 10 ⁻⁹
H ₂ O ₂	2 × 10 ⁻⁹
NO ₂	0
NO	0
CH ₄	1.8 × 10 ⁻⁰⁶
HCHO	4.0 × 10 ⁻⁰⁹
CO	100 × 10 ⁻⁰⁹
CH ₃ OH	3.0 × 10 ⁻⁰⁹
CH ₃ OOH	5.0 × 10 ⁻⁰⁹
HCOOH	350 × 10 ⁻¹²
CH ₃ C(O)O ₂ NO ₂ (PAN)	0
CH ₃ CHO	2.0 × 10 ⁻⁰⁹
HOCH ₂ CHO	1.5 × 10 ⁻⁰⁹
GLYOX	100 × 10 ⁻¹²
CH ₃ CO ₂ H	2.0 × 10 ⁻⁰⁹
CH ₃ CO ₃ H	1.5 × 10 ⁻⁰⁹
CH ₃ COCH ₂ OH	4.0 × 10 ⁻⁰⁹
CH ₃ COCHO	500 × 10 ⁻¹²
MVK	1.5 × 10 ⁻⁰⁹
MACR	1.5 × 10 ⁻⁰⁹
ISOPAOOH	500 × 10 ⁻¹²
ISOPBOOH	2.0 × 10 ⁻⁰⁹
ISOPCOOH	500 × 10 ⁻¹²
ISOPDOOH	1.5 × 10 ⁻⁰⁹
HC4ACHO	600 × 10 ⁻¹²
HC4CCHO	600 × 10 ⁻¹²
C ₅ H ₈ (isoprene)	3.0 × 10 ⁻⁰⁹

computed by MCM. Despite the substantial extensions to MCM, MCMEv1 computes a OH concentration that is only 2.5 times higher. On the 5th model day most of the secondary OH production in MCMEv1 (and MCM) comes from the photolysis of organic hydroperoxides (ROOH) whose mixing ratios significantly build up in contrast to the GABRIEL field measurements of about 1 nmol/mol (Lelieveld et al. (2008), Stickler et al. (2007)). However, mixing ratios of simple C₅-hydroperoxides computed with MCMEv2 are a factor of 20 lower than with MCM. The daytime isoprene mixing ratio mirrors the corresponding OH concentrations for each mechanism. MCMEv2 computes a noon isoprene minimum of 1.5 nmol/mol, that is quite close to the average value of 2 nmol/mol measured during GABRIEL in the boundary layer (Lelieveld et al. (2008)), in contrast to the 6 nmol/mol computed by MCM. HCHO is substantially lower in the simulation with MCMEv2, while MCMEv1 significantly diverges from MCM on the 4th model day. This is also the case with respect to the sum of MVK and MACR that is greatly reduced in MCMEv2 compared to both MCM and MCMEv1. This is mainly the consequence of the new routes discovered by Peeters et al. (2009) which do not lead to MVK and MACR production. As a result mixing ratios of HCHO, MVK and MACR are substantially

reduced being more consistent with field measurements. For instance, [Butler et al. \(2008\)](#) showed that 3D simulations with MIM2 overestimate the measured HCHO and MVK+MACR mixing ratios by 1-2 nmol/mol. [Butler et al. \(2008\)](#) also showed a large underestimation of the model (MIM2) with respect to CH₃CHO. This underestimation is larger for MCMEv2 mainly because of the much higher OH mixing ratios. Provided that no substantial CH₃CHO source could be identified in the isoprene oxidation, it is likely that the major atmospheric sources are ozonolysis of higher terpenes and/or decomposition of dissolved organic matter in the ocean, followed by sea-air transfer of CH₃CHO ([Kieber et al. \(1990\)](#), [Millet et al. \(2008a\)](#)). The species denoted as IEPOX is the epoxydiol identified by [Paulot et al. \(2009b\)](#). It is formed in the reaction of C₅-hydroperoxides with OH in which after addition OH is eliminated by the –OOH group. IEPOX turns out to be a major isoprene oxidation product with mixing ratios higher than 0.5 nmol/mol throughout the simulation. This implies a substantial OH recycling. Moreover, IEPOX has been indicated as the missing link in SOA formation from isoprene, via the heterogeneous production on aerosols of tetrols which have been measured in SOA ([Claeys et al. \(2004a\)](#)). Inclusion of IEPOX in the model makes the tetrol mixing ratios computed by MCMEv1 decrease from 13 (max. value) to 1 pmol/mol in MCMEv2. This indicates the likely predominance of the heterogeneous acid-catalyzed hydrolysis of IEPOX on the homogeneous gas-phase mechanism to form tetrols in aerosols ([Böge et al. \(2006b\)](#), [Edney et al. \(2005\)](#)).

5.1.3 Case 2: NO_x-rich boundary layer

The three oxidation mechanisms considered here are also tested under "mid-NO_x" conditions in which the NO emissions have been set to be 3.33×10^{10} molecule cm⁻² s⁻¹. Depending on the mechanism used, the NO_x mixing ratios oscillates between 100 and 650 pmol/mol (see [Fig. 5.2](#)). MCMEv1 and v2 show significantly lower NO_x mixing ratios, reflected in the lower O₃ production compared to MCM. The reason lies in the different capacity of the two versions of MCME and MCM to store nitrogen in the form of alkyl nitrates (see [Sec. 4.3.7.2](#)). The patterns of differences between the mechanisms are similar to those in the NO_x-free scenario. The highest HO_x concentrations are again computed by MCMEv2. Both MCME versions compute lower mixing ratios of CH₃OOH with differences reaching 3 nmol/mol though the difference is much less than in the NO_x-free scenario. At noon of the 2nd model day the OH concentration is 2.5 times higher than computed by MCM. Under this scenario the epoxide (IEPOX) appears still to be a relatively important product.

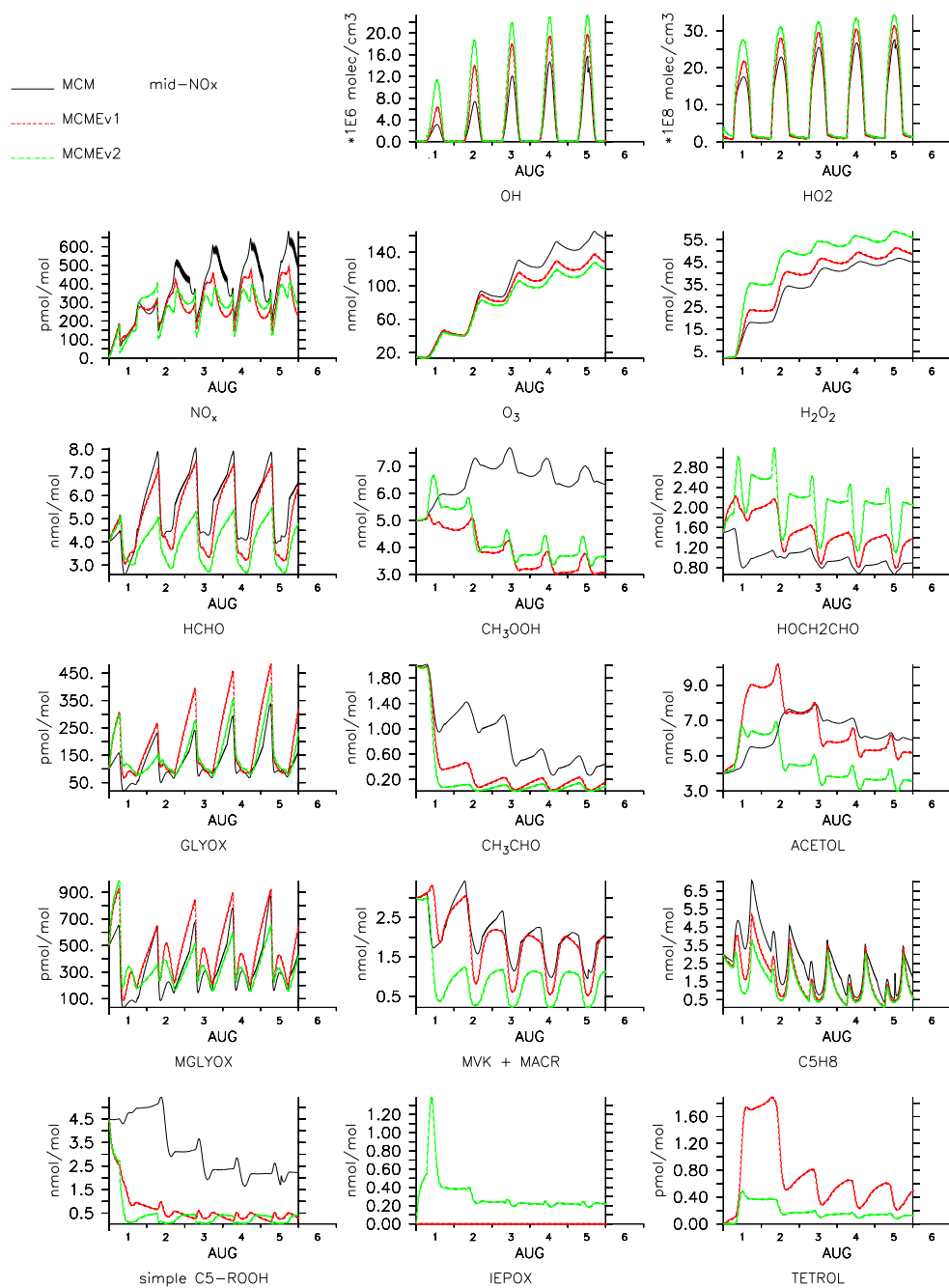


FIGURE 5.2: Comparison of MCME v1 and v2 with MCM for a NO_x-rich boundary layer.

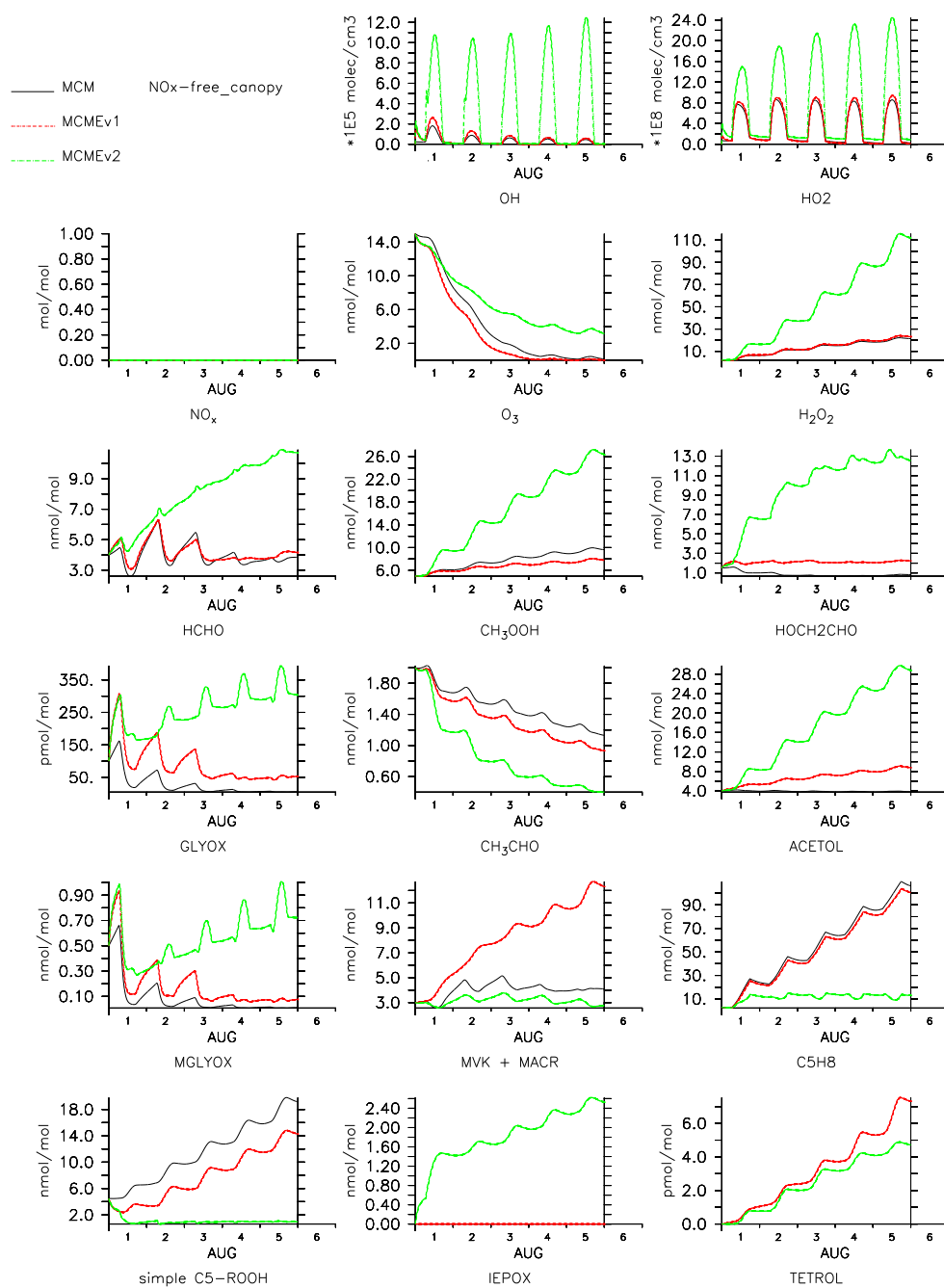


FIGURE 5.3: Comparison of MCME v1 and v2 with MCM for a within-canopy scenario.

5.1.4 Case 3: within the canopy

The enhanced HO_x levels shown by field measurements and these simulations might significantly affect the emissions of biogenic VOC. In fact, fast oxidation within the canopy affects the net amount of VOC that is emitted into the overlying atmosphere. For instance, [Stroud et al. \(2005\)](#) estimated β -caryophyllene to escape the canopy with an efficiency lower than 40% under all conditions. In that study traditional chemistry with little OH-recycling under low- NO_x was used. Isoprene was estimated to escape the canopy with an efficiency greater than 90%. Therefore representing the enhanced isoprene oxidation in canopies will reduce this efficiency and might help reconciling the large discrepancies between “top-down” and “bottom-up” VOC emissions estimates ([Guenther et al. \(2007\)](#)).

Box model simulations are not well suited to estimate the effect of chemistry on the net isoprene emissions from a canopy. However, they can be used to get an idea of the order of magnitude of such potential effect. For this purpose another set of simulations is shown in [Fig. 5.3](#) in which all photolysis frequencies have been reduced by 80%. This reduction represents the maximum intensity reduction of the photosynthetic active radiation (PAR) in a canopy ([Grant \(1997\)](#)). Under these conditions on the 2nd model day the OH concentrations computed by MCMEv2 are 10 times higher than the ones computed by both MCM and MCMEv1. Correspondingly, the isoprene mixing ratios computed by MCMEv2 are 2 times lower than by both MCM and MCMEv1 on the first model day and 3 times lower on the second model day. This might well explain why local “bottom-up” estimates of isoprene emission can exceed the “top-down” estimates by a factor of 2 or more ([Guenther et al. \(2007\)](#)).

5.2 Box model constrained with field measurements

5.2.1 Simulation setup

In order to assess which oxidation mechanism better reproduces the measurements, the box model has been constrained with actual measurements taken during the GABRIEL field campaign. They comprise radical species like OH, HO_2 and NO and long-lived species like H_2O_2 , HCHO, isoprene, acetone, methanol, pinene and the sum of MVK and MACR. Furthermore, the mixing ratio of the total organic hydroperoxides has also been measured. In the free troposphere this quantity corresponds approximately to the CH_3OOH mixing ratio. Besides the basic physical quantities like temperature and pressure, $J(\text{NO}_2)$ was also measured. Further details on the preparation of data for constrained box model simulations have been reported by [Madronich and Flocke \(1998\)](#).

For a given location and time, the species mixing ratios were initialized with either the measured value or with a typical one taken from preliminary simulations. In the case of organic hydroperoxides, simulations with MCMEv1 showed that in an isoprene-rich scenario about 70% is made of CH₃OOH and the rest made mainly of the MCM species ISOPBOOH. The organic hydroperoxides mixing ratios were assigned according to this ratios. For simplicity this initial mixing ratios are used for the isoprene-poor simulations in which the measured value should be assigned only to CH₃OOH. However, since the C₅ organic hydroperoxides disappear quickly this assumption does not significantly affect the results. The pinene mixing ratio was set to its average measured value in the boundary layer during the campaign (300 pmol/mol). In the simulations pinene represents a simple OH sink as only the first oxidation step is represented.

Photolysis frequencies are as in [Kubistin et al. \(2008\)](#) and kept constant during each simulation. They were calculated with the TUV model using a total ozone column of 265 D.U. (GOME satellite data). The photolysis frequencies were then corrected for cloud and aerosol effects by scaling to the measured J(NO₂) ([Madronich and Flocke \(1998\)](#)). The simulations were performed constraining only a limited number of species to the measured values and letting the model run for 2 simulation hours. The constrained species were NO, O₃, CO, CH₄, CH₃COCH₃, pinene and isoprene. No dry deposition was included since the simulations were short and partly representative of the free troposphere.

5.2.2 Case 1: isoprene-poor troposphere

In order to first examine the differences in C₁-chemistry, before going in to the more complex ones the oxidation mechanisms were first compared to a set of measurements for an isoprene-poor region at specific location and time (Fig. 5.4). Despite the mixing ratios for pinene and the simple C₅ ROOH being unrealistically set to non-zero values, all mechanisms overestimate the OH concentration by about a factor of 4.5. These simulations do not include significant contributions by other VOC that the forest may emit. For example, the contributions by monoterpenes other than pinene, sesquiterpene oxidation products and in general directly emitted oxygenated VOC may well bring the modeled OH concentrations close to the measurements. Since the detection limit for the isoprene measurements was 100 pmol/mol ([Eerdekens et al. \(2009\)](#)) a sensitivity simulation with that amount of isoprene was performed. The overestimation of the OH concentration by all mechanisms is thereby reduced to a factor of 4. On the other hand, the HO₂ concentration is underestimated by a factor of 6.4. Under very low-NO_x conditions, 14 pmol/mol in this case, HO₂ and OH are chemically “decoupled” because of the negligible role of the NO + HO₂ → OH + NO₂ reaction. Therefore, the discrepancy

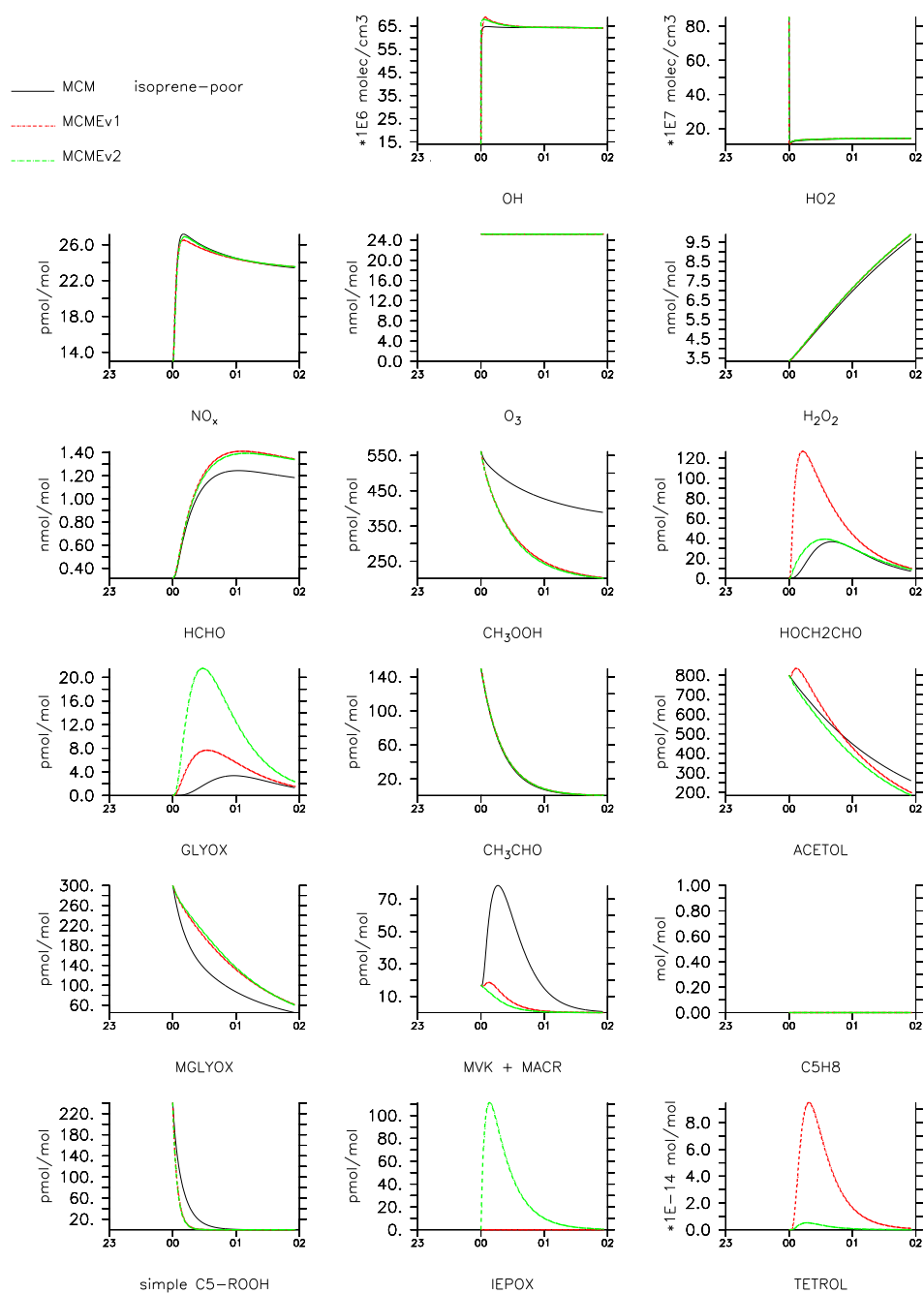


FIGURE 5.4: Results for simulations constrained with GABRIEL measurements in the free troposphere for which isoprene is below the detection limit and assumed to be not present.

TABLE 5.2: Measured OH concentrations and modeled-to-measured ratios for the different mechanisms after 20 minutes simulations time. MCMEv2seg include a 50% reduction in the rate constant of isoprene + OH.

altitude	C ₅ H ₈	OH	OH _{meas} /OH _{mod}		
(m)	(nmol/mol)	(molecule cm ⁻³)	MCM	MCMEV2	MCMEv2seg
1264	< 0.10	1.18×10 ⁷	0.23	0.23	0.23
735	3.19	6.18×10 ⁶	3.1	1.1	0.94

concerning HO₂ may be likely due to too low mixing ratios of VOC other than isoprene whose oxidation produces HO₂. The substantial model overestimation of HCHO mixing ratio is difficult to pin down without a budgeting analysis. However, a likely explanation is an increased HCHO production due to the overestimation of the OH concentration. On the other hand, the differences between MCM and MCME are easier to identify. One reason is that, compared to MCM, the last IUPAC recommendations include a much higher rate constant of the HCHO-producing channel in the CH₃OOH + OH reaction and a direct HCHO production in the reaction of glycolaldehyde and hydroxyacetone with OH. In addition, the reaction CH₃CO + O₂ should significantly contribute as well (see Sec. 4.3.6.2). With respect to hydroxyacetone (ACETOL in the plot) the differences between MCM and MCME are likely due to the new IUPAC recommendations for the rate constant for the ACETOL + OH being a factor of 1.5 higher than in MCM at 298 K. As mentioned in Sec. 5.2.1 the initialization of simple C₅ hydroperoxides causes transient production for intermediates like glycolaldehyde and glyoxal.

5.2.3 Case 2: isoprene-rich boundary layer

MCM and MCMEv2 have been compared for a region in which the isoprene mixing ratio was about 3 nmol/mol. MCMEv2 has also been modified (MCMEv2seg) by reducing the rate constant for the reaction of isoprene with OH by 50%. This is because the heterogeneity of isoprene emissions and the short OH lifetime result in a species segregation whose effect is the reduction of the effective rate constant (Krol et al. (2000)). A reduction of 50%, together with a 40-50% OH-recycling, was found necessary in order to match the GABRIEL and OP3 field measurements (Butler et al. (2008), Pugh et al. (2009)). The results from the three mechanisms, MCM, MCMEv2 and MCMEv2seg, are shown in Fig. 5.5. MCMEv1 is not shown since it produces similar results to MCM with respect to HO_x and many other species. Under these conditions intermediate species mostly accumulate with time decreasing OH in the long term. A fair compromise is to look at the HO_x levels at about 20 minutes simulation time when NO_x has reached the stationary state. MCM underestimates the observed OH concentration of 6.18×10⁶ molecule cm⁻³

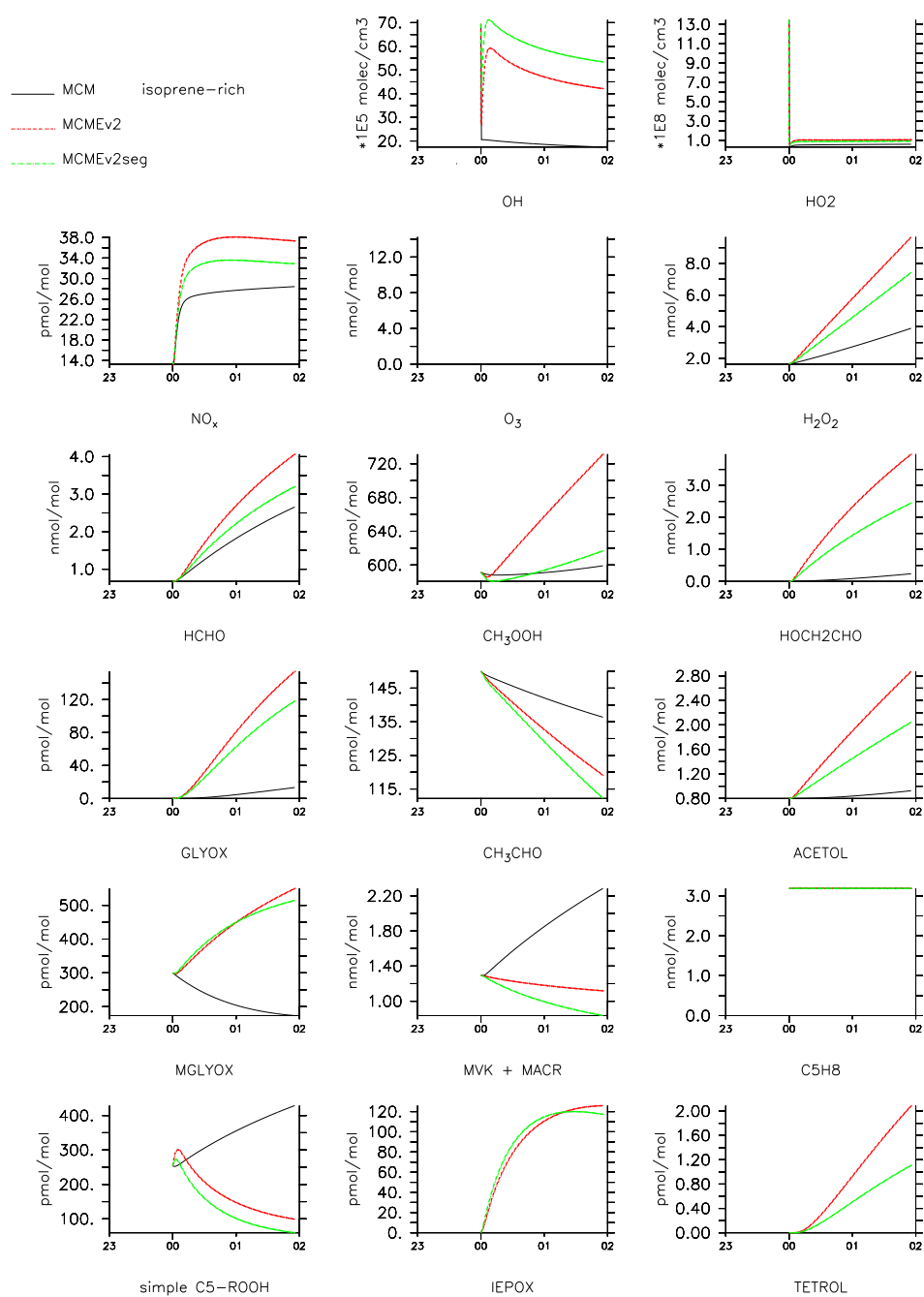


FIGURE 5.5: Results for simulations constrained with GABRIEL measurements in the boundary layer for which isoprene is about 3 nmol/mol. MCMEv2seg includes a 50% reduction of $k_{OH+C_5H_8}$.

by a factor of 3.1 while MCMEv2 by a factor of about 1.1 and MCMEv2seg agrees very well (Tab. 5.2). The new routes proposed by Paulot et al. (2009b) and Peeters et al. (2009) together with the segregation effect appear to be crucial in reconciling the model with the field data. Despite these breakthroughs, the underestimation of HO₂ remains substantial, although halved by MCMEv2. One of the possible causes for this persisting underestimation might be presence in the air of VOC that are not related to isoprene, whose oxidation produce HO₂ and consume OH. After 1-2 hours simulation time, the mixing ratios of species with a lifetime of a day or more are not very representative and normally expected to accumulate because of the absence of dry deposition and transport in the simulation setup. However, some negative trends provide further support for the new chemistry in MCMEv2. In contrast to MCM, MCMEv2 computes mixing ratios for the sum MVK+MACR and the simple C₅ hydroperoxides that decrease rather than accumulate with time. In fact, it was found that the MCM isoprene chemistry greatly overestimates the mixing ratios for the sum MVK+MACR and the organic hydroperoxides (Butler et al. (2008), Pugh et al. (2009)). It is worth noting that the isoprene epoxydiol discovered by Paulot et al. (2009b) reaches a mixing ratio of 100 pmol/mol in one simulation hour.

Chapter 6

Conclusions and outlook

6.1 Conclusions

6.1.1 A new oxidation mechanism for 3D models

With a simple set of mechanism reduction principles, the development of a new isoprene oxidation mechanism for regional and global atmospheric models was possible. It has been described and evaluated against the MCM in a box model representative of a tropical continental boundary layer. The mechanism, called MIM2, is mass conserving with respect to carbon, including CO₂. Compared to its predecessor MIM, MIM2 offers several improvements, as summarized below. The mechanism was found to compute small average relative biases (<6%) for most of the intermediate species under all NO_x regimes studied (see Table 3.2). For instance, this is the case for C₅-alkyl nitrates, hydroperoxides and diols. The C₅-hydroperoxides are suggested to be precursors for organic aerosol nucleation and growth from isoprene oxidation (Kroll et al., 2006) and the C₅-diols are precursors of tetrols found recently in aerosols (Böge et al., 2006a, Claeys et al., 2004a). MIM2 (MIM) was found to compute relative biases for formic and acetic acid, which are important components of the gas and aqueous phase of the atmosphere (Chebbi and Carlier, 1996), reaching about -10% (+300%) and +10% (-40%), respectively. HCHO nocturnal production is close to the rate in the MCM with the average relative bias being less than 1%. Chemical production of CH₃OH has been improved substantially under all NO_x conditions. The representation of the organic nitrogen has been improved remarkably due to the consideration of eight alkyl nitrates (RONO₂) and four peroxy acyl nitrates (RC(O)OONO₂), causing the NO_x relative bias to be always less than 10%. With respect to MIM, MIM2 represents many important new species like glycolaldehyde, α -nitrooxy acetone, two more peroxy acyl nitrates, as well as MVK and MACR, which were previously lumped. In comparison to the isoprene chemistry implemented

in MCM v3.1, the overall improvement in the computation of key atmospheric species and of the isoprene oxidation intermediates is substantial and it will be reflected in the applications with 3D atmospheric models. Because of its low level of species lumping, MIM2 is especially suitable for implementation of new results regarding the isoprene oxidation. An example was given with the modified mechanism, MIM2mod, in which a selection of recent results of VOC chemistry were easily implemented. This will make it straightforward to evaluate the global impacts of new oxidation routes, especially in low-NO_x regions.

MIM2 has been preliminarily implemented in a global atmospheric chemistry model. It has been compared to the modified version of MIM, here referred to as MIMvK, that is used in the EMAC model (Jöckel et al., 2006). Higher OH concentrations are computed compared to the previously implemented isoprene mechanisms. The overall increase in OH and the decrease in isoprene mixing ratios, however, are not enough to match the observations which were made during the GABRIEL campaign (Lelieveld et al., 2008). A more in-depth discussion of the model-measurement comparison during this campaign for OH, isoprene and many other intermediates is presented in Butler et al. (2008). Amongst the new species present in MIM2, the global chemical production of important species like acetaldehyde, propene and glyoxal has been found to be 7.3, 9.5 and 33.8 Tg/yr, respectively.

6.1.2 A new master oxidation mechanism

Lelieveld et al. (2008), based on field observations, proposed that isoprene could sustain the atmospheric oxidation capacity even in pristine environments. In order to test this hypothesis, the MCM for isoprene has been extended from about 600 to 3800 reactions with new rate constant estimates and experimental results. A second version of this extended mechanism, MCMEv2 which was slightly modified to include recent findings, has been shown to produce much higher OH concentrations under NO_x-free conditions. When used to reproduce a subset of the GABRIEL field measurements, MCMEv2 has been able to compute OH concentrations very close to the measurements. The major contributors to the enhanced OH concentration has been found to be the new oxidation routes discovered by Paulot et al. (2009b) and Peeters et al. (2009). However, their relative importance remains to be investigated with either a detailed budget analysis of the mechanism or by neglecting one route at a time. Furthermore, the MCMEv2 has been able to halve the substantial discrepancy with the HO₂ measurement. With respect to other species like organic hydroperoxides, MVK, MACR, HCHO and isoprene itself, model improvements have been achieved.

The great extent of OH recycling in isoprene oxidation may substantially affect estimates

of net VOC emissions from forest canopies. In fact, a significant part of the VOC emitted could be oxidized before it escapes the forest canopy. An attempt to estimate this effect has been made with the box model. The new isoprene chemistry might well explain why local “bottom-up” estimates of isoprene emission can exceed the “top-down” estimates by a factor of 2 or more (Guenther et al., 2007). This effect should be taken into account in global atmospheric studies.

Finally, the implementation of the dihydroxy epoxide production from isoprene hydroperoxides oxidation (Paulot et al., 2009b) provides support for a crucial role of heterogeneous hydrolysis as major formation pathway of tetrols (Böge et al., 2006b, Edney et al., 2005). The gas-phase mechanism of tetrol production should only play a minor role.

6.2 Outlook

6.2.1 Budgeting of OH recycling routes

An important future step will be evaluation of the relative importance of the OH recycling routes. This may be accomplished by budgeting analysis for many species, especially HO_x (Butler, 2009). Suggestions for resolving other model-observation discrepancies may come from such an analysis.

6.2.2 New chemistry and the global atmospheric composition

It is planned to assess the impacts of the new isoprene oxidation routes in a global atmospheric model (Jöckel et al., 2006). Such a task is only feasible after a reduced mechanism with a performance close to MCMEv2 has been developed. MIM2 presents a good starting basis for such a development as demonstrated with MIM2mod (Sec. 3.12). The reduced mechanism will be evaluated against MCMEv2 in a box model in an analogous way to MIM2 versus MCM. An initial focus in the 3D model study will be how well the atmospheric composition in the continental boundary layer is simulated. Following this, the impact of the new oxidation mechanism on the global mean OH concentration and the methane lifetime will be examined. Other possible focal topics include the transport of oxidation products from isoprene emission hot spots, particularly to the upper troposphere, as well as the sensitivity to a simplistic representation of isoprene oxidation within the canopy, which could be implemented by replacing a fraction of the isoprene emission fluxes with a corresponding amount of products of its reaction with OH.

6.2.3 Further mechanism development

Despite much effort, still a few recent experimental results remain to be included in the detailed oxidation mechanism. Two of them are mostly relevant under NO_x -rich conditions.

Paulot et al. (2009a) reported that Z-1,4-hydroxyalkoxy radicals from isoprene undergo an isomerization (H-shift), forming enolic peroxy radicals. This and subsequent chemistry was firstly predicted by Dibble (2002) and Dibble (2004). The net effect of this new oxidation route should be the reduction of $\text{NO} \rightarrow \text{NO}_2$ conversions in the current mechanism.

The fate of alkyl nitrates affects the ozone production efficiencies of air masses. In fact, the fraction of NO_2 produced during the oxidation of the unsaturated C_5 -alkyl nitrates from isoprene is uncertain and considered to be unity in MCM as well as in MCMEv2. Paulot et al. (2009a) also reported the branching ratios for the reaction of OH with all six isomers of C_5 -alkyl nitrates from isoprene. This new chemistry results in about 50% NO_2 recycling efficiency and is expected to significantly affect the O_3 production.

The oxidation mechanism at 298 K for glycolaldehyde and hydroxyacetone as determined by Butkovskaya et al. (2006a) and Butkovskaya et al. (2006b) have already been implemented in MCMEv2. However, it has been established that the yields of products like OH, HCHO, HCOOH and $\text{CH}_3\text{CO}_2\text{H}$ depend strongly on the temperature. At temperatures typical of the upper troposphere these yields are much greater than at 298 K. Therefore, inclusion of such temperature dependent product yields will be important in 3D model studies.

6.2.4 Investigation of new routes

Current computational tools, eg. GAUSSIAN09 (Frisch et al., 2009) and MULTIWELL (Barker, 2001), could be used in order to determine the likely fate of species whose fate is currently unknown. Two potential applications are shown in Fig. 6.1. One could be the fate of the isoprene-related epoxides discovered by Paulot et al. (2009b). After H-abstraction by OH, the heterocyclic three-membered ring could rearrange unimolecularly via cleavage of either a C–C or O–C bonds (see Fig. 6.1a). Estimates of the k_{a1} and k_{a2} would provide a valuable guide in the mechanism development. The second application could be the fate of isoprene-related alkyl nitrates. The extent to which they recycle NO_x in the first degradation steps is thought to be important in determining the O_3 production potential of isoprene in air masses. Their gas phase fate was studied by Paulot et al. (2009a) in presence of 500 nmol/mol NO. Under these conditions the lifetime of the corresponding peroxy radicals (RO_2) is greatly reduced, precluding pathways that are

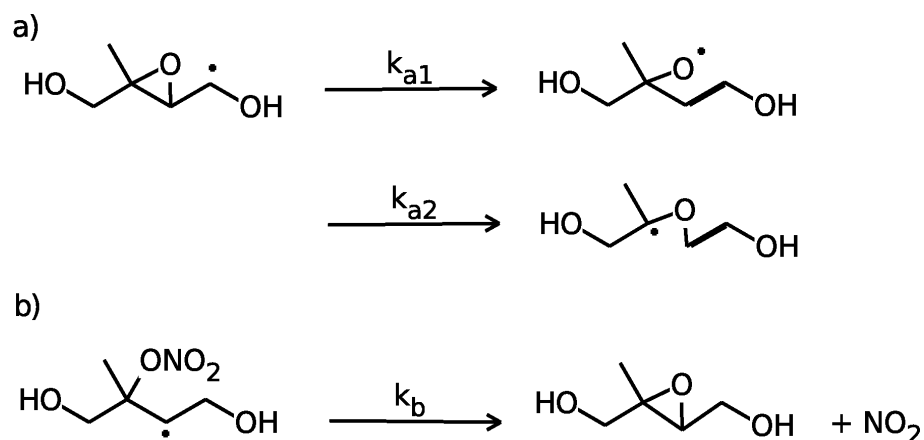


FIGURE 6.1: Molecular decompositions that could be theoretically investigated for further mechanism development.

potentially accessible under more typical (tropical forest) atmospheric conditions. For example, OH addition to one of the unsaturated isoprene nitrates produces a radical like the one shown on the lower left in Fig. 6.1b. In analogy with the formation of epoxides from isoprene hydroperoxides, NO_2 could be eliminated after formation of the three membered ring. Formation of epoxides has been reported in studies of isoprene + NO_3 in which similar radicals are formed (Berndt and Böge (1997)). If calculations were to support this newly hypothesized route, the implications for mechanism development and SOA formation would be significant. In fact, formation of epoxides (SOA precursors) under high- NO_x conditions would provide the missing link explaining the enhanced concentration of tetrols found in organic aerosols during biomass burning periods (Claeys et al., 2004b).

6.3 Catalytic oxidation in the atmosphere

The ultimate oxidant in the atmosphere is O_2 which is present in high concentrations ($\approx 21\%$). Over the last 500 million years the O_2 concentration remained in a relatively narrow range between 10 and 30% (Falkowski and Isozaki, 2008, and references therein). O_2 is continuously produced biologically via the oxidation of water driven by the energy from the Sun. On time scales of millions of years more organic matter was buried in the Earth's crust than respired allowing a substantial accumulation of O_2 in the atmosphere. O_2 has a lifetime of 4 million years according to (Keeling et al., 1993) and is not able to initiate the oxidation of any non-radical atmospheric species. Therefore, atmospheric oxidation can only take place with the help of catalyzers like O_3 and OH. O_3 is produced primarily in the stratosphere via O_2 -photolysis and in the upper troposphere

via lightning NO_x production. The second and most important catalyzer is OH that results from the photolysis of O_3 in the presence of water. An essential characteristic of a catalyzer is that it is recycled during the chemical processes. Although the atmosphere is not an idealized mono-phase system the current work shows that the extent of OH recycling is still substantial and can be higher than 50%. This has an impact on the abundance of OH that ultimately determines the speed at which oxidation proceeds in the troposphere. When added, this OH recycling makes the atmospheric models reconcile with the Earth system behaviour. Under pristine conditions the enhanced oxidation of isoprene, and possibly of other BVOCs, is in fact essential in allowing:

- a sustained self-cleansing capacity of the atmosphere
- BVOCs gradients whereby plant-plant and plant-insect interactions can take place
- protection at both leaf- and forest-level from damages caused by O_3
- a self-fertilizing mechanism for N-poor forests via foliar uptake of alkyl nitrates
- an enhanced formation aerosol precursors that might affect cloud formation and climate

It will be a challenge to elucidate the chemistry of complex mixtures of hydrocarbons emitted by the vegetation and assess the level of OH recycling and the driving mechanisms.

Appendix A

MIM2 mechanism

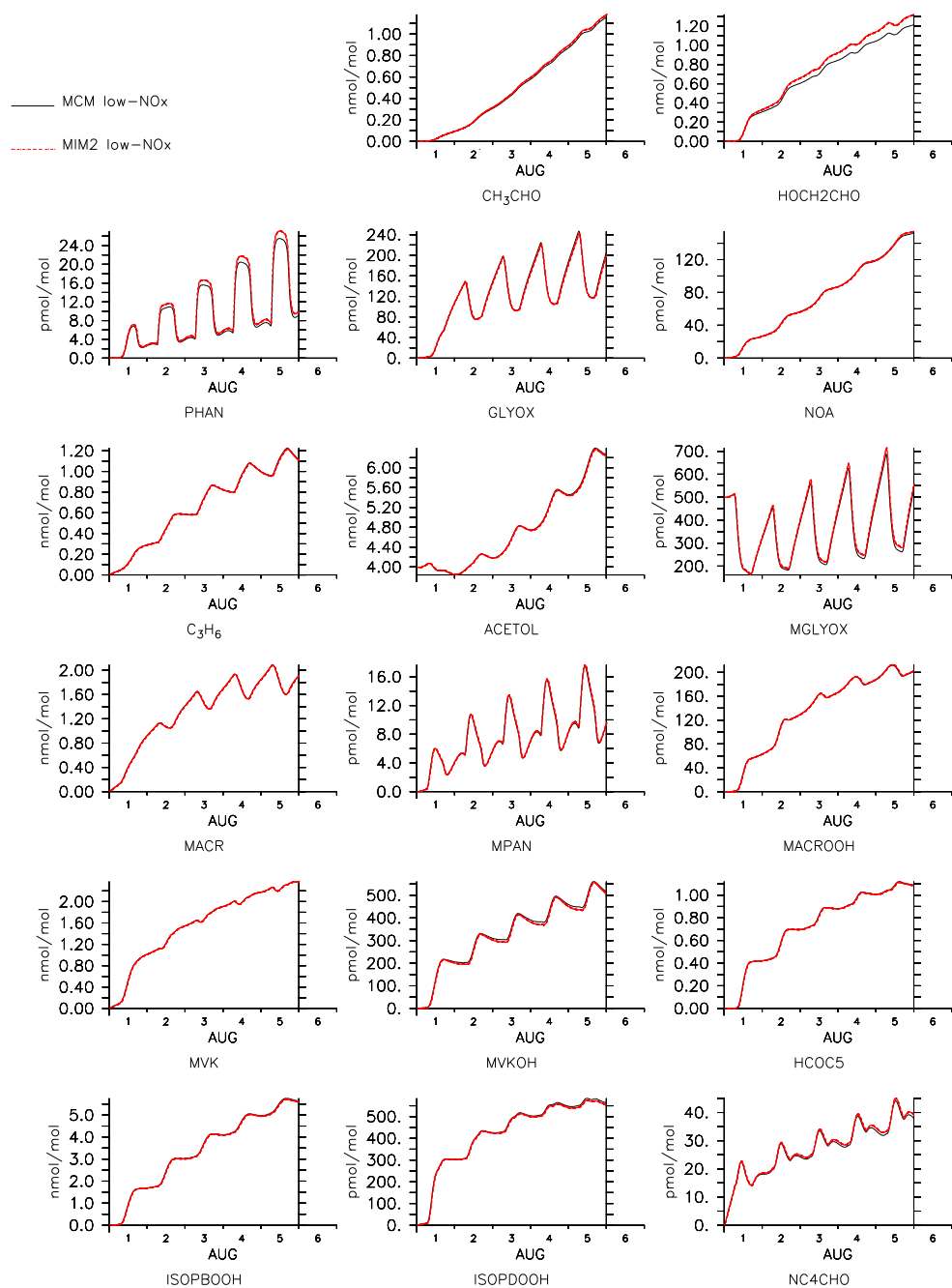


FIGURE A.1: A selection of the most prominent among the news species present now in MIM2. A comparison between MIM2 and MCM in the low-NO_x scenario is shown.

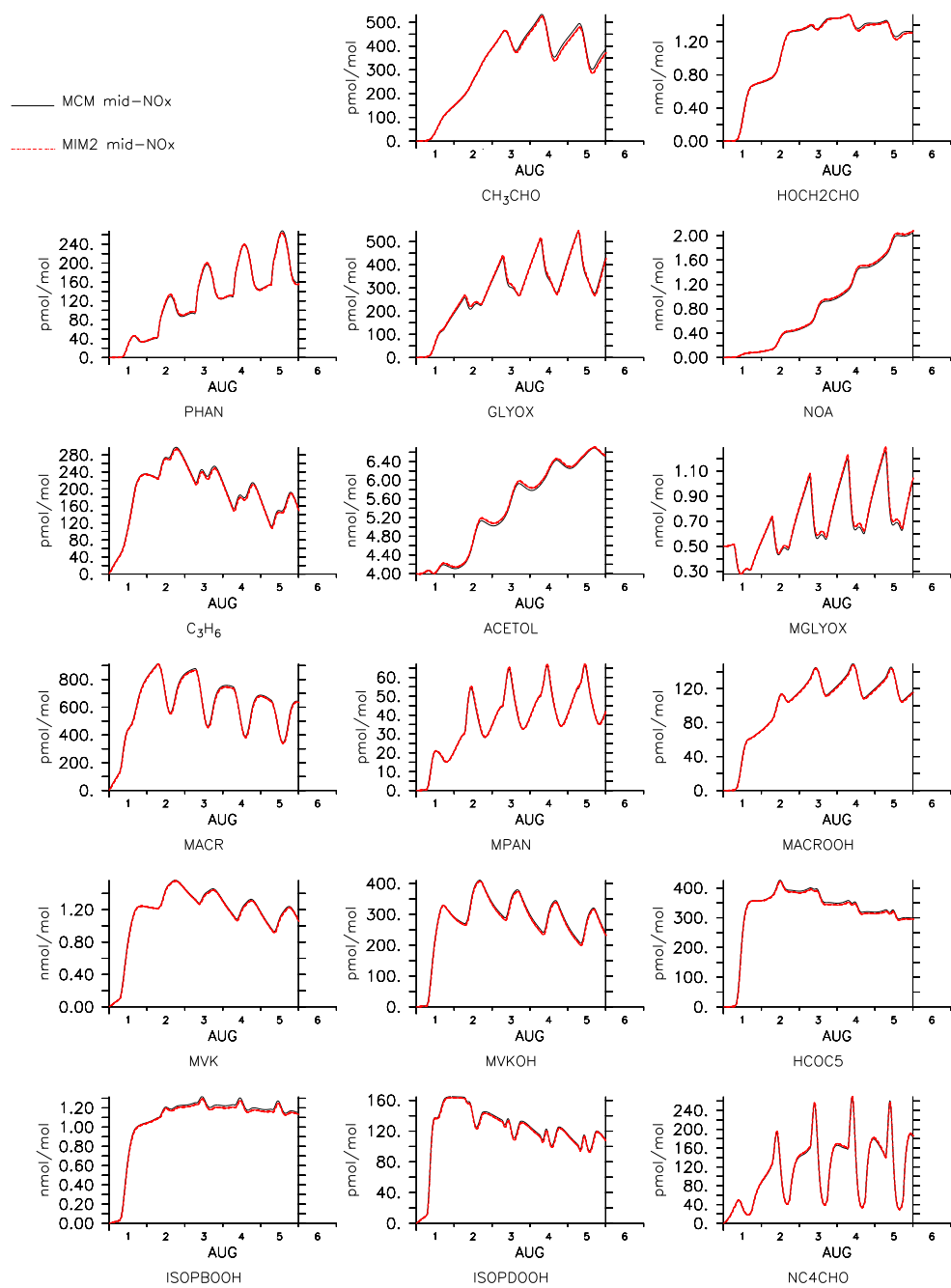


FIGURE A.2: A selection of the most prominent among the news species present now in MIM2. A comparison between MIM2 and MCM in the mid-NO_x scenario is shown.

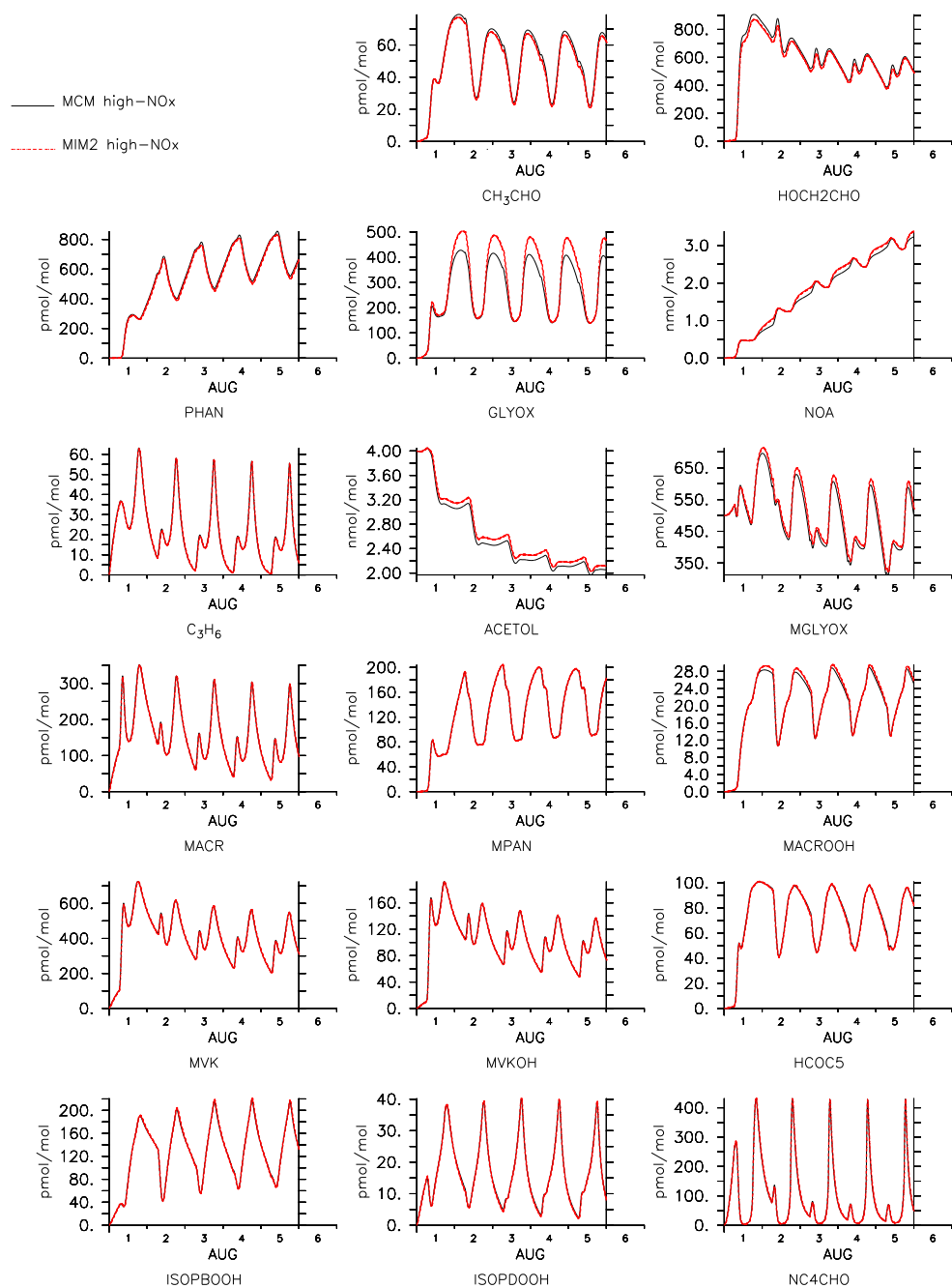


FIGURE A.3: A selection of the most prominent among the news species present now in MIM2. A comparison between MIM2 and MCM in the high-NO_x scenario is shown.

TABLE A.1: MIM2 species. For the lumped species based on isomers in MCM only the condensed formulae are shown. For lumped species representing non-isomeric species the condensed formulae are not shown.

MIM2 name	Formula	Description	Transported
C₅ Stable species			
C5H8	CH ₂ =C(CH ₃)CH=CH ₂	2-methyl-1,3-butadiene (isoprene)	yes
LISOPACOOH	C ₅ H ₁₀ O ₃ lumped	see Tab. A.2	yes
ISOPBOOH	HOCH ₂ C(CH ₃)(OOH)CH=CH ₂	β -hydroxyperoxide	yes
ISOPDOOH	CH ₂ =C(CH ₃)CHOOHCH ₂ OH	β -hydroxyperoxide	yes
ISOPAHOH	HOCH ₂ C(CH ₃)=CHCH ₂ OH	E-2-methyl-2-butene-1,4-diol	yes
ISOPBOH	HOCH ₂ C(CH ₃)OHCH=CH ₂	2-methyl-3-butene-1,2-diol	yes
ISOPDOH	CH ₂ =C(CH ₃)CHOHCH ₂ OH	3-methyl-3-butene-1,2-diol	yes
LISOPACNO3	C ₅ H ₁₀ NO ₄ lumped	see Tab. A.2	yes
ISOPBNO3	HOCH ₂ C(CH ₃)ONONO ₂ CH=CH ₂	alkyl nitrate	yes
ISOPDNO3	CH ₂ =C(CH ₃)CHONO ₂ CH ₂ OH	alkyl nitrate	yes
NISOPOOH	O ₂ NOCH ₂ C(CH ₃)=CHCH ₂ OOH	nitro-hydro-peroxide	yes
NC4CHO	O ₂ NOCH ₂ C(CH ₃)=CHCHO	nitro-aldehyde	yes
LNISOOH	C ₅ H ₇ NO _{6.5} lumped	see Tab. A.2	yes
LHC4ACCHO	C ₅ H ₈ O ₂ lumped	see Tab. A.2	yes
LC578OOH	C ₅ H ₁₀ O ₅ lumped	see Tab. A.2	yes
LHC4ACCO2H	C ₅ H ₈ O ₃ lumped	see Tab. A.2	yes
LHC4ACCO3H	C ₅ H ₈ O ₄ lumped	see Tab. A.2	yes
LC5PAN1719	C ₅ H ₇ NO ₆ lumped	see Tab. A.2	yes
HCOC5	CH ₂ =C(CH ₃)COCH ₂ OH		yes
C59OOH	HOCH ₂ C(CH ₃)(OOH)COCH ₂ OH		yes
C₅-peroxy radicals			
LISOPACO2	C ₅ H ₉ O ₃ lumped	δ -hydroxyperoxy radical see Tab. A.2	no
ISOPBO2	HOCH ₂ CO ₂ (CH ₃)CH=CH ₂	β -hydroxyperoxy radical	no
ISOPDO2	CH ₂ =C(CH ₃)CO ₂ CH ₂ OH	β -hydroxyperoxy radical	no
NISOPO2	O ₂ NOCH ₂ C(CH ₃)=CHCH ₂ O ₂	nitro-peroxy radical	no
LNISO3	C ₅ H ₇ NO _{6.5} lumped	nitro-peroxy radical see Tab. A.2	no
LHC4ACCO3	C ₅ H ₇ O ₄ lumped	δ -hydroxyperoxyacyl radical see Tab. A.2	no
LC578O2	C ₅ H ₉ O ₅ lumped	see Tab. A.2	no
C59O2	C ₅ H ₉ O ₅	alkyl peroxy radicals from the C ₅ -hydroxy ketone (HCOC5)	no
C₄ Stable species			
MACR	CH ₂ =C(CH ₃)CHO	methacrolein	yes
MACROOH	HOCH ₂ C(CH ₃)(OOH)CHO	methacrolein peroxide	yes
MACROH	HOCH ₂ C(CH ₃)(OH)CHO	1,2-dihydroxy-2-methylpropanaldehyde	yes
MACO2H	CH ₂ =C(CH ₃)CO ₂ H	methacroleic acid	yes
MACO3H	CH ₂ =C(CH ₃)CO ₃ H	methacroleic peroxyacid	yes
MPAN	CH ₂ =C(CH ₃)C(O)OONO ₂	peroxy methacroleil nitrate	yes

TABLE A.1: MIM2 species (continued)

MIM2 name	Formula	Description	Transported
C₄ Stable species			
MVK	CH ₂ =CHC(O)CH ₃	butenone (methyl vinyl ketone)	yes
LHMVKABOOH	C ₄ H ₈ O ₄ lumped	see Tab. A.2	yes
MVKOH	CH ₂ =CHC(O)CH ₂ OH	β -hydroxy methyl vinyl ketone	yes
LMVKOHABOOH	C ₄ H ₈ O ₅ lumped	see Tab. A.2	yes
CO2H3CHO	CH ₃ COCH ₂ (OH)CHO		yes
CO2H3CO3H	CH ₃ COCH ₂ (OH)CO ₃ H		yes
BIACETOH	CH ₃ C(O)C(O)CH ₂ OH		yes
HO12CO3C4	CH ₃ C(O)CH(OH)CH ₂ OH		yes
C₄ Peroxy radicals			
MACRO2	HOCH ₂ C(CH ₃)(O ₂)CHO		no
MACO3	CH ₂ =C(CH ₃)CO ₃		no
LHMVKABO2	C ₄ H ₇ O ₄ lumped	see Tab. A.2	no
LMVKOHABO2	C ₄ H ₇ O ₅ lumped	see Tab. A.2	no
CO2H3CO3	CH ₃ COCH ₂ (OH)CO ₃		no
C₃ Stable species			
C3H6	C ₃ H ₆	propene	yes
HYPROPO2H	CH ₃ CH(OOH)CH ₂ OH	β -hydroxyhydroperoxides	yes
PR2O2HNO3	CH ₃ CH(OOH)CH ₂ ONO ₂		yes
ACETOL	CH ₃ C(O)CH ₂ OH	hydroxyacetone	yes
MGLYOX	CH ₃ C(O)CHO	methylglyoxal	yes
NOA	CH ₃ C(O)CH ₂ ONO ₂	α -nitrooxy acetone	yes
HOCH2COCHO	HOCH ₂ C(O)CHO		yes
HOCH2COCO2H	HOCH ₂ C(O)CO ₂ H		yes
C₃ Peroxy radicals			
HYPROPO2	CH ₃ CH(O ₂)CH ₂ OH	β -hydroxy peroxy radical	no
PRONO3BO2	CH ₃ CH(O ₂)CH ₂ ONO ₂	nitro peroxy radical from C3H6	no
C₂ compounds			
CH3CHO	CH ₃ CHO	acetaldehyde	yes
CH3CO2H	CH ₃ CO ₂ H	acetic acid	yes
CH3CO3H	CH ₃ CO ₃ H	peroxy acetic acid	yes
PAN	CH ₃ C(O)OONO ₂	peroxy acetyl nitrate	yes
HOCH2CHO	HOCH ₂ CHO	glycolaldehyde	yes
HOCH2CO2H	HOCH ₂ CO ₂ H	carboxylic acid from	yes
		HOCH2CHO	
HOCH2CO3H	HOCH ₂ CO ₃ H	peroxy carboxylic acid from	yes
		HOCH2CHO	
PHAN	HOCH ₂ C(O)OONO ₂	homologues of PAN for	yes
		HOCH2CHO	
GLYOX	CHOCHO	glyoxal	yes
HCOCO2H	HCOCO ₂ H	carboxylic acid from GLYOX	yes
HCOCO3H	HCOCO ₃ H	peroxy carboxylic acid from	yes
		GLYOX	
C₂ Peroxy radicals			
CH3CO3	CH ₃ CO ₃	peroxy acetyl radical	no
HOCH2CO3	HOCH ₂ CO ₃	peroxy acyl radical from	no
		HOCH2CHO	
HCOCO3	HCOCO ₃	peroxy acyl radical from GLYOX	no

TABLE A.2: Composition of lumped species in MIM2 is given in terms of MCM species.

Lumped species	Compositions	Kind
LISOPACO2	0.5 ISOPAO2 + 0.5 ISOPCO2	δ -hydroxyperoxy radical (internal double bond)
LISOPACOOH	0.5 ISOPAOOH + 0.5 ISOPCOOH	δ -hydroxyperoxides (internal double bond)
LISOPACNO3	0.5 ISOPANO3 + 0.5 ISOPCNO3	alkyl nitrates (internal double bond)
LNISO3	0.5 C510O2 + 0.5 NC4CO3	nitro-peroxy radicals from NC4CHO
LNISOOH	0.5 C510OOH + 0.5 NC4CO3H	nitro-peroxides from LNISO3
LHC4ACCO3	0.5 HC4ACO3 + 0.5 HC4CCO3	acyl peroxy radicals from C ₅ -hydroxy aldehydes
LHC4ACCHO	0.5 HC4ACCHO + 0.5 HC4CCHO	carbonyls (internal double bond)
LHC4ACCO2H	0.5 HC4ACO2H + 0.5 HC4CCO2H	carboxylic acids (internal double bond)
LHC4ACCO3H	0.5 HC4ACO3H + 0.5 HC4CCO3H	percarboxylic acids (internal double bond)
LC5PAN1719	0.5 C5PAN17 + 0.5 C5PAN19	homologues of PAN from LHC4ACCO3
LC578O2	0.5 C57O2 + 0.5 C58O2	peroxy radicals from C ₅ -hydroxy aldehydes
LC578OOH	0.5 C57OOH + 0.5 C58OOH	hydroperoxides from LC578O2
LHMKABO2	0.3 HMKAO2 + 0.7 HMKBO2	peroxy radicals from MVK
LHMKABOOH	0.3 HMKAOOH + 0.7 HMKBOOH	hydroperoxides from LHMKABO2
LMVKOHABO2	0.3 MVKOHAO2 + 0.7 MVKOHBO2	peroxy radicals from MVKOH
LMVKOHABOOH	0.3 MVKOHAOOH + 0.7 MVKOHBOOH	hydroperoxides from LMVKOHABO2

TABLE A.3: List of MIM2 reactions. The expressions for the simple MCM rate coefficients (KRO2NO, KRO2HO2, KAPHO2, KAPNO, KRO2NO3, KNO3AL) are shown in Tab. A.4. The expressions for the complex MCM rate coefficients (KFPAN, KBPAN and KMT16) are shown in Tab. A.5. M is the concentration of air in molec cm^{-3} and T is the temperature in K.

Chemical reaction	Rate coefficient
C₅ compounds	
C5H8 + OH	$\rightarrow 0.25 \text{ LISOPACO2} + 0.491 \text{ ISOPBO2} + 0.259 \text{ ISOPDO2}$ $2.54\text{E-}11 \times \exp(410/T)$
C5H8 + O3	$\rightarrow 0.051 \text{ CH3O2} + 0.1575 \text{ CH3CO3} + 0.054 \text{ LHMVKABO2} + 0.522 \text{ CO} + 0.06875 \text{ HCOOH} + 0.11 \text{ H2O2} + 0.32475 \text{ MACR} + 0.1275 \text{ C3H6} + 0.2625 \text{ HO2} + 0.255 \text{ CO2} + 0.74975 \text{ HCHO} + 0.04125 \text{ MACO2H} + 0.27 \text{ OH} + 0.244 \text{ MVK}$ $7.86\text{E-}15 \times \exp(-1913/T)$
C5H8 + NO3	$\rightarrow \text{NISOPO2}$ $3.03\text{E-}12 \times \exp(-446/T)$
LISOPACO2 + HO2	$\rightarrow \text{LISOPACOOH}$ $0.706 \times \text{KRO2HO2}$
LISOPACO2 + NO	$\rightarrow 0.892 \text{ LHC4ACCHO} + 0.892 \text{ HO2} + 0.892 \text{ NO2} + 0.108 \text{ LISOPACNO3}$ KRO2NO
LISOPACO2 + NO3	$\rightarrow \text{LHC4ACCHO} + \text{HO2} + \text{NO2}$ KRO2NO3
LISOPACO2	$\rightarrow 0.9 \text{ LHC4ACCHO} + 0.8 \text{ HO2} + 0.1 \text{ ISOPA0H}$ $2.4\text{E-}12 \times \text{RO2}$
LISOPACOOH + OH	$\rightarrow \text{LHC4ACCHO} + \text{OH}$ $1.07\text{E-}10$
LISOPACOOH + $h\nu$	$\rightarrow \text{LHC4ACCHO} + \text{HO2} + \text{OH}$ $\text{J}(41)$
ISOPA0H + OH	$\rightarrow \text{LHC4ACCHO} + \text{HO2}$ $9.30\text{E-}11$
LISOPACNO3 + OH	$\rightarrow \text{LHC4ACCHO} + \text{NO2}$ $8.91\text{E-}11$
LISOPACNO3 + $h\nu$	$\rightarrow \text{LHC4ACCHO} + \text{HO2} + \text{NO2}$ $\text{J}(53)$
ISOPBO2 + HO2	$\rightarrow \text{ISOPBOOH}$ $0.706 \times \text{KRO2HO2}$
ISOPBO2 + NO	$\rightarrow 0.696 \text{ MVK} + 0.232 \text{ MVKOH} + 0.696 \text{ HCHO} + 0.696 \text{ HO2} + 0.232 \text{ CH3O2} + 0.928 \text{ NO2} + 0.072 \text{ ISOPBNO3}$ KRO2NO
ISOPBO2 + NO3	$\rightarrow 0.75 \text{ MVK} + 0.25 \text{ MVKOH} + 0.75 \text{ HCHO} + 0.75 \text{ HO2} + 0.25 \text{ CH3O2} + \text{NO2}$ KRO2NO3
ISOPBO2	$\rightarrow 0.6 \text{ MVK} + 0.2 \text{ MVKOH} + 0.6 \text{ HCHO} + 0.6 \text{ HO2} + 0.2 \text{ CH3O2} + 0.2 \text{ ISOPBOH}$ $8.\text{E-}13 \times \text{RO2}$
ISOPBOOH + OH	$\rightarrow \text{ISOPBO2}$ $4.2\text{E-}11$
ISOPBOOH + $h\nu$	$\rightarrow 0.75 \text{ MVK} + 0.25 \text{ MVKOH} + 0.75 \text{ HCHO} + 0.75 \text{ HO2} + 0.25 \text{ CH3O2} + \text{OH}$ $\text{J}(41)$
ISOPBOH + OH	$\rightarrow 0.75 \text{ MVK} + 0.25 \text{ MVKOH} + 0.75 \text{ HCHO} + 0.75 \text{ HO2} + 0.25 \text{ CH3O2}$ $3.85\text{E-}11$
ISOPBNO3 + OH	$\rightarrow \text{MVK} + \text{HCHO} + \text{NO2}$ $3.55\text{E-}11$
ISOPBNO3 + $h\nu$	$\rightarrow 0.75 \text{ MVK} + 0.25 \text{ MVKOH} + 0.75 \text{ HCHO} + 0.75 \text{ HO2} + 0.25 \text{ CH3O2} + \text{NO2}$ $\text{J}(55)$
ISOPDO2 + HO2	$\rightarrow \text{ISOPDOOH}$ $0.706 \times \text{KRO2HO2}$
ISOPDO2 + NO	$\rightarrow 0.855 \text{ MACR} + 0.855 \text{ HCHO} + 0.855 \text{ HO2} + 0.855 \text{ NO2} + 0.145 \text{ ISOPDNO3}$ KRO2NO
ISOPDO2 + NO3	$\rightarrow \text{MACR} + \text{HCHO} + \text{HO2} + \text{NO2}$ KRO2NO3
ISOPDO2	$\rightarrow 0.8 \text{ MACR} + 0.8 \text{ HCHO} + 0.8 \text{ HO2} + 0.1 \text{ HCOC5} + 0.1 \text{ ISOPDOH}$ $2.9\text{E-}12 \times \text{RO2}$
ISOPDOOH + OH	$\rightarrow \text{HCOC5} + \text{OH}$ $1.07\text{E-}10$
ISOPDOOH + $h\nu$	$\rightarrow \text{MACR} + \text{HCHO} + \text{HO2} + \text{OH}$ $\text{J}(41)$
ISOPDOH + OH	$\rightarrow \text{HCOC5} + \text{HO2}$ $7.38\text{E-}11$
ISOPDNO3 + OH	$\rightarrow \text{HCOC5} + \text{NO2}$ $6.1\text{E-}11$
ISOPDNO3 + $h\nu$	$\rightarrow \text{MACR} + \text{HCHO} + \text{HO2} + \text{NO2}$ $\text{J}(54)$

TABLE A.3: MIM2 reactions (continued)

Chemical reaction	Rate coefficient
C₅ compounds	
NISOPO2	→ 0.8 NC4CHO + 0.6 HO2 + 0.2 LISOPACNO3 1.3E-12×RO2
NISOPO2 + NO	→ NC4CHO + HO2 + NO2 KRO2NO
NISOPO2 + NO3	→ NC4CHO + HO2 + NO2 KRO2NO3
NISOPO2 + HO2	→ NISOPOOH .706×KRO2HO2
NISOPOOH + OH	→ NC4CHO + OH 1.03E-10
NISOPOOH + hν	→ NC4CHO + HO2 + OH J(41)
NC4CHO + OH	→ LNISO3 4.16E-11
NC4CHO + O3	→ 0.445 NO2 + 0.89 CO + 0.075625 H2O2 + 0.034375 HCOCO2H + 0.555 NOA + 0.445 HO2 + 0.520625 GLYOX + 0.89 OH + 0.445 MGLYOX 2.40E-17
NC4CHO + NO3	→ LNISO3 + HNO3 KNO3AL×4.25
NC4CHO + hν	→ NOA + 2 CO + 2 HO2 J(18)
LNISO3 + NO	→ NOA + 0.5 GLYOX + 0.5 CO + HO2 + NO2 + 0.5 CO2 (KAPNO + KRO2NO)/2
LNISO3 + NO3	→ NOA + 0.5 GLYOX + 0.5 CO + HO2 + NO2 + 0.5 CO2 1.3×KRO2NO
LNISO3 + HO2	→ LNISOOH (0.706×KRO2HO2 + KAPHO2)/2
LNISOOH + OH	→ LNISO3 2.65E-11
LNISOOH + hν	→ NOA + OH + 0.5 GLYOX + 0.5 CO + HO2 + 0.5 CO2 J(41)
LHC4ACCHO + OH	→ 0.52 LC578O2 + 0.48 LHC4ACCO3 4.52E-11
LHC4ACCHO + O3	→ 0.2225 CH3CO3 + 0.89 CO + 0.0171875 HOCH2CO2H + 0.075625 H2O2 + 0.0171875 HCOCO2H + 0.2775 ACETOL + 0.6675 HO2 + 0.2603125 GLYOX + 0.2225 HCHO + 0.89 OH + 0.2603125 HOCH2CHO + 0.5 MGLYOX 2.40E-17
LHC4ACCHO + NO3	→ LHC4ACCO3 + HNO3 KNO3AL×4.25
LHC4ACCHO + hν	→ 0.5 LHC4ACCO3 + 0.25 ACETOL + 0.25 HOCH2CHO + 0.25 CH3CO3 + 0.75 CO + 1.25 HO2 2×J(19)
LC578O2	→ 0.5 ACETOL + 0.5 MGLYOX + 0.5 GLYOX + 0.5 HOCH2CHO + HO2 9.20E-14×RO2
LC578O2 + HO2	→ LC578OOH KRO2HO2×0.706
LC578O2 + NO	→ 0.5 ACETOL + 0.5 MGLYOX + 0.5 GLYOX + 0.5 HOCH2CHO + HO2 + NO2 KRO2NO
LC578O2 + NO3	→ 0.5 ACETOL + 0.5 MGLYOX + 0.5 GLYOX + 0.5 HOCH2CHO + HO2 + NO2 KRO2NO3
LC578OOH + OH	→ LC578O2 3.16E-11
LC578OOH + hν	→ 0.5 ACETOL + 0.5 MGLYOX + 0.5 GLYOX + 0.5 HOCH2CHO + HO2 + OH J(41)

TABLE A.3: MIM2 reactions (continued)

Chemical reaction	Rate coefficient
C₅ compounds	
LHC4ACCO3	→ 0.3 LHC4ACCO2H + 0.35 ACETOL + 0.35 HOCH2CHO + 0.35 CH3CO3 + 0.35 CO + 0.35 HO2 + 0.7 CO2 1.00E-11×RO2
LHC4ACCO3 + HO2	→ 0.71 LHC4ACCO3H + 0.29 LHC4ACCO2H + 0.29 O3 KAPHO2
LHC4ACCO3 + NO	→ 0.5 ACETOL + 0.5 HOCH2CHO + 0.5 CH3CO3 + 0.5 CO + 0.5 HO2 + NO2 + CO2 KAPNO
LHC4ACCO3 + NO3	→ 0.5 ACETOL + 0.5 HOCH2CHO + 0.5 CH3CO3 + 0.5 CO + 0.5 HO2 + NO2 + CO2 1.6×KRO2NO3
LHC4ACCO3 + NO2	→ LC5PAN1719 KFPAN(T,M)
LHC4ACCO2H + OH	→ 0.5 ACETOL + 0.5 HOCH2CHO + 0.5 CH3CO3 + 0.5 CO + 0.5 HO2 + CO2 2.52E-11
LHC4ACCO3H + OH	→ LHC4ACCO3 2.88E-11
LHC4ACCO3H + hν	→ 0.5 ACETOL + 0.5 HOCH2CHO + 0.5 CH3CO3 + 0.5 CO + 0.5 HO2 + OH + CO2 J(41)
LC5PAN1719	→ LHC4ACCO3 + NO2 KBPAN(T,M)
LC5PAN1719 + OH	→ 0.5 MACROH + 0.5 HO12CO3C4 + CO + NO2 2.52E-11
HCOC5 + OH	→ C59O2 3.81E-11
HCOC5 + hν	→ CH3CO3 + HCHO + HOCH2CO3 J(24)
C59O2	→ ACETOL + HOCH2CO3 9.20E-14×RO2
C59O2 + NO	→ ACETOL + HOCH2CO3 + NO2 KRO2NO
C59O2 + NO3	→ ACETOL + HOCH2CO3 + NO2 KRO2NO3
C59O2 + HO2	→ C59OOH KRO2HO2×0.706
C59OOH + OH	→ C59O2 9.7E-12
C59OOH + hν	→ ACETOL + HOCH2CO3 + OH J(22)+J(41)
C₄ compounds	
MACR + OH	→ 0.57 MACO3 + 0.43 MACRO2 1.86E-11×exp(175/T)
MACR + O3	→ 0.59 MGLYOX + 0.41 CH3CO3 + 0.03375 HCOOH + 0.55625 HCHO + 0.82 CO + 0.12375 H2O2 + 0.41 HO2 + 0.82 OH 1.36E-15×exp(-2112/T)
MACR + NO3	→ MACO3 + HNO3 KNO3AL×2.0
MACR + hν	→ 0.5 MACO3 + 0.5 CH3CO3 + 0.5 HCHO + 0.5 CO + HO2 J(18)+J(19)
MACO3	→ 0.7 CH3CO3 + 0.7 HCHO + 0.7 CO2 + 0.3 MACO2H 1.00E-11×RO2
MACO3 + HO2	→ 0.71 MACO3H + 0.29 MACO2H + 0.29 O3 KAPHO2
MACO3 + NO	→ CH3CO3 + HCHO + NO2 + CO2 8.70E-12×exp(290/T)
MACO3 + NO3	→ CH3CO3 + HCHO + NO2 + CO2 1.6×KRO2NO3
MACO3 + NO2	→ MPAN KFPAN(T,M)
MACRO2	→ 0.7 ACETOL + 0.7 HCHO + 0.7 HO2 + 0.3 MACROH 9.20E-14×RO2
MACRO2 + NO	→ ACETOL + HCHO + HO2 + NO2 KRO2NO
MACRO2 + NO3	→ ACETOL + HCHO + HO2 + NO2 KRO2NO3
MACRO2 + HO2	→ MACROOH KRO2HO2×0.625

TABLE A.3: MIM2 reactions (continued)

Chemical reaction	Rate coefficient
C₄ compounds	
MACROOH + OH	→ MACRO2 2.82E-11
MACROOH + hν	→ ACETOL + HCHO + HO2 + OH J(41)
MACROOH + hν	→ ACETOL + CO + HO2 + OH J(17)
MACROH + OH	→ ACETOL + HCHO + HO2 2.46E-11
MACROH + hν	→ ACETOL + CO + HO2 + HO2 J(17)
MPAN	→ MACO3 + NO2 KBPAN(T,M)
MPAN + OH	→ ACETOL + CO + NO2 3.60E-12
MACO2H + OH	→ CH3CO3 + HCHO + CO2 1.51E-11
MACO3H + OH	→ MACO3 1.87E-11
MACO3H + hν	→ CH3CO3 + HCHO + OH + CO2 J(41)
MVK + OH	→ LHMVKABO2 4.13E-12 × exp(452/T)
MVK + O3	→ 0.28 CH3CO3 + 0.56 CO + 0.225 LCARBON + 0.075 HCOOH + 0.09 H2O2 + 0.28 HO2 + 0.1 CO2 + 0.1 CH3CHO + 0.645 HCHO + 0.36 OH + 0.545 MGLYOX 7.51E-16 × exp(-1521/T)
MVK + hν	→ 0.5 C3H6 + 0.5 CH3CO3 + 0.5 HCHO + CO + 0.5 HO2 2 × J(23)
LHMVKABO2	→ 0.06 CO2H3CHO + 0.18 HO2 + 0.18 HCHO + 0.18 MGLYOX + 0.42 CH3CO3 + 0.42 HOCH2CHO + 0.2 HO12CO3C4 + 0.14 BIACETOH (0.3 × 2.00E-12 + 0.7 × 8.80E-13) × RO2
LHMVKABO2 + HO2	→ LHMVKABOOH KRO2HO2 × 0.625
LHMVKABO2 + NO	→ 0.3 MGLYOX + 0.7 HOCH2CHO + 0.7 CH3CO3 + 0.3 HCHO + 0.3 HO2 + NO2 KRO2NO
LHMVKABO2 + NO3	→ 0.3 MGLYOX + 0.7 HOCH2CHO + 0.7 CH3CO3 + 0.3 HCHO + 0.3 HO2 + NO2 KRO2NO3
LHMVKABOOH + OH	→ 0.3 CO2H3CHO + 0.7 BIACETOH + OH 0.3 × 5.77E-11 + 0.7 × 3.95E-11
LHMVKABOOH + hν	→ 0.3 MGLYOX + 0.7 CH3CO3 + 0.7 HOCH2CHO + 0.3 HCHO + 0.3 HO2 + OH J(41)
MVKOH + OH	→ LMVKOHABO2 4.60E-12 × exp(452/T)
MVKOH + O3	→ 0.56 CO + 0.545 HOCH2COCHO + 0.075 HOCH2COCO2H + 0.075 HCOOH + 0.09 H2O2 + 0.28 HOCH2CO3 + 0.28 HO2 + 0.2 CO2 + 0.545 HCHO + 0.36 OH + 0.1 HOCH2CHO 7.51E-16 × exp(-1521/T)
MVKOH + hν	→ 0.5 HCHO + 0.5 HO2 + 0.5 HOCH2CO3 + CO + 1.5 LCARBON 2 × J(23)
LMVKOHABO2	→ 0.7 HOCH2CHO + 0.7 HOCH2CO3 + 0.3 HOCH2COCHO + 0.3 HCHO + 0.3 HO2 (0.3 × 2.00E-12 + 7 × 8.80E-13) × RO2
LMVKOHABO2 + NO	→ 0.3 HOCH2COCHO + 0.3 HCHO + 0.3 HO2 + 0.7 HOCH2CHO + 0.7 HOCH2CO3 + NO2 KRO2NO
LMVKOHABO2 + NO3	→ 0.3 HOCH2COCHO + 0.3 HCHO + 0.3 HO2 + 0.7 HOCH2CHO + 0.7 HOCH2CO3 + NO2 KRO2NO3
LMVKOHABO2 + HO2	→ LMVKOHABOOH KRO2HO2 × 0.625
LMVKOHABOOH + OH	→ 0.7 HO12CO3C4 + 0.3 CO2H3CHO + OH 5.98E-11
LMVKOHABOOH + hν	→ 0.3 HOCH2COCHO + 0.3 HCHO + 0.3 HO2 + 0.7 HOCH2CHO + 0.7 HOCH2CO3 + OH J(22) + J(41)

TABLE A.3: MIM2 reactions (continued)

Chemical reaction	Rate coefficient
C₄ compounds	
CO ₂ H ₃ CHO + OH → CO ₂ H ₃ CO ₃	2.45E-11
CO ₂ H ₃ CHO + NO ₃ → CO ₂ H ₃ CO ₃ + HNO ₃	KNO ₃ AL×4.0
CO ₂ H ₃ CHO + hν → MGLYOX + CO + HO ₂ + HO ₂	J(15)
CO ₂ H ₃ CO ₃ → MGLYOX + HO ₂ + CO ₂	1.00E-11×RO ₂
CO ₂ H ₃ CO ₃ + HO ₂ → CO ₂ H ₃ CO ₃ H	KAPHO ₂
CO ₂ H ₃ CO ₃ + NO → MGLYOX + HO ₂ + NO ₂ + CO ₂	KAPNO
CO ₂ H ₃ CO ₃ + NO ₃ → MGLYOX + HO ₂ + NO ₂ + CO ₂	1.6×KRO ₂ NO ₃
CO ₂ H ₃ CO ₃ H + OH → CO ₂ H ₃ CO ₃	7.34E-12
CO ₂ H ₃ CO ₃ H + hν → MGLYOX + HO ₂ + OH + CO ₂	J(41)
CO ₂ H ₃ CO ₃ H + hν → CH ₃ CO ₃ + HO ₂ + HCOCO ₃ H	J(22)
HO ₁₂ CO ₃ C ₄ + OH → BIACETOH + HO ₂	1.88E-11
HO ₁₂ CO ₃ C ₄ + hν → CH ₃ CO ₃ + HOCH ₂ CHO + HO ₂	J(22)
BIACETOH + hν → CH ₃ CO ₃ + HOCH ₂ CO ₃	J(35)
C₃ compounds	
C ₃ H ₆ + OH → HYPROPO ₂	KMT16(T,M)
C ₃ H ₆ + O ₃ → 0.28 CH ₃ O ₂ + 0.1 CH ₄ + 0.075 CH ₃ CO ₂ H + 0.56 CO + 0.075 HCOOH + 0.09 H ₂ O ₂ + 0.28 HO ₂ + 0.2 CO ₂ + 0.545 CH ₃ CHO + 0.545 HCHO + 0.36 OH	5.51E-15×exp(-1878/T)
C ₃ H ₆ + NO ₃ → PRONO ₃ BO ₂	9.4E-15
HYPROPO ₂ + HO ₂ → HYPROPO ₂ H	KRO ₂ HO ₂ ×0.520
HYPROPO ₂ + NO → CH ₃ CHO + HCHO + HO ₂ + NO ₂	KRO ₂ NO
HYPROPO ₂ + NO ₃ → CH ₃ CHO + HCHO + HO ₂ + NO ₂	KRO ₂ NO ₃
HYPROPO ₂ → CH ₃ CHO + HCHO + HO ₂	8.80E-13×RO ₂
HYPROPO ₂ H + OH → HYPROPO ₂	1.90E-12×exp(190/T)
HYPROPO ₂ H + OH → ACETOL + OH	2.44E-11
HYPROPO ₂ H + hν → CH ₃ CHO + HCHO + HO ₂ + OH	J(41)
PRONO ₃ BO ₂ + NO → NOA + HO ₂ + NO ₂	KRO ₂ NO
PRONO ₃ BO ₂ + NO ₃ → NOA + HO ₂ + NO ₂	KRO ₂ NO ₃
PRONO ₃ BO ₂ + HO ₂ → PR ₂ O ₂ HNO ₃	KRO ₂ HO ₂ ×0.520
PR ₂ O ₂ HNO ₃ + OH → PRONO ₃ BO ₂	1.90E-12×exp(190/T)
PR ₂ O ₂ HNO ₃ + OH → NOA + OH	3.47E-12
PR ₂ O ₂ HNO ₃ + hν → NOA + HO ₂ + OH	J(41)
ACETOL + OH → MGLYOX + HO ₂	3.00E-12
ACETOL + hν → CH ₃ CO ₃ + HCHO + HO ₂	J(22)
MGLYOX + OH → CH ₃ CO ₃ + CO	1.72E-11
MGLYOX + NO ₃ → CH ₃ CO ₃ + CO + HNO ₃	KNO ₃ AL×2.4
MGLYOX + hν → CH ₃ CO ₃ + CO + HO ₂	J(34)
NOA + OH → MGLYOX + NO ₂	1.30E-13
NOA + hν → CH ₃ CO ₃ + HCHO + NO ₂	J(56)+J(57)
HOCH ₂ COCHO + OH → HOCH ₂ CO ₃ + CO	1.44E-11
HOCH ₂ COCHO + NO ₃ → HOCH ₂ CO ₃ + CO + HNO ₃	KNO ₃ AL×2.4
HOCH ₂ COCHO + hν → HOCH ₂ CO ₃ + CO + HO ₂	J(34)
HOCH ₂ COCO ₂ H + OH → HOCH ₂ CO ₃ + CO ₂	2.89E-12
HOCH ₂ COCO ₂ H + hν → HOCH ₂ CO ₃ + HO ₂ + CO ₂	J(34)

TABLE A.3: MIM2 reactions (continued)

Chemical reaction	Rate coefficient
C₂ compounds	
CH ₃ CO ₃	→ 0.7 CH ₃ O ₂ + 0.7 CO ₂ + 0.3 CH ₃ CO ₂ H 1.00E-11×RO ₂
CH ₃ CO ₃ + HO ₂	→ 0.71 CH ₃ CO ₃ H + 0.29 CH ₃ CO ₂ H + 0.29 O ₃ KAPHO ₂
CH ₃ CO ₃ + NO ₂	→ PAN KFPAN(T,M)
CH ₃ CO ₃ + NO	→ NO ₂ + CH ₃ O ₂ + CO ₂ KAPNO
CH ₃ CO ₃ + NO ₃	→ NO ₂ + CH ₃ O ₂ + CO ₂ KRO ₂ NO ₃ ×1.60
CH ₃ CO ₂ H + OH	→ CH ₃ O ₂ + CO ₂ 8.00E-13
CH ₃ CO ₃ H + OH	→ CH ₃ CO ₃ 3.70E-12
CH ₃ CO ₃ H + hν	→ CH ₃ O ₂ + OH + CO ₂ J(41)
CH ₃ CHO + OH	→ CH ₃ CO ₃ 5.55E-12× exp(311/T)
CH ₃ CHO + NO ₃	→ CH ₃ CO ₃ + HNO ₃ KNO ₃ AL
CH ₃ CHO + hν	→ CH ₃ O ₂ + HO ₂ + CO J(13)
PAN	→ CH ₃ CO ₃ + NO ₂ KBPAN(T,M)
PAN + OH	→ HCHO + CO + NO ₂ 9.50E-13× exp(-650/T)
HOCH ₂ CHO + OH	→ 0.8 HOCH ₂ CO ₃ + 0.2 GLYOX + 0.2 HO ₂ 1.00E-11
HOCH ₂ CHO + NO ₃	→ HOCH ₂ CO ₃ + HNO ₃ KNO ₃ AL
HOCH ₂ CHO + hν	→ HO ₂ + HCHO + HO ₂ + CO J(15)
HOCH ₂ CO ₃ + NO ₂	→ PHAN KFPAN(T,M)
HOCH ₂ CO ₃ + HO ₂	→ 0.71 HOCH ₂ CO ₃ H + 0.29 HOCH ₂ CO ₂ H + 0.29 O ₃ KAPHO ₂
HOCH ₂ CO ₃	→ 0.7 HCHO + 0.7 CO ₂ + 0.7 HO ₂ + 0.3 HOCH ₂ CO ₂ H 1.00E-11×RO ₂
HOCH ₂ CO ₃ + NO	→ NO ₂ + HO ₂ + HCHO + CO ₂ KAPNO
HOCH ₂ CO ₃ + NO ₃	→ NO ₂ + HO ₂ + HCHO + CO ₂ 1.6×KRO ₂ NO ₃
HOCH ₂ CO ₂ H + OH	→ HCHO + HO ₂ + CO ₂ 2.73E-12
HOCH ₂ CO ₃ H + OH	→ HOCH ₂ CO ₃ 6.19E-12
HOCH ₂ CO ₃ H + hν	→ HCHO + HO ₂ + OH + CO ₂ J(41)
PHAN	→ HOCH ₂ CO ₃ + NO ₂ KBPAN(T,M)
PHAN + OH	→ HCHO + CO + NO ₂ 1.12E-12
GLYOX + OH	→ 1.2 CO + 0.6 HO ₂ + 0.4 HCOCO ₃ 1.14E-11
GLYOX + NO ₃	→ 1.2 CO + 0.6 HO ₂ + 0.4 HCOCO ₃ + HNO ₃ KNO ₃ AL
GLYOX + hν	→ 2 CO + H ₂ J(31)
GLYOX + hν	→ HCHO + CO J(32)
GLYOX + hν	→ 2 CO + 2 HO ₂ J(33)
HCOCO ₃	→ 0.7 CO + 0.7 HO ₂ + 0.7 CO ₂ + 0.3 HCOCO ₂ H 1.00E-11×RO ₂
HCOCO ₃ + HO ₂	→ 0.71 HCOCO ₃ H + 0.29 HCOCO ₂ H + 0.29 O ₃ KAPHO ₂
HCOCO ₃ + NO	→ HO ₂ + CO + NO ₂ + CO ₂ KAPNO
HCOCO ₃ + NO ₃	→ HO ₂ + CO + NO ₂ + CO ₂ 1.6×KRO ₂ NO ₃
HCOCO ₂ H + OH	→ CO + HO ₂ + CO ₂ 1.23E-11
HCOCO ₂ H + hν	→ 2 HO ₂ + CO + CO ₂ J(34)
HCOCO ₃ H + OH	→ HCOCO ₃ 1.58E-11
HCOCO ₃ H + hν	→ HO ₂ + CO + OH + CO ₂ J(41)+J(15)

The total peroxy radicals are defined as: RO₂ = LISOPACO₂ + ISOPBO₂ + ISOPDO₂ + NISOPO₂ + LHC4ACCO₃ + LC578O₂ + C59O₂ + LNISO₃ + LHMVK-ABO₂ + LMVKOHABO₂ + MACO₃ + MACRO₂ + CO₂H₃CO₃ + HYPROPO₂ + PRONO₃BO₂ + CH₃CO₃ + HOCH₂CO₃ + HCOCO₃ + CH₃O₂.

TABLE A.4: MCM simple rate constants. T is the temperature in K.

name	expression
KRO2NO	$2.54\text{E-}12 \times \exp(360/T)$
KRO2HO2	$2.91\text{E-}13 \times \exp(1300/T)$
KAPHO2	$4.30\text{E-}13 \times \exp(1040/T)$
KAPNO	$8.10\text{E-}12 \times \exp(270/T)$
KRO2NO3	2.50E-12
KNO3AL	$1.44\text{E-}12 \times \exp(-1862/T)$

TABLE A.5: Parameters for the MCM complex rate constants used in MIM2. M is the concentration of air in molec cm⁻³ and T is the temperature in K.

rate constant	parameters
KMT16	
K0	$8.00 \times 10^{-27} \times (T/300)^{-3.5} \times M$
KI	3.00×10^{-11}
FC	0.5
KFPAN	
K0	$2.70 \times 10^{-28} \times (T/300)^{-7.1} \times M$
KI	$1.20 \times 10^{-11} \times (T/300)^{-0.9}$
FC	0.3
KBPAN	
K0	$4.90 \times 10^{-03} \times \exp(-12100/T) \times M$
KI	$5.40 \times 10^{+16} \times \exp(-13830/T)$
FC	0.3

The rate constants are then calculated according to the following expressions: $k_{comp} = K0 \cdot KI \cdot F / (K0 + KI)$, where $F = 10^{\log FC / (1 + (\log krd/nu)^2)}$ and $nu = 0.75 - 1.27 \cdot \log FC$.

TABLE A.6: Photolysis Parameters (l , m and n) from MCM and used in the box model evaluation (Saunders et al., 2003). They J-values (in s^{-1}) are computed with the expression $J = l \times (\cos(\theta))^m \times \exp(-n \sec(\theta))$, where θ is the solar zenith angle.

J	l	m	n	structural pattern
$J(1)$	6.073E-05	1.743	0.474	
$J(2)$	4.775E-04	0.298	0.080	
$J(3)$	1.041E-05	0.723	0.279	
$J(4)$	1.165E-02	0.244	0.267	
$J(5)$	2.485E-02	0.168	0.108	
$J(6)$	1.747E-01	0.155	0.125	
$J(7)$	2.644E-03	0.261	0.288	
$J(8)$	9.312E-07	1.230	0.307	
$J(11)$	4.642E-05	0.762	0.353	HCHO
$J(12)$	6.853E-05	0.477	0.323	HCHO
$J(13)$	7.344E-06	1.202	0.417	CH ₃ CHO
$J(14)$	2.879E-05	1.067	0.358	C ₂ H ₅ CHO
$J(15)$	2.792E-05	0.805	0.338	C ₃ H ₇ CHO
$J(16)$	1.675E-05	0.805	0.338	C ₅ H ₁₁ CHO
$J(17)$	7.914E-05	0.764	0.364	RCHOHCHO
$J(18)$	1.140E-05	0.396	0.298	RR'C=CR''CHO
$J(19)$	1.140E-05	0.396	0.298	RR'C=CR''CHO
$J(21)$	7.992E-07	1.578	0.271	CH ₃ COCH ₃
$J(22)$	5.804E-06	1.092	0.377	RCOCHR'/OH
$J(23)$	1.836E-05	0.395	0.296	CH ₃ COCH=CH ₂
$J(24)$	1.836E-05	0.395	0.296	RCOCR'=CH ₂
$J(31)$	6.845E-05	0.130	0.201	(HCO) ₂
$J(32)$	1.032E-05	0.130	0.201	(HCO) ₂
$J(33)$	3.802E-05	0.644	0.312	(HCO) ₂
$J(34)$	1.537E-04	0.170	0.208	RCOCHO
$J(35)$	3.326E-04	0.148	0.215	RCOCOR'
$J(41)$	7.649E-06	0.682	0.279	ROOH
$J(51)$	1.588E-06	1.154	0.318	CH ₃ NO ₃
$J(52)$	1.907E-06	1.244	0.335	C ₂ H ₅ NO ₃
$J(53)$	2.485E-06	1.196	0.328	RR'CHNO ₃
$J(54)$	4.095E-06	1.111	0.316	RR'CHNO ₃
$J(55)$	1.135E-05	0.974	0.309	RR'R''CNO ₃
$J(56)$	7.549E-06	1.015	0.324	RCOCHR'/NO ₃
$J(57)$	3.363E-06	1.296	0.322	RCOCHR'/NO ₃
$J(61)$	7.537E-04	0.499	0.266	

Bibliography

- Arnth, A., Monson, R. K., Schurgers, G., Niinemets, U., and Palmer, P. I.: Why are estimates of global terrestrial isoprene emissions so similar (and why is this not so for monoterpenes)?, *Atmos. Chem. Phys.*, 8, 4605–4620, 2008.
- Aschmann, S. M. and Atkinson, R.: Formation yields of methyl vinyl ketone and methacrolein from the gas-phase reaction of O₃ with isoprene, *Environ. Sci. Technol.*, 28, 1539–1542, 1994.
- Atkinson, R.: A structure-activity relationship for the estimation of rate constants for the gas-phase reactions of OH radicals with organic compounds, *Int. J. Chem. Kinetics*, 19, 799–828, 1987.
- Atkinson, R.: Atmospheric reactions of alkoxy and β -hydroxyalkoxy radicals, *Int. J. Chem. Kinetics*, 29, 99–111, 1997a.
- Atkinson, R.: Gas-phase tropospheric chemistry of volatile organic compounds: 1. Alkanes and alkenes, *J. Phys. Chem. Ref. Data*, 26, 215–290, 1997b.
- Atkinson, R.: R. S. Boethling and D. Mackay Eds., Atmospheric Oxidation. Contribution to “Handbook of Property Estimation Methods for Chemicals: Environmental and Health Sciences”, CRC Press, 2000.
- Atkinson, R.: Rate constants for the atmospheric reactions of alkoxy radicals: An updated estimation method, *Atmos. Environ.*, 41, 8468–8485, 2007.
- Atkinson, R. and Arey, J.: Atmospheric Degradation of Volatile Organic Compounds, *Chemical Reviews*, 103(12), 4605–4638, 2003a.
- Atkinson, R. and Arey, J.: Gas-phase tropospheric chemistry of biogenic volatile organic compounds: a review, *Atmos. Environ.*, 2, S197–S219, 2003b.
- Atkinson, R., Ashmann, S. M., Tuazon, E. C., Arey, J., and Zielinska, B.: Formation of 3-Methylfuran from the gas-phase reaction of OH radicals with isoprene and the rate constant for its reaction with the OH radical, *Int. J. Chem. Kinetics*, 21, 953–604, 1989.

- Atkinson, R., Aschmann, S. M., Arey, J., and Shorees, B.: Formation of OH radicals in the gas-phase reaction of O₃ with a series of terpenes, *J. Geophys. Res.*, **97**, 6065–6073, 1992.
- Atkinson, R., Arey, J., Aschmann, S. M., and Tuazon, E. C.: Formation of O(3P) atoms and epoxides from the gas-phase reaction of O₃ with isoprene, *Res. in Chem. Intermediates*, **20**, 385–394, 1994.
- Atkinson, R., Baulch, D. L., Cox, R. A., Crowley, J. N., Hampson, R. F., Hynes, R. G., Jenkin, M. E., Rossi, M. J., and Troe, J.: Evaluated kinetic and photochemical data for atmospheric chemistry: Volume II gas phase reactions of organic species, *Atmos. Chem. Phys.*, **6**, 3625–4055, 2006.
- Baeza-Romero, M. T., Glowacki, D. R., Blitz, M. A., Heard, D., Pilling, M. J., Rickard, A., and Seakins, P.: A combined experimental and theoretical study of the reaction between methylglyoxal and OH/OD radical: OH regeneration, *Phys. Chem. Chem. Phys.*, **9**, 4114–4128, doi:10.1039/b702916k, 2007.
- Barker, J. H.: Multiple-Well, Multiple-Path Unimolecular Reaction Systems. I. Multi-Well Computer Program Suite, *Int. J. Chem. Kinetics*, **33**, 232–245, 2001.
- Baulch, D. L., Bowman, C. T., Cobos, C., Cox, R. A., Just, T., Kerr, J. A., Pilling, M. J., Stocker, D., Troe, J., Tsang, W., Walker, R. W., and Warnatz, J.: Evaluated Kinetic Data for Combustion Modeling: Supplement II, *J. Phys. Chem. Ref. Data*, **34**, 757–1397, 2005.
- Benkelberg, H. J., Böge, O., Seuwen, R., and Warneck, P.: Product distributions from the OH radical-induced oxidation of but-1-ene, methyl-substituted but-1-enes and isoprene in NO_x-free air, *Phys. Chem. Chem. Phys.*, **2**, 4029–4039, 2000.
- Berndt, T. and Böge, O.: Gas-Phase Reaction of NO₃ Radicals With Isoprene: A Kinetic and Mechanistic Study, *Int. J. Chem. Kinetics*, **29**, 755–765, 1997.
- Biesenthal, T. A., Bottenheim, J. W., Shepson, P. B., Li, S.-M., and Brickell, P. C.: The chemistry of biogenic hydrocarbons at a rural site in eastern Canada, *J. Geophys. Res.*, **103**, 25 487–25 498, 1998.
- Blitz, M. A., Heard, D. W., and Pilling, M. J.: OH formation from CH₃CO + O₂: a convenient experimental marker for acetylradical, *Chem. Phys. Lett.*, **365**, 374–379, 2002.
- Böge, O., Miao, Y., Plewka, A., and Herrmann, H.: Formation of secondary organic particle phase compounds from isoprene gas-phase oxidation products: An aerosol chamber and field study, *Atmos. Environ.*, **40**, 2501–2509, 2006a.

- Böge, O., Miao, Y., Plewka, A., and Herrmann, H.: Formation of secondary organic particle phase compounds from isoprene gas-phase oxidation products: An aerosol chamber and field study, *Atmos. Environ.*, 40, 2501–2509, 2006b.
- Brasseur, G. P., Hauglustaine, D. A., Walters, S., Rasch, P. J., Müller, J.-F., Granier, C., and Tie, X. X.: MOZART, a global chemical transport model for ozone and related chemical tracers 1. Model description, *J. Geophys. Res.*, 103, 28 265–28 290, 1998.
- Butkovskaya, N. I., Kukui, A., and Le Bras, G.: Branching Fractions for H₂O Forming Channels of the Reaction of OH Radicals with Acetaldehyde, *J. Phys. Chem. A*, 108, 1160–1168, 2004.
- Butkovskaya, N. I., Pouvesle, N., Kukui, A., and Le Bras, G.: Mechanism of the OH-Initiated Oxidation of Glycolaldehyde over the Temperature Range 233-296 K, *J. Phys. Chem. A*, 110, 13 492–13 499, 2006a.
- Butkovskaya, N. I., Pouvesle, N., Kukui, A., Mu, Y., and Le Bras, G.: Mechanism of the OH-Initiated Oxidation of Hydroxyacetone over the Temperature Range 236-298 K, *J. Phys. Chem. A*, 110, 6833–6843, 2006b.
- Butler, T. M.: Automated sequence analysis of atmospheric oxidation pathways: SEQUENCE version 1.0, *Geosci. Model. Dev. Discuss.*, 2, 1001–1021, 2009.
- Butler, T. M., Taraborrelli, D., Brühl, C., Fischer, H., Harder, H., Lawrence, M. G., Martinez, M., Williams, J., and Lelieveld, J.: Improved simulation of isoprene oxidation chemistry with the ECHAM5/MESSy chemistry-climate model: Lessons from the GABRIEL airborne field campaign, *Atmos. Chem. Phys.*, 8, 4529–4546, 2008.
- Capouet, M., Peeters, J., Noziere, B., , and Müller, J.-F.: Alpha-pinene oxidation by OH: simulations of laboratory experiments, *Atmos. Chem. Phys.*, 4, 2285–2311, 2004.
- Carlton, A. G., Turpin, B. J., Altieri, K. E., Seitzinger, S., Reff, A., Lime, H.-J., and Ervens, B.: Atmospheric oxalic acid and SOA production from glyoxal: Results of aqueous photooxidation experiments, *Atmos. Environ.*, 41, 7588–7602, 2007.
- Carlton, A. G., Wiedinmyer, C., and Kroll, J. H.: A review of Secondary Organic Aerosol (SOA) formation from isoprene, *Atmos. Chem. Phys.*, 9, 4987–5005, 2009.
- Carr, S. A., Baeza-Romero, M. T., Blitz, M. A., Price, B. J. S., and Seakins, P.: Ketone Photolysis in the Presence of Oxygen: A Useful Source of OH for Flash Photolysis Kinetics Experiments, *Int. J. Chem. Kinetics*, 40, 504–514, 2008.

- Carslaw, N., Creasey, D. J., Heard, D. E., Lewis, A. C., McQuaid, J. B., Pilling, M. J., Monks, P. S., Bandy, B. J., and Penkett, S. A.: Modeling OH, HO₂, and RO₂ radicals in the marine boundary layer - 1. Model construction and comparison with field measurements, *J. Geophys. Res.*, 104(D23), 30 241–30 255, 1999a.
- Carslaw, N., Jacobs, P. J., and Pilling, M. J.: Modeling OH, HO₂, and RO₂ radicals in the marine boundary layer 2. Mechanism reduction and uncertainty analysis, *J. Geophys. Res.*, 104(D23), 30 257–30 273, 1999b.
- Carslaw, N., Harrison, D., Heard, D. E., Hunter, M. C., Jacobs, P. J., Jenkin, M. E., Lee, J. D., Lewis, A. C., Pilling, M. J., Saunders, S. M., and Seakins, P. W.: OH and HO₂ radical chemistry in a forested region of north-western Greece, *Atmos. Environ.*, 35, 4725–4737, 2001.
- Carter, W. P. L.: Documentation of the SAPRC-99 chemical mechanism for VOC reactivity assessment, Final report to California air resources board contract 92-329 and contract 95-308, Air pollution research center and college of engineering center for environmental research and technology University of California, Riverside, CA, 2000.
- Carter, W. P. L. and Atkinson, R.: Development and evaluation of a detailed mechanism for atmospheric reactions of isoprene and NO_x, *Int. J. Chem. Kinetics*, 28, 497–530, 1996.
- Chebbi, A. and Carlier, P.: Carboxylic acids in the troposphere, occurrence, sources and sinks: a review, *Atmos. Environ.*, 30, 4233–4249, 1996.
- Chen, X., Hulbert, D., and Shepson, P. B.: Measurement of the organic nitrate yield from OH reaction with isoprene, *J. Geophys. Res.*, 103, 25 563–25 568, 1998.
- Chen, Z. M., Wang, H. L., Zhu, L. H., Wang, C. X., Jie, C. Y., and Hua, W.: Aqueous-phase ozonolysis of methacrolein and methyl vinyl ketone: a potentially important source of aqueous oxidants, *Atmos. Chem. Phys. Discuss.*, 7, 17 599–17 623, 2007.
- Claeys, M., Graham, B., Vas, G., Wang, W., Vermeylen, R., Pashynska, V., Cafmeyer, J., Guyon, P., Andreae, M. O., Artaxo, P., and Maenhaut, W.: Formation of Secondary Organic Aerosols Through Photooxidation of Isoprene, *Science*, 303, 1173–1176, 2004a.
- Claeys, M., Wang, W., Iona, A. C., Kourtcheva, I., Gelencsér, A., and Maenhaut, W.: Formation of secondary organic aerosols from isoprene and its gas-phase oxidation products through reaction with hydrogen peroxide, *Atmos. Environ.*, 38, 4093–4098, 2004b.

- Clifford, E., Wenthold, P. G., Gareyev, R., Lineberger, W. C., DePuy, C. H., Bierbaum, V. M., and Ellison, G. B.: Photoelectron spectroscopy, gas phase acidity, and thermochemistry of tert-butyl hydroperoxide: Mechanisms for the rearrangement of peroxy radicals, *J. Chem. Phys.*, 109, 10 293–10 310, 1998.
- de Gouw, J. and Warneke, C.: Measurements of volatile organic compounds in the Earth's atmosphere using proton-transfer-reaction mass spectrometry, *Mass Spectrometry Reviews*, 26, 223–257, 2007.
- Di Carlo, P.: Missing OH reactivity in a forest: Evidence for unknown reactive biogenic VOCs, *Science*, 304, 722–725, 2004.
- Dibble, T. S.: Isomerization of OH-isoprene adducts and hydroxyalkoxy isoprene radicals, *J. Phys. Chem. A*, 106, 6643–6650, 2002.
- Dibble, T. S.: Prompt chemistry of alkenoxy radical products of the double H-atom transfer of alkoxy radicals from isoprene, *J. Phys. Chem. A*, 108, 2208–2215, 2004.
- Dillon, T. J. and Crowley, J. N.: Direct detection of OH formation in the reactions of HO₂ with CH₃C(O)O₂ and other substituted peroxy radicals, *Atmos. Chem. Phys.*, 8, 4877–4889, 2008.
- Edney, E., Kleindienst, T., Jaouib, M., Lewandowski, M., Offenberg, J., Wang, W., and Claeys, M.: Formation of 2-methyl tetrols and 2-methylglyceric acid in secondary organic aerosol from laboratory irradiated isoprene/NOX/SO₂/air mixtures and their detection in ambient PM_{2.5} samples collected in the eastern United States, *Atmos. Environ.*, 39, 5281–5289, 2005.
- Eerdeken, G., Ganzeveld, L., de Arellano, J. V.-G., Klpfel, T., Sinha, V., N. Yassaa, J. W., Harder, H., Kubistin, D., Martinez, M., and Lelieveld, J.: Flux estimates of isoprene, methanol and acetone from airborne PTR-MS measurements over the tropical rainforest during the GABRIEL 2005 campaign, *Atmos. Chem. Phys.*, 9, 4207–4227, 2009.
- Elrod, M. J., Ranschaert, D. L., and Schneider, N. J.: Direct kinetics study of the temperature dependence of the CH₂O branching channel for the CH₃O₂ + HO₂ reaction, *Int. J. Chem. Kinetics*, 33, 363–376, 2001.
- Emmons, L. K., Carroll, M. A., Hauglustaine, D. A., Brasseur, G. P., Atherton, C., Penner, J., Sillman, S., Levy, H., Rohrer, F., Wauben, W. M. F., Velthoven, P. F. J. V., Wang, Y., Jacob, D., Bakwin, P., Dickerson, R., Doddridge, B., Gerbig, C., Honrath, R., Hbler, G., Jaffe, D., Kondo, Y., Munger, J. W., Torres, A., and Volz-Thomas, A.: Climatologies of NO_x and NO_y: A comparison of data and models, *Atmos. Environ.*, 31, 1851–1904, 1997.

- Falkowski, P. G. and Isozaki, Y.: The story of O₂, *Science*, 322, doi:10.1126/science.1162641, 2008.
- Fan, J. and Zhang, R.: Atmospheric oxidation mechanism of isoprene, *Environ. Chem.*, 1, 140–149, 2004.
- Fehsenfeld, F., Calvert, J., Fall, R., Goldan, P., Guenther, A. B., Hewitt, C. N., Lamb, B., Liu, S., Trainer, M., Westberg, H., and Zimmerman, P.: Emissions of volatile organic compounds from vegetation and the implications for atmospheric chemistry, *Global Biogeochem. Cycles*, 6, 389–430, 1992.
- Feierabend, K. J., Zhu, L., Talukdar, R. K., and Burkholder, J. B.: Rate coefficients for the OH + HC(O)C(O)H (Glyoxal) reaction between 210 and 390 K, *J. Phys. Chem. A*, 112, 73–82, 2008.
- Feng, W. and Wang, B.: Reaction of Vinyl Radical with O₂ Studied by Time-Resolved Infrared Emission Spectroscopy, *Chem. Phys. Lett.*, 365, 505–510, 2002.
- Finlayson-Pitts, B. J. and Pitts, Jr., J. N.: *Chemistry of the upper and lower atmosphere*, Academic Press, 2000.
- Folberth, G. A., Hauglustaine, D. A., Lathière, J., and Brocheton, F.: Interactive chemistry in the Laboratoire de Météorologie Dynamique general circulation model: model description and impact analysis of biogenic hydrocarbons on tropospheric chemistry, *Atmos. Chem. Phys.*, 34, 2273–2319, 2006.
- Frisch, M. J., Trucks, G. W., Schlegel, H. B., Scuseria, G. E., Robb, M. A., Cheeseman, J. R., Scalmani, G., Barone, V., Mennucci, B., Petersson, G. A., Nakatsuji, H., Caricato, M., Li, X., Hratchian, H. P., Izmaylov, A. F., Bloino, J., Zheng, G., Sonnenberg, J. L., Hada, M., Ehara, M., Toyota, K., Fukuda, R., Hasegawa, J., Ishida, M., Nakajima, T., Honda, Y., Kitao, O., Nakai, H., Vreven, T., Jr., M., A., J., Peralta, J. E., Ogliaro, F., Bearpark, M., Heyd, J. J., Brothers, E., Kudin, K. N., Staroverov, V. N., Kobayashi, R., Normand, J., Raghavachari, K., Rendell, A., Burant, J. C., Iyengar, S. S., Tomasi, J., Cossi, M., Rega, N., Millam, J. M., Klene, M., Knox, J. E., Cross, J. B., Bakken, V., Adamo, C., Jaramillo, J., Gomperts, R., Stratmann, R. E., Yazyev, O., Austin, A. J., Cammi, R., Pomelli, C., Ochterski, J. W., Martin, R. L., Morokuma, K., Zakrzewski, V. G., Voth, G. A., Salvador, P., Dannenberg, J. J., Dapprich, S., Daniels, A. D., Farkas, O., Foresman, J. B., Ortiz, J. V., Cioslowski, J., and Fox, D. J.: *Gaussian 09 Revision A.1*, 2009.
- Geiger, H., Barnes, I., Bejan, I., Benter, T., and Spittler, M.: The tropospheric degradation of isoprene: an updated module for the regional atmospheric chemistry mechanism, *Atmos. Environ.*, 37, 1503–1519, 2003.

- Giacopelli, P., Ford, K., Espada, C., and Shepson, P. B.: Comparison of the measured and simulated isoprene nitrate distributions above a forest canopy, *J. Geophys. Res.*, 110, doi:10.1029/2004JD005123, 2005.
- Goldstein, A. H. and Galbally, I. E.: Known and Unexplored Organic Constituents in the Earth's Atmosphere, *Environ. Sci. Technol.*, 41(5), 1515–1521, 2007.
- Goldstein, A. H., McKay, M., Kurpius, M. R., Schade, G. W., Lee, A., Holzinger, R., and Rasmussen, R. A.: Forest thinning experiment confirms ozone deposition to forest canopy is dominated by reaction with biogenic VOCs, *Geophys. Res. Lett.*, 31, doi:10.1029/2004GL021259, 2004.
- Grant, R. H.: Partitioning of biologically active radiation in plant canopies, *Int. J. Biometeorol.*, 40, 26–40, 1997.
- Grosjean, D., Williams, E. L., and Grosjean, E.: Atmospheric chemistry of isoprene and its carbonyl products, *Environ. Sci. Technol.*, 27, 830–840, 1993.
- Grosjean, E. and Grosjean, D.: Rate constants for the gas-phase reactions of ozone with unsaturated aliphatic alcohols, *Int. J. Chem. Kinetics*, 26, 1185–1191, 1994.
- Guenther, A., Hewitt, C. N., Erickson, D., Fall, R., Geron, C., Graedel, T., Harley, P., Klinger, L., Lerdau, M., McKay, W. A., Pierce, T., Scholes, B., Steinbrecher, R., Tallamraju, R., Taylor, J., and Zimmerman, P.: A global model of natural volatile organic compound emissions, *J. Geophys. Res.*, 100, 8873–8892, 1995.
- Guenther, A., Karl, T., Harley, P., Wiedinmyer, C., Palmer, P. I., and Geron, C.: Estimates of global terrestrial isoprene emissions using MEGAN (Model of Emissions of Gases and Aerosols from Nature), *Atmos. Chem. Phys.*, 6, 3181–3210, 2006.
- Guenther, A., Karl, T., Wiedinmyer, C., Barkley, M., Palmer, P., Muller, J. F., Stavrov, T., and Millet, D.: Reconciling bottom-up, top-down, and direct measurements of biogenic VOC emissions, *Eos, Trans. AGU (Abstract Supplement)*, 88(52), A14D–07, 2007.
- Gutbrod, R., Meyer, S., Rahman, M. M., and Schindler, R. N.: On the use of CO as scavenger for OH radicals in the ozonolysis of simple alkenes and isoprene, *Int. J. Chem. Kinetics*, 29, 717–723, 1997.
- Gutman, D. and Nelson, H. H.: Gas-phase reactions of the vinoxy radical with O₂ and NO, *J. Phys. Chem.*, 87, 3902–3905, 1983.
- Harwood, M. H., Roberts, J. M., Frost, G. J., Ravishankara, A. R., and Burkholder, J. B.: Photochemical Studies of CH₃C(O)OONO₂ (PAN) and CH₃CH₂C(O)OONO₂ (PPN): NO₃ Quantum Yields, *J. Phys. Chem. A*, 107, 1148–1154, 2003.

- Hasson, A. S., Orzechowska, G., and Paulson, S. E.: Production of stabilized Criegee intermediates and peroxides in the gas phase ozonolysis of alkenes 1. Ethene, trans-2-butene, and 2,3-dimethyl-2-butene, *J. Geophys. Res.*, 106, 34 131–34 142, 2001a.
- Hasson, A. S., Orzechowska, G., and Paulson, S. E.: Production of stabilized Criegee intermediates and peroxides in the gas phase ozonolysis of alkenes 2. Asymmetric and biogenic alkenes, *J. Geophys. Res.*, 106, 34 143–34 153, 2001b.
- Hasson, A. S., Chung, M. Y., Kuwata, K. K., Converse, A. D., Krohn, D., and Paulson, S. E.: Reaction of Criegee Intermediates with Water Vapors—An Additional Source of OH Radicals in Alkene Ozonolysis?, *J. Phys. Chem. A*, 107, 6176–6182, 2003.
- Hasson, A. S., Tyndall, G. S., and Orlando, J. J.: A Product Yield Study of the Reaction of HO₂ Radicals with Ethyl Peroxy (C₂H₅O₂), Acetyl Peroxy (CH₃C(O)O₂), and Acetonyl Peroxy (CH₃C(O)CH₂O₂) Radicals, *J. Phys. Chem. A*, 108, 5979–5989, 2004.
- Hastings, W. P., Koehler, C. A., Bailey, E. L., and De Haan, D. O.: Secondary organic aerosol formation by glyoxal hydration and oligomer formation: humidity effects and equilibrium shifts during analysis, *Environ. Sci. Technol.*, 39, 8728–8735, 2005.
- Heard, A. C., Pilling, M. J., and Tomlin, A. S.: Mechanism reduction techniques applied to tropospheric chemistry, *Atmos. Environ.*, 32, 1059–1073, 1998.
- Horowitz, L. W., Fiore, A. M., Milly, G. P., Cohen, R. C., Perring, A., Wooldridge, P. J., Hess, P. G., Emmons, L. K., and Lamarque, J.-F.: Observational constraints on the chemistry of isoprene nitrates over the eastern United States, *J. Geophys. Res.*, 112, doi:10.1029/2006JD007747, 2007.
- Houweling, S., Dentener, F., and Lelieveld, J.: The impact of nonmethane hydrocarbon compounds on tropospheric photochemistry, *J. Geophys. Res.*, 103(D9), 10 673–10 696, 1998.
- Ito, A., Sillman, S., and Penner, J. E.: Global chemical transport model study of ozone response to changes in chemical kinetics and biogenic volatile organic compounds emissions due to increasing temperatures: Sensitivities to isoprene nitrate chemistry and grid resolution, *J. Geophys. Res.*, 114, doi:10.1029/2008JD011254, 2009.
- Jacob, D. J., Field, B. D., Li, Q., Blake, D. R., de Gouw, J., Warneke, C., Hansel, A., Wisthaler, A., Singh, H. B., and Guenther, A.: Global budget of methanol: Constraints from atmospheric observations, *J. Geophys. Res.*, 110, doi:10.1029/2004JD005172, 2005.
- Jenkin, M. E. and Hayman, G. D.: Kinetics of reactions of primary, secondary and tertiary β -hydroxy peroxy radicals, *J. Chem. Soc. Faraday Trans.*, 91, 1911–1922, 1995.

- Jenkin, M. E., Saunders, S. M., and Pilling, M. J.: The Tropospheric Degradation of Volatile Organic Compounds: a Protocol for Mechanism Development, *Atmos. Environ.*, 31, 81–104, 1997.
- Jenkin, M. E., Boyd, A. A., and Lesclaux, R.: Peroxy radical kinetics resulting from the OH-initiated oxidation of 1,3-butadiene, 2,3-dimethyl-1,3-butadiene and isoprene, *J. Atmos. Chem.*, 29, 267–298, 1998.
- Jenkin, M. E., Hurley, M. D., and Wallington, T. J.: Investigation of the radical product channel of the $\text{CH}_3\text{C}(\text{O})\text{O}_2 + \text{HO}_2$ reaction in the gas phase, *Phys. Chem. Chem. Phys.*, 9, 3149–3162, doi:10.1039/b702757e, 2007.
- Jöckel, P., Tost, H., Pozzer, A., Brühl, C., Buchholz, J., Ganzeveld, L., Hoor, P., Kerckweg, A., Lawrence, M. G., Sander, R., Steil, B., Stiller, G., Tanarhte, M., Taraborrelli, D., van Ardenne, J., and Lelieveld, J.: The atmospheric chemistry general circulation model ECHAM5/MESSy1: consistent simulation of ozone from the surface to the mesosphere, *Atmos. Chem. Phys.*, 6, 5067–5104, 2006.
- Johnson, D. and Marston, G.: The gas-phase ozonolysis of unsaturated volatile organic compounds in the troposphere, *Chem. Soc. Rev.*, 37, 699–716, 2008.
- Johnson, D., Cassanelli, P., and Cox, R. A.: Correlation-type structure activity relationships for the kinetics of the decomposition of simple and β -substituted alkoxy radicals, *Atmos. Environ.*, 38, 1755–1765, 2004.
- Kanakidou, M. and Crutzen, P. J.: The photochemical source of carbon monoxide: Importance, uncertainties and feedbacks, *Chemosphere - Global Change Science*, 1, 91–109, 1999.
- Karl, M., Dorn, H.-P., Holland, F., Koppmann, R., Poppe, D., Rupp, L., Schaub, A., and Wahner, A.: Product study of the reaction of OH radicals with isoprene in the atmosphere simulation chamber SAPHIR, *J. Atmos. Chem.*, 55, 167–187, 2006.
- Karunanandan, R., Hölscher, D., Dillon, T. J., Horowitz, A., Crowley, J. N., Vereecken, L., and Peeters, J.: Reaction of HO with Glycolaldehyde, HOCH_2CHO : Rate Coefficients (240–362 K) and Mechanism, *J. Phys. Chem. A*, 111, 897–908, 2007.
- Keeling, R. F., Najjar, R. P., Bender, M. L., and Tans, P. P.: What Atmospheric Oxygen Measurements Can Tell Us About the Global Carbon Cycle, *Global Biogeochem. Cycles*, 7(37), 37–67, 1993.
- Kieber, R. J., Zhou, X., and Mopper, K.: Formation of Carbonyl Compounds from UV-Induced Photodegradation of Humic Substances in Natural Waters: Fate of Riverine Carbon in the Sea, *Limnol. Oceanogr.*, 35, 1503–1515, 1990.

- Kiendler-Scharr, A., Wildt, J., Dal Maso, M., Hohaus, T., Kleist, E., Mentel, T. F., Tillmann, R., Uerlings, R., Schurr, U., and Wahner, A.: New particle formation in forests inhibited by isoprene emissions, *Nature*, 461, doi:10.1038/nature08292, 2009.
- Krol, M. C., Molemaker, M. J., and de Arellano, J. V.-G.: Effects of turbulence and heterogeneous emissions on photochemically active species in the convective boundary layer, *J. Geophys. Res.*, 105, 6871–6884, 2000.
- Kroll, J. H., Clarke, J. S., Donahue, N. M., Anderson, J. G., and Demerjian, K. L.: Mechanism of HO_x Formation in the Gas-Phase Ozone-Alkene Reaction. 1. Direct, Pressure-Dependent Measurements of Prompt OH Yields, *J. Phys. Chem. A*, 105, 1554–1560, 2001a.
- Kroll, J. H., Sahay, S. R., Anderson, J. G., Demerjian, K. L., and Donahue, N. M.: Mechanism of HO_x Formation in the Gas-Phase Ozone-Alkene Reaction. 2. Prompt versus Thermal Dissociation of Carbonyl Oxides to Form OH, *J. Phys. Chem. A*, 105, 4446–4457, 2001b.
- Kroll, J. H., Ng, N. L., Murphy, S. M., Flagan, R. C., and Seinfeld, J. H.: Secondary organic aerosol formation from isoprene photooxidation, *Environ. Sci. Technol.*, 40, 1869–1877, 2006.
- Kubistin, D., Harder, H., Martinez, M., Rudolf, M., Sander, R., Bozem, H., Eerdekens, G., Fischer, H., Gurk, C., Klüpfel, T., Knigstedt, R., U. Parchatka, C. S., Stickler, A., Taraborelli, D., Williams, J., and Lelieveld, J.: Hydroxyl radicals in the tropical troposphere over the Suriname rain forest: comparison of measurements with the box model MECCA, *Atmos. Chem. Phys. Discuss.*, 8, 15 491–15 536, 2008.
- Kulmala, M.: How particles nucleate and grow, *Science*, 302, doi:10.1126/science.1090848, 2003.
- Kurpius, M. R. and Goldstein, A. H.: Gas-phase chemistry dominates O₃ loss to a forest, implying a source of aerosols and hydroxyl radicals to the atmosphere, *Geophys. Res. Lett.*, 30, doi:10.1029/2002GL016785, 2003.
- Kuwata, K. T., Templeton, K. L., and Hasson, A. S.: Computational Studies of the Chemistry of Syn Acetaldehyde Oxide, *J. Phys. Chem. A*, 107, 11 525–11 532, 2003.
- Kuwata, K. T., Hasson, A. S., r. v. Dickinson, Petersen, E. R., and Valin, L. C.: Quantum Chemical and Master Equation Simulations of the Oxidation and Isomerization of Vinyloxy Radicals, *J. Phys. Chem. A*, 109, 2514–2524, 2005.
- Kwok, E. S. C. and Atkinson, R.: Estimation of hydroxyl radical reaction rate constants for gas-phase organic compounds using a structure-reactivity relationship: An update, *Atmos. Environ.*, 29, 1685–1695, 1995.

- Kwok, E. S. C., Atkinson, R., and Arey, J.: Observation of hydroxycarbonyls from the OH radical-initiated reaction of isoprene, *Environ. Sci. Technol.*, **29**, 2467–2469, 1995.
- Laothawornkitkul, J., Paul, N. D., Vickers, C. E., Possell, M., Mullineaux, P. M., Hewitt, C. N., and Taylor, J. E.: The role of isoprene in insect herbivory, *Plant Signaling and Behavior*, **3**, 1141–1142, 2008a.
- Laothawornkitkul, J., Paul, N. D., Vickers, C. E., Possell, M., Taylor, J. E., Mullineaux, P. M., and Hewitt, C. N.: Isoprene emissions influence herbivore feeding decisions, *Plant, Cell and Environ.*, **31**, doi:10.1111/j.1365-3040.2008.01849.x, 2008b.
- Laothawornkitkul, J., Taylor, J. E., Paul, N. D., and Hewitt, C. N.: Biogenic volatile organic compounds in the Earth system, *New Phytologist*, **183**, 27–51, 2009.
- Lathière, J., Hauglustaine, D. A., Friend, A. D., Noblet-Ducoudré, N. D., Viovy, N., and Folberth, G. A.: Impact of climate variability and land use changes on global biogenic volatile organic compound emissions, *Atmos. Chem. Phys.*, **6**, 2129–2146, 2006.
- Lawrence, M. G., Rasch, P. J., von Kuhlmann, R., Williams, J., Fischer, H., de Reus, M., Lelieveld, J., Crutzen, P. J., Schultz, M., Stier, P., Huntrieser, H., Heland, J., Stohl, A., Forster, C., Elbern, H., Jakobs, H., and Dickerson, R. R.: Global chemical weather forecasts for field campaign planning: predictions and observations of large-scale features during MINOS, CONTRACE, and INDOEX, *Atmos. Chem. Phys.*, **3**, 267–289, 2003.
- Lee, W., Baasandorj, M., Stevens, P. S., and Hites, R. A.: Monitoring OH-initiated oxidation kinetics of isoprene and its products using online mass spectrometry, *Environ. Sci. Technol.*, **39**, 1030–1036, doi:10.1021/es049438f, 2005.
- Lei, W., Zhang, R., McGivern, W. S., Derecskei-Kovacs, A., and North, S.: Theoretical study of OH-O₂-isoprene peroxy radicals, *J. Phys. Chem. A*, **105**, 471–477, 2001.
- Lelieveld, J., Butler, T. M., Dillon, T. J., Fischer, H., Ganzeveld, L., Harder, H., Lawrence, M. G., Martinez, M., Taraborrelli, D., and Williams, J.: Atmospheric oxidation capacity sustained by a tropical forest, *Nature*, **452**, doi:10.1038/nature06870, 2008.
- Lewin, A. G., Johnson, D., Price, D. W., and Marston, G.: Aspects of the kinetics and mechanism of the gas-phase reaction of ozone with conjugated dienes, *Phys. Chem. Chem. Phys.*, **3**, 1253–1261, 2001.
- Lockwood, A. L., Filley, T. R., Rodhes, D., and Shepson, P. B.: Foliar uptake of atmospheric organic nitrates, *J. Geophys. Res.*, **35**, doi:10.1029/2008GL034714, 2008.

- Loeffler, K. W., Koehler, C. A., Paul, N. M., and De Haan, D. O.: Oligomer formation in evaporating glyoxal and methyl glyoxal solutions, *Environ. Sci. Technol.*, 40, 6318–6323, 2006.
- Loivamäki, M., Mummb, R., Dicke, M., and Schnitzler, J.-P.: Isoprene interferes with the attraction of bodyguards by herbaceous plants, *Proc. Nat. Accademy of Sciences*, 105, doi:10.1073/pnas.0804488105, 2008.
- Loreto, F. and Velikova, V.: Isoprene Produced by Leaves Protects the Photosynthetic Apparatus against Ozone Damage, Quenches Ozone Products, and Reduces Lipid Peroxidation of Cellular Membranes, *Plant Phys.*, 127, 1781–1787, 2001.
- Loreto, F., Mannozi, M., Maris, C., Nascetti, P., Ferranti, F., and Pasqualini, S.: Ozone Quenching Properties of Isoprene and Its Antioxidant Role in Leaves, *Plant Phys.*, 126, 993–1000, 2001.
- Madronich, S. and Calvert, J. G.: The NCAR Master Mechanism of Gas Phase Chemistry - Version 2.0, Technical note, NCAR, 1989.
- Madronich, S. and Calvert, J. G.: Permutation reactions of organic peroxy radicals in the troposphere, *J. Geophys. Res.*, 95D, 5697–5715, 1990.
- Madronich, S. and Flocke, S.: The role of solar radiation in atmospheric chemistry, Springer, New York, 1998.
- Magneron, I., Mellouki, A., Bras, G. L. L., Moortgat, G. K., Horowitz, A., and Wirtz, K.: Photolysis and OH-Initiated Oxidation of Glycolaldehyde under Atmospheric Conditions, *J. Phys. Chem. A*, 109, 4552–4561, 2005.
- Martinez, M., Harder, H., Kubistin, D., Rudolf, M., Bozem, H., Eerdeken, G., Fischer, H., Gurk, C., Klpfel, T., Knigstedt, R., Parchatka, U., Schiller, C. L., Stickler, A., Williams, J., , and Lelieveld, J.: Hydroxyl radicals in the tropical troposphere over the Suriname rainforest: airborne measurements, *Atmos. Chem. Phys. Discuss.*, 8, 15 491–15 536, 2008.
- Mereau, R., Rayez, M.-T., Caralp, F., and Rayez, J.-C.: Theoretical study on the comparative fate of 1-butoxy and β -hydroxy-1-butoxy radicals, *Phys. Chem. Chem. Phys.*, 2, 1919–1928, 2000.
- Mereau, R., Rayez, M.-T., Rayez, J.-C., Caralp, F., and Lesclaux, R.: Theoretical study on the atmospheric fate of carbonyl radicals : kinetics of decomposition reactions, *Phys. Chem. Chem. Phys.*, 3, 4712–4717, 2001.

- Millet, D. B., Custer, T. G., de Gouw, J. A., Karl, T., Singh, H. B., Warneke, C., and Williams, J.: Top-down constraints on the atmospheric acetaldehyde budget, *Eos, Trans. AGU (Abstract Supplement)*, 89(53), A21H-03, 2008a.
- Millet, D. B., Jacob, D. J., Custer, T. G., de Gouw, J. A., Goldstein, A. H., Karl, T., Singh, H. B., Sive, B. C., Talbot, R. W., Warneke, C., , and Williams, J.: New constraints on terrestrial and oceanic sources of atmospheric methanol, *Atmos. Chem. Phys. Discuss.*, 8, 7609–7655, 2008b.
- Miyoshi, A., Atakeyama, S., and Washida, N.: OH radical- initiated photooxidation of isoprene: An estimate of global CO production, *J. Geophys. Res.*, 99, 18 779–18 787, 1994.
- Müller, J.-F., Stavrou, T., Wallens, S., Smedt, I. D., Roozendaal, M. V., Potosnak, M. J., Rinne, J., Munger, B., Goldstein, A., and Guenther, A. B.: Global isoprene emissions estimated using MEGAN, ECMWF analyses and a detailed canopy environment model, *Atmos. Chem. Phys.*, 8, 1329–1341, 2008.
- Myriokefalitakis, S., Vrekoussis, M., Tsigaridis, K., Wittrock, F., Richter, A., Brhl, C., Volkamer, R., Burrows, J. P., and Kanakidou, M.: The influence of natural and anthropogenic secondary sources on the glyoxal global distribution, *Atmos. Chem. Phys.*, 8, 4965–4981, 2008.
- Neeb, P. and Moortgat, G. K.: Formation of OH radicals in the gas-phase reaction of propene, isobutene, and isoprene with O₃, *J. Phys. Chem. A*, 103, 9003–9012, 1999.
- Neeb, P., Sauer, F., Horie, O., and Moortgat, G. K.: Formation of hydroxymethyl hydroperoxide and formic acid in alkene ozonolysis in the presence of water vapor, *Atmos. Environ.*, 31, 1417–1423, 1997.
- Neeb, P., Horie, O., and Moortgat, G. K.: The ethene-ozone reaction in the gas phase, *J. Phys. Chem. A*, 102, 6778–6785, 1998.
- Nenes, A., Charlson, R. J., Facchini, M. C., Kulmala, M., Laaksonen, A., and Seinfeld, J. H.: Can chemical effects on cloud droplet number rival the first indirect effect?, *Geophys. Res. Lett.*, 29, doi:10.1029/2002GL015295, 2002.
- Nguyen, T. L., Peeters, J., and Vereecken, L.: Theoretical study of the gas-phase ozonolysis of β -pinene (C₁₀H₁₆), *Phys. Chem. Chem. Phys.*, doi:10.1039/b822984h, 2009.
- Niinemets, M., Loreto, F., and Reichstein, M.: Physiological and physicochemical controls on foliar volatile organic compound emissions, *TRENDS in Plant Science*, 9, doi:10.1016/j.tplants.2004.02.006, 2004.

- Niki, H., Maker, P. D., Savage, C. M., and Breitenbach, L. P.: An FTIR study of the Cl-atom-initiated reaction of glyoxal, *Int. J. Chem. Kinetics*, 17, 547–558, 1983.
- Niki, H., Maker, P. D., Savage, C. M., Breitenbach, L. P., and Hurley, M. D.: FTIR spectroscopic study of the mechanism for the gas-phase reaction between ozone and tetramethylethylene, *J. Phys. Chem.*, 91, 941–946, 1987.
- Nizkorodov, S. A., Crouse, J. D., Fry, J. L., Roehl, C. M., and Wennberg, P. O.: Near-IR photodissociation of peroxy acetyl nitrate, *Atmos. Chem. Phys.*, 5, 385–392, 2005.
- Orlando, J. J. and Tyndall, G. S.: The atmospheric chemistry of the HC(O)CO radical, *Int. J. Chem. Kinetics*, 33, 149–156, 2001.
- Orlando, J. J., Tyndall, G. S., and Paulson, S. E.: Mechanism of the OH-initiated oxidation of methacrolein, *Geophys. Res. Lett.*, 26, 1999.
- Orlando, J. J., Tyndall, G. S., Vereecken, L., and Peeters, J.: The atmospheric chemistry of acetonoxyl radical, *J. Phys. Chem. A*, 104, 11 578–11 588, 2000.
- Patchen, A. K., Pennino, M. J., Kiep, A. C., and Elrod, M. J.: Direct kinetics study of the product-forming channels of the reaction of isoprene-derived hydroperoxy radicals with NO, *Int. J. Chem. Kinetics*, 39, 353–361, 2007.
- Paulot, F., Crouse, J. D., Kjaergaard, H. G., Kroll, J. H., Seinfeld, J. H., and Wennberg, P. O.: Isoprene photooxidation: new insights into the production of acids and organic nitrates, *Atmos. Chem. Phys.*, 9, 1479–1501, 2009a.
- Paulot, F., Crouse, J. D., Kjaergaard, H. G., Krten, A., St. Clair, J. M., Seinfeld, J. H., and Wennberg, P. O.: Unexpected Epoxide Formation in the Gas-Phase Photooxidation of Isoprene, *Science*, 325, doi:10.1126/science.1172910, 2009b.
- Paulson, S. E., Flagan, R. C., and Seinfeld, J. H.: Atmospheric photooxidation of isoprene Part I: the OH and O(3P) reactions, *Int. J. Chem. Kinetics*, 24, 79–101, 1992a.
- Paulson, S. E., Flagan, R. C., and Seinfeld, J. H.: Atmospheric Photooxidation of isoprene Part II: The ozone-isoprene reaction, *Int. J. Chem. Kinetics*, 24, 103–125, 1992b.
- Paulson, S. E., Chung, M., Sen, A. D., and Orzechowska, G.: Measurement of OH radical formation from the reaction of ozone with several biogenic alkenes, *J. Geophys. Res.*, 103, 25 533–25 539, 1998.

- Peeters, J., Fantechi, G., and Vereecken, L.: A generalized Structure-activity relationship for the decomposition of (substituted) alkoxy radicals, *J. Atmos. Chem.*, 48, 59–80, 2004.
- Peeters, J., Boullart, W., Pultau, V., Vandenberg, S., and Vereecken, L.: Structure-activity relationship for the addition of OH to (poly)alkenes: site-specific and total rate constants, *J. Phys. Chem. A*, 111, 1618–1631, 2007.
- Peeters, J., Nguyen, T. L., and Vereecken, L.: HO_x radical regeneration in the oxidation of isoprene, *Phys. Chem. Chem. Phys.*, doi:10.1039/b908511d, 2009.
- Penuelas, J. and Llusà, J.: Plant VOC emissions: making use of the unavoidable, *TRENDS in Plant Science*, 19, doi:10.1016/j.tree.2004.06.002, 2004.
- Pfister, G. G., Emmons, L. K., Hess, P. G., Lamarque, J.-F., Orlando, J. J., Walters, S., Guenther, A., Palmer, P. I., and Lawrence, P. J.: Contribution of isoprene to chemical budgets: A model tracer study with the NCAR CTM MOZART-4, *J. Geophys. Res.*, 113, doi:10.1029/2007JD008948, 2008.
- Pinho, P. G., Pio, C. A., and Jenkin, M. E.: Evaluation of isoprene degradation in the detailed tropospheric chemical mechanism, MCM v3, using environmental chamber data, *Atmos. Environ.*, 39, 1303–1322, 2005.
- Pöschl, U., von Kuhlmann, R., Poisson, N., and Crutzen, P. J.: Development and intercomparison of condensed isoprene oxidation mechanisms for global atmospheric modeling, *J. Atmos. Chem.*, 37, 29–52, 2000.
- Pozzer, A., Jöckel, P., Tost, H., Sander, R., Ganzeveld, L., Kerkweg, A., and Lelieveld, J.: Simulating organic species with the global atmospheric chemistry general circulation model ECHAM5/MESSy1: a comparison of model results with observations, *Atmos. Chem. Phys.*, 7, 2527–2550, 2007.
- Pugh, T. A. M., MacKenzie, A. R., Hewitt, C. N., Langford, B., Edwards, P. M., Furneaux, K. L., Heard, D. E., Hopkins, J. R., Jones, C. E., Karunaharan, A., Lee, J., Mills, G., Misztal, P., Moller, S., Monks, P. S., and Whalley, L. K.: Simulating atmospheric composition over a South-East Asian tropical rainforest: Performance of a chemistry box model, *Atmos. Chem. Phys. Discuss.*, 9, 19 243–19 278, 2009.
- Raber, W. H. and Moortgat, G. K.: *Progress and Problems in atmospheric chemistry*, World Scientific, 1995.
- Ren, X., Olson, J. R., Crawford, J. H., Brune, W. H., Mao, J., Long, R. B., Chen, Z., Chen, G., Avery, M. A., Sachse, G. W., Barrick, J. D., Diskin, G. S., Huey, L. G., Fried, A., Cohen, R. C., Heikes, B., Wennberg, P. O., Singh, H. B., Blake, D. R., and Shetter,

- R. E.: HO_x chemistry during INTEX-A 2004: Observation, model calculation, and comparison with previous studies, *J. Geophys. Res.*, 106, doi:10.1029/2007JD009166, 2008.
- Rickard, A. R., Johnson, D., McGill, C. D., and Marston, G.: OH yields in the gas-phase reactions of ozone with alkenes, *J. Phys. Chem. A*, 103, 7656–7664, 1999.
- Rohrer, F. and Berresheim, H.: Strong correlation between levels of tropospheric hydroxyl radicals and solar ultraviolet radiation, *Nature*, 442, doi:10.1038/nature04924, 2006.
- Ruppert, L. and Becker, K. H.: A product study of the OH radical-initiated oxidation of isoprene: formation of C₅-unsaturated diols, *Atmos. Environ.*, 34, 1529–1542, 2000.
- Sander, R.: Compilation of Henrys Law Constants for Inorganic and Organic Species of Potential Importance in Environmental Chemistry, Tech. rep., Max-Planck Institute for Chemistry, PO Box 3060 55020 Mainz, Germany, <http://www.mpch-mainz.mpg.de/~sander/res/henry.html>, 1999.
- Sander, R., Kerkweg, A., Jöckel, P., and Lelieveld, J.: Technical note: The new comprehensive atmospheric chemistry module MECCA, *Atmos. Chem. Phys.*, 5, 445–450, 2005.
- Sandu, A. and Sander, R.: Technical note: Simulating chemical systems in Fortran90 and Matlab with the Kinetic PreProcessor KPP-2.1, *Atmos. Chem. Phys.*, 6, 187–195, 2006.
- Sandu, A., Verwer, J. G., and E. J. Spee, J. G. B., Carmichael, G. R., and Potra, F. A.: Benchmarking stiff ODE solvers for atmospheric chemistry problems II: Rosenbrock solvers, *Atmos. Environ.*, 31, 3459–3472, 1997.
- Sauer, F., Schfer, C., Neeb, P., Horie, O., and Moortgat, G. K.: Formation of hydrogen peroxide in the ozonolysis of isoprene and simple alkenes under humid conditions, *Atmos. Environ.*, 33, 229–241, 1999.
- Saunders, S. M., Jenkin, M. E., Derwent, R. G., and Pilling, M. J.: Protocol for the Development of the Master Chemical Mechanism, MCM v3 (Part A): tropospheric degradation of non-aromatic volatile organic compounds, *Atmos. Chem. Phys.*, 34, 161–180, 2003.
- Sharkey, T. D. and Singsaas, E. L.: Why plants emit isoprene, *Nature*, 374, doi:10.1038/374769a0, 1995.
- Sharkey, T. D., Chen, X., and Yeh, S.: Isoprene Increases Thermotolerance of Fostmidomycin-Fed Leaves, *Plant Phys.*, 125, 2001–2006, 2001.

- Shepson, P., Mackay, E., and Muthuramu, K.: Henry's law constants and removal processes of several atmospheric β -hydroxy alkyl radicals, *Environ. Sci. Technol.*, 30, 3618–3623, 1996.
- Singh, H., Chen, Y., Staudt, A., Jacob, D., Blake, D., Heikes, B., and Snow, J.: Evidence from the Pacific troposphere for large global sources of oxygenated organic compounds, *Nature*, 410, doi:10.1038/35074067, 2001.
- Singsaas, E. L., Lerdau, M., Winter, K., and Sharkey, T. D.: Isoprene Increases Thermotolerance of Isoprene-Emitting Species, *Plant Phys.*, 115, 1413–1420, 1997.
- Sinreich, R., Volkamer, R., Filsinger, F., Frie, U., Kern, C., Platt, U., Sebastian, O., and Wagner, T.: MAX-DOAS detection of glyoxal during ICARTT 2004, *Atmos. Chem. Phys.*, 7, 12931303, 2007.
- Sprengnether, M., Demerjian, K. L., Donahue, N., and Anderson, J. G.: Product analysis of the OH oxidation of isoprene and 1,3-butadiene in the presence of NO, *J. Geophys. Res.*, 107, doi:10.1029/2006JD007747, 2002.
- Stark, M. S.: Epoxidation of Alkenes by Peroxyl Radicals in the Gas Phase: Structure-Activity Relationships, *J. Phys. Chem. A*, 101, 8296–8301, 1997.
- Stark, M. S.: Addition of Peroxyl Radicals to Alkenes and the Reaction of Oxygen with Alkyl Radicals, *J. Am. Chem. Soc.*, 122, 4162–4170, 2000.
- Stickler, A., Fischer, H., Bozem, H., Gurk, C., Schiller, C., Martinez-Harder, M., Kubistin, D., Harder, H., Williams, J., Eerdeken, G., Yassaa, N., Ganzeveld, L., Sander, R., and Lelieveld, J.: Chemistry, transport and dry deposition of trace gases in the boundary layer over the tropical Atlantic Ocean and the Guyanas during the GABRIEL field campaign, *Atmos. Chem. Phys.*, 7, 3933–3956, 2007.
- Stockwell, W., Kirchner, F., Kuhn, M., and Seefeld, S.: A new mechanism for regional atmospheric chemistry modeling, *Atmos. Environ.*, 102, 25 847–25 879, 1997.
- Stroud, C., Makar, P., Karl, T., Guenther, A., Geron, C., Turnipseed, A., Nemitz, E., Baker, B., Potosnak, M., and Fuentes, J. D.: Role of canopy-scale photochemistry in modifying biogenic-atmosphere exchange of reactive terpene species: Results from the CELTIC field study, *J. Geophys. Res.*, 110, doi:10.1029/2005JD005775, 2005.
- Talukdar, R. K., Burkholder, J. B., Schmoltner, A.-M., Roberts, J. M., Wilson, R. R., and Ravishankara, A. R.: Investigation of the loss processes for peroxyacetyl nitrate in the atmosphere - UV photolysis and reaction with OH, *J. Geophys. Res.*, 100, 14 163–14 173, 1995.

- Tan, D., Faloon, I., Simpas, J. B., Brune, W., Shepson, P. B., Couch, T. L., Summer, A. L., Carroll, M. A., Apel, T. E., Remier, D., and Stockwell, W.: HO_x budgets in a deciduous forest: Results from the PROPHET summer 1998 campaign, *J. Geophys. Res.*, 106, 24 407–24 427, 2001.
- Torres, A. L. and Buchan, H.: Tropospheric nitric oxide measurements over the Amazon Basin, *J. Geophys. Res.*, 93, 1396–1406, 1988.
- Treves, K., Shragina, L., and Rudich, Y.: Henry's law constants of some β -, γ -, and δ -hydroxy alkyl nitrates of atmospheric interest, *Environ. Sci. Technol.*, 34, 1197–1203, 2000.
- Tuazon, E. and Atkinson, R.: A product study of the gas-phase reaction of isoprene with the OH radical in the presence of NO_x, *Int. J. Chem. Kinetics*, 22, 1221–1236, 1990a.
- Tuazon, E. and Atkinson, R.: A product study of the gas-phase reaction of methacrolein with the OH radical in the presence of NO_x, *Int. J. Chem. Kinetics*, 22, 591–602, 1990b.
- Tyndall, G. S., Orlando, J. J., Wallington, T. J., and Hurley, M. D.: Pressure Dependence of the Rate Coefficients and Product Yields for the Reaction of CH₃CO Radicals with O₂, *Int. J. Chem. Kinetics*, 29, 655–663, 1997.
- Vereecken, L. and Peeters, J.: H-atom abstraction by OH-radicals from (biogenic) (poly)alkenes: C-H bond strengths and abstraction rates, *J. Phys. Chem. A*, 333, 162–168, 2001.
- Vereecken, L. and Peeters, J.: Nontraditional (per)oxy ring-closure paths in the atmospheric oxidation of isoprene and monoterpenes, *J. Phys. Chem. A*, 108, 5197–5204, 2004.
- Vereecken, L., Nguyen, T., Hermans, I., and Peeters, J.: Computational study of the stability of α -hydroperoxyl or α -alkylperoxyl substituted alkyl radicals, *Chem. Phys. Lett.*, 393, 432–436, 2004.
- Vereecken, L., Müller, J.-F., and Peeters, J.: Low-volatility poly-oxygenates in the OH-initiated atmospheric oxidation of α -pinene: impact of non-traditional peroxy radical chemistry, *Phys. Chem. Chem. Phys.*, 9, 5241–5248, doi:10.1039/b708023a, 2007.
- Volkamer, R., Molina, L. T., Molina, M. J., Shirley, T., and Brune, W. H.: DOAS measurement of glyoxal as an indicator for fast VOC chemistry in urban air, *Geophys. Res. Lett.*, 32, doi:10.1029/2005GL022616, 2005.

- Volkamer, R., Martini, F. S., Molina, L. T., Salcedo, D., Jimenez, J. L., and Molina, M. J.: A missing sink for gas-phase glyoxal in Mexico City: Formation of secondary organic aerosol, *Geophys. Res. Lett.*, 34, doi:10.1029/2007GL030752, 2007.
- von Kuhlmann, R., Lawrence, M. G., Crutzen, P. J., and Rasch, P. J.: A model for studies of tropospheric ozone and nonmethane hydrocarbons: Model evaluation of ozone-related species, *J. Geophys. Res.*, 108, doi:10.1029/2002JD003348, 2003.
- von Kuhlmann, R., Lawrence, M. G., Pöschl, U., and Crutzen, P. J.: Sensitivities in global scale modeling of isoprene, *Atmos. Chem. Phys.*, 4, 1–17, 2004.
- Wang, K. Y. and Shallcross, D. E.: Modelling terrestrial biogenic isoprene fluxes and their potential impact on global chemical species using a coupled LSM-CTM model, *Atmos. Environ.*, 34, 2909–2925, 2000.
- Wang, Y., Jacob, D. J., and Logan, J. A.: Global simulation of tropospheric O₃-NO_x-hydrocarbon chemistry 1. Model formulation, *J. Geophys. Res.*, 103, 10 713–10 725, 1998.
- Warneke, C., Holzinger, R., Hansel, A., Jordan, A., Lindinger, W., Pöschl, U., Williams, J., Hoor, P., Fischer, H., Crutzen, P. J., Scheeren, H. A., and Lelieveld, J.: Isoprene and its oxidation products methyl vinyl ketone, methacrolein, and isoprene related peroxides measured online over the tropical rain forest of Surinam in March 1998, *J. Atmos. Chem.*, 38, 167–185, 2001.
- Whitehouse, L. E., Tomlin, A. S., and Pilling, M. J.: Systematic reduction of complex tropospheric chemical mechanisms, Part I: sensitivity and time-scale analyses, *Atmos. Chem. Phys.*, 4, 2025–2056, 2004a.
- Whitehouse, L. E., Tomlin, A. S., and Pilling, M. J.: Systematic reduction of complex tropospheric chemical mechanisms, Part II: Lumping using a time-scale based approach, *Atmos. Chem. Phys.*, 4, 2057–2081, 2004b.
- Wijaya, C. D., Sumathi, R., and Green, W. H.: Thermodynamic properties and kinetic parameters for cyclic ether formation from hydroperoxyalkyl radicals, *J. Phys. Chem. A*, 107, 4908–4920, 2003.
- Williams, J., Pöschl, U., Crutzen, P. J., Hansel, A., Holzinger, R., Warneke, C., Lindinger, W., and Lelieveld, J.: An Atmospheric Chemistry Interpretation of Mass Scans Obtained from a Proton Transfer Mass Spectrometer Flown over the Tropical Rainforest of Surinam, *J. Atmos. Chem.*, 38, 133–166, 2001.
- Wittrock, F., Richter, A., Oetjen, H., Burrows, J. P., Kanakidou, M., Myriokefalitakis, S., Volkamer, R., Beirle, S., Platt, U., and Wagner, T.: Simultaneous global

observations of glyoxal and formaldehyde from space, *Geophys. Res. Lett.*, **33**, doi: 10.1029/2006GL026310, 2006.

Yokouchi, Y.: Seasonal and diurnal variation of isoprene and its reaction products in a semi-rural area, *Atmos. Environ.*, **28**, 2651–2658, 1994.

Zhu, L. and G. Johnston: Kinetics and products of the reaction of the vinoxy radical with O₂, *J. Phys. Chem.*, **99**, 15 114–15 119, 1995.